N73-11261

NASA TECHNICAL NOTE

NASA TN D-6965

NASA TN D-6965

CASE FILE COPY

EXPERIMENTAL STUDY OF NOZZLE WALL BOUNDARY LAYERS AT MACH NUMBERS 20 TO 47

by Joseph H. Kemp, Jr., and F. Kevin Owen

Ames Research Center

Moffett Field, Calif. 94035

NATIONAL AERONAUTICS AND SPACE ADMINISTRATION • WASHINGTON, D. C. • OCTOBER 1972

1. Report No. NASA TN D-6965	2. Government Accession No.	3. Recipient's Catalog No.
4. Title and Subtitle EXPERIMENTAL STUDY OF NOZZLE WALL BOUNDARY LAYERS AT MACH NUMBERS 20 TO 47		5. Report Date October 1972
		6. Performing Organization Code
7. Author(s) Joseph H. Kemp, Jr., and F. Kevin Owen		8. Performing Organization Report No. A-4359
9. Performing Organization Name and Address NASA Ames Research Center Moffett Field, Calif. 94035		10. Work Unit No. 136-13-01-16-00-21
		11. Contract or Grant No.
12. Sponsoring Agency Name and Address National Aeronautics and Space Administration Washington, D.C. 20546		13. Type of Report and Period Covered Technical Note
		14. Sponsoring Agency Code
15. Supplementary Notes		

16. Abstract

The nozzle wall boundary layer of the Ames M-50 helium tunnel has been thoroughly investigated with pitot pressure, total temperature, skin friction, and wall heat transfer measurements at five stations and hot wire measurements at two stations. The results indicate that the boundary layer was turbulent with a thick viscous sublayer. Pressure gradients were observed across the boundary layer; the effect of these gradients on the equations of motion are discussed in this paper.

The direct skin friction measurements were higher than expected from empirical predictions; the Reynolds analogy factors however, $2C_H/C_f$, were lower than expected. Hot wire measurements indicated mass flow fluctuations as large as 80 percent of the local mean mass flow at the edge of the viscous sublayer with a maximum value relative to the edge mass flow of about 15 percent at $y/\delta \approx 0.8$.

17. Key Words (Suggested by Author(s)) Hypersonic flow, Turbulent boundary layers, Nozzle wall	18. Distribution Statement Unclassified – Unlimited

19. Security Classif. (of this report)	20. Security Classif. (of this page)	21. No. of Pages	22. Price*
Unclassified	Unclassified	106	$3.00

*For sale by the National Technical Information Service, Springfield, Virginia 22151

TABLE OF CONTENTS

SYMBOLS

C_f friction coefficient, $\dfrac{2\tau_w}{\rho_e u_e^2}$

C_H Stanton number, $\dfrac{q}{\rho_e u_e C_p(T_{aw} - T_w)}$

C_p pressure coefficient

d diameter of thermocouple wire used in heat-transfer gage, cm

D diameter of wire in total temperature probe, cm

e voltage

f frequency

F_c transformation function for C_f

F_{R_θ} transformation function for Re_θ

h heat-transfer coefficient, $\dfrac{q}{(T_{aw} - T_w)}$

k thermal conductivity

K Bach's relaminarization parameter (ref. 24), $\dfrac{\mu_e}{\rho_e u_e^2} \dfrac{du_e}{dx}$

M Mach number

Nu Nusselt number, $\dfrac{hd}{k}$

p pressure, atm

q wall heat-transfer rate, W/m^2

Q_r total radial heat conduction at radius r in the thin skin at the heat-transfer gage

r radius, cm

r_f recovery factor

R Reynolds number

t	thickness of sensing element in heat transfer gage, cm
T	temperature, °K
u	velocity, m/sec
u^+	transformed velocity
x	longitudinal distance downstream from the nozzle throat
y	distance normal to the surface, cm
y^+	transformed distance normal to the surface
Γ	energy thickness, $r_W - r_W \left[1 - \frac{2}{r_W} \int_o^{\delta} \frac{\rho u}{\rho_e u_e} \left(\frac{T - T_e}{T_W - T_e}\right) \left(1 - \frac{y}{r_W}\right) dy\right]^{1/2}$
δ	boundary–layer thickness, cm
δ^*	displacement thickness, $r_W - r_W \left[1 - \frac{2}{r_W} \int_o^{\delta} \left(1 - \frac{\rho u}{\rho_e u_e}\right) \left(1 - \frac{y}{r_W}\right) dy\right]^{1/2}$
θ	momentum thickness, $r_W - r_W \left[1 - \frac{2}{r_W} \int_o^{\delta} \frac{\rho u}{\rho_e u_e} \left(1 - \frac{u}{u_e}\right) \left(1 - \frac{y}{r_W}\right) dy\right]^{1/2}$
μ	coefficient of viscosity
ν	kinematic viscosity
ρ	density, kg/m^3
τ	shear stress

Subscripts

act	actual value
aw	adiabatic wall condition
c	at disk center
e	outer edge of the boundary layer
l	local value

L	outer edge of the viscous sublayer
m	measured value
r	at radius r
T	at nozzle throat based on throat diameter
$VD\ I$	Van Driest I
w	wall or wire
o	local stagnation condition
2	static value behind a normal shock
θ	based on momentum thickness

Superscripts

$'$	fluctuating part of dependent variable
$-$	time-averaged part of dependent variable

EXPERIMENTAL STUDY OF NOZZLE WALL BOUNDARY LAYERS AT MACH NUMBERS 20 TO 47

Joseph H. Kemp, Jr. and F. Kevin Owen

Ames Research Center

SUMMARY

The nozzle wall boundary layer of the Ames M-50 helium tunnel has been thoroughly investigated using pitot pressure, total temperature, skin friction, and wall heat-transfer measurements at five stations covering about 85 percent of the nozzle length and with hot wire measurements at two stations near the nozzle exit. Data were obtained for temperature ratios varying from 0.35 to 1 and Reynolds numbers based on momentum thickness varying from 900 to 5600. The results indicate that the boundary layer is turbulent with a thick viscous sublayer. Pressure gradients observed across the boundary layer are large relative to the static pressure but small relative to the dynamic pressure.

The direct skin-friction measurements were higher than expected from empirical predictions: the Reynolds analogy factors $2C_H/C_f$, however, were lower than expected. Hot-wire measurements indicated mass flow fluctuations as large as 80 percent of the local mean mass flow at the edge of the viscous sublayer with a maximum value relative to the edge mass flow of about 15 percent at $y/\delta = 0.8$.

INTRODUCTION

The development of flow models and provision of test cases for hypersonic turbulent boundary-layer theories and prediction techniques require experimental data over the full range of conditions for which such theories and techniques may be used. Such data should include independent measurements of skin friction, wall heat transfer, and two flow property distributions across the boundary layer (usually pitot pressure and stagnation temperature).

Although more than 50 studies of hypersonic boundary layers have been reported, it is still difficult to make satisfactory tests of theories and prediction techniques because researchers have not measured all four quantities listed above except in the studies reported in references 1 through 4. Furthermore, the data are even more limited at the higher hypersonic Mach numbers where density ratios across the boundary layer become very large. For example, the only published data above Mach number 15 appear to be those presented in references 4 through 8.

The present investigation was undertaken to augment available data by providing data on turbulent boundary layers with very high edge Mach numbers. The data include direct measurements of skin friction, wall heat-transfer rates, and mean and fluctuating measurements across the

boundary layer. The data obtained on the nozzle wall of the Ames M–50 helium tunnel cover a broad range of test conditions with measurements at five stations covering 85 percent of the nozzle length, wall temperature ratios varying from 0.35 to 1, and Reynolds numbers based on momentum thickness varying from 900 to 5600. The boundary layer thickness varied from 2.4 cm to 29 cm, and the nozzle exit radius was 36 cm.

EXPERIMENTAL PROCEDURES

Facility

Tests were conducted on the nozzle wall of the Ames M–50 helium tunnel, which is a blow-down tunnel with an axisymmetric contoured nozzel and an open test section (ref. 9). It uses helium (heated by an electrical resistance heater) as a test gas and operates at nominal exit Mach numbers of 42 to 47 for test times up to 20 min.

Figure 1 shows the five survey stations where pitot pressure, total temperature, and wall temperature were measured, together with the ten wall pressure stations. Wall heat transfer and skin friction were measured at the last four survey stations; the hot-wire surveys were made at the last two survey stations. The tunnel was operated at reservoir pressures ranging from 65 to 272 atm and total temperatures from 300° to 900° K.

Pressure Measurements

Primary pitot pressure surveys between x = 1.067 m and 3.56 m were obtained by traversing a single 0.476–cm–dia probe through the boundary layers. In addition a 0.159–cm–dia probe was used to check the effects of probe diameter on measured pitot pressure at these stations and to obtain survey data at x = 0.508 m.

Pressures were measured by a capacitance type transducer system similar to one described in reference 10. With this system, one transducer provides accurate readings over the full pressure range encountered in the boundary layer (0.004 to 0.14 atm). Errors in pressure resulting from nonlinearity and temperature effects on the transducer sensitivity were less than ±1 percent of the measured value. Additional errors due to variations in reference pressures were less than 4 percent of the minimum pressure measured.

No corrections were made for the various rarefaction effects on the pressure measurements. However, the possible variations attributable to these effects are summarized as follows. The effects of thermal transpiration errors due to temperature variations along the tube connecting the orifice and the transducer are negligible (refs. 11,12). Errors in wall pressure resulting from orifice effects due to heat transfer to the wall are less than 3 percent (ref. 13). Errors due to viscous interaction and rarefaction effects on the pitot pressure measurements are less than 4 percent for the outer region of the boundary layer (ref. 14). Near the wall, these effects may introduce larger errors; however, the the conclusions of this report do not depend on these data.

Stagnation Temperature Measurements

Stagnation temperatures were measured with a single shielded thermocouple probe (fig. 2) designed specifically to have low conduction losses at very low density flow conditions.

The probe was calibrated in the free-jet facility described in reference 15, which produced flows at Mach numbers ranging from 5 to 40 and flow densities comparable to those encountered in the boundary layer of the M-50 tunnel.

The probe calibration is shown in figure 3 where the data are correlated over a wide range of temperatures and pressures. These data could not be correlated solely on the basis of conduction error as proposed by Winkler (ref. 16). The present correlation parameters were derived using the assumption that radiation losses constituted the major source of error (appendix A).

Conduction effects probably cause some scatter in the data. Nevertheless, the correlation is reasonably good for a wide range of temperatures, and there is substantial agreement between data from the calibration in the free jet and the test points in the M-50, where differences in support temperatures should cause significant differences in the conduction effects.

Skin-Friction Measurements

Skin friction was measured using a floating element, magnetically nulling balance similar to the one described in reference 17. At each station, the elements were contoured to the local nozzle surface. The balance had an accuracy of ±2 percent.

The effects of floating element position, both above and below the surface, were investigated, and it was found that the measured skin friction was much less sensitive to the element position than has been observed previously at lower Mach numbers (refs. 18-20). Indeed, the indicated skin friction increased by only 10 percent when the element was raised 0.0075 cm above the surface, and no differences were observed when the element was recessed the same distance below the surface. The relative insensitivity of the data to element position is probably due to the combination of large boundary-layer thickness and low wall density.

Heat-Transfer Measurements

Wall heat transfer was determined from the steady-state heat conduction in a thin-skin gage contoured to the nozzle wall. The local temperatures were measured by chromel-constantan thermocouples spot-welded to the thin skin at the locations shown in figure 4.

Since the temperature variation between the center of the thin skin and the wall was small, relative to the driving potential,

$$\frac{(T_c - T_w)}{T_{0e} - T_w} \leqslant 0.06$$

constant heat transfer over the gage surface area was assumed. With this assumption, the equation governing the heat transfer in the gage is

$$Q_R = -2\pi Rkt\frac{dT}{dR} = \pi R^2 q$$

Solving for the temperature, one obtains

$$q = \left(\frac{T_c - T_R}{R^2}\right)4tk$$

In the present experiments, heat transfer rates corresponding to the temperature difference between the center and each of the other three thermocouples (fig. 4) were calculated and the results averaged to obtain the values presented in this paper. The individual measurements were generally within ±5 percent; however, in a few cases the variations were as high as ±10 percent.

Errors due to conduction down the thermocouple wires, convection from the back of the gage, and radiation losses have not been accounted for in the data reduction. However, conduction errors were held low by using small diameter wires, $d/t \leqslant 0.6$. Convection losses were held down by evacuating the back of the gage to pressures less than or equal to the local wall pressure; and radiation errors were not large, since the temperature difference between the gage surface and the surrounding radiative media was small ($T_c - T_w < 35°$ K). It is estimated that the combined error due to these effects is less than 5 percent. Basic instrument accuracy and the accuracy of the normalizing quantities (ρ, u, T_{aw}) also introduce error in the heat-transfer coefficient. Consequently, the overall accuracy of the heat-transfer coefficient is estimated to be about ±12 percent.

Boundary-Layer Fluctuation Measurements

The character of the fluctuations across the boundary layer at $x = 3.56$ m were obtained with a constant temperature anemometer system, which uses a water-cooled platinum film probe similar to the one described in reference 21. Water cooling permitted film operation at a temperature well below the free-stream total temperature. The upper frequency limit (−3dB) of the system, as determined by a standard square-wave technique, was found to be 60 kHz. Since the boundary layer is approximately 29 cm thick at the survey station, this frequency response makes it possible to measure fluctuations with a length scale down to one-eighth the boundary layer thickness. In light of the work by Kistler (ref. 22), over 90 percent of the energy should be contained within this frequency range. Mass flow and temperature fluctuation intensities were measured at $x = 2.793$ m using a constant temperature anemometer with a 0.00063-cm-dia by 0.317-cm-long platinum 10 percent iridium wire.

A preliminary calibration of the probe was made in the free-jet facility (see ref. 15). In this calibration, the voltage across the wire e_w was measured for various wire temperatures T_w, stream total temperatures T_o, and mass flows ρu. The measurements were then plotted against ρu and T_o for constant values of T_w and T_o or ρu. From the calibration it was found that

$$\left(\frac{\partial e_W{}^2}{\partial T_O}\right)_{\rho u,\ T_W} \quad \text{and} \quad \left(\frac{\partial e_W{}^2}{\partial \rho u}\right)_{T_O,\ T_W}$$

were approximately constant for the flow conditions of the present tests. This is consistent with the indication that for this diameter wire the flow would be essentially free molecular. The fluctuation levels were obtained at a number of points through the boundary layer using a technique similar to that of Kistler. The wire was operated at six different over–heat values and a least-squares parabolic fit of the data was made to the equation

$$(\Delta e)^2 = \left(\frac{\partial e}{\partial T_O}\right)^2 \overline{(\Delta T_O)^2} + \left(\frac{\partial e}{\partial \rho u}\right)^2 \overline{\Delta(\rho' u')^2} + 2\frac{\partial e}{\partial \rho u}\frac{\partial e}{\partial T_O}\ \overline{\Delta(\rho' u')\Delta T_O'}$$

where $\partial e/\partial T_O$ and $\partial e/\partial \rho u$ were obtained from the calibration.

RESULTS AND DISCUSSION

Throat Reynolds Number and Possible Relaminarization Effects

The effects of Reynolds number based on throat diameter and relaminarization due to favorable pressure gradient have been examined through comparisons with the work of Bach et al. (refs. 23,24). In figure 5 the relaminarization parameter K of Bach et al. is plotted against x. The data presented are for the throat region of the nozzle only; farther downstream the data continue the trend established here and should be of little importance.

Presented are the limiting cases for the present tests. For the high pressure limit (p_O = 270 atm) with a throat Reynolds number of 4.8 million and a maximum value of K of about 2.6×10^6, the work of Bach et al. indicates the flow should definitely be turbulent at the throat with no discernible effects of relaminarization. For the lower pressure limit (p_O = 65 atm), the throat Reynolds number of 0.5 million is on the borderline for turbulent flow (ref. 23), and the value of K is sufficiently high that a significant region of relaminarization might occur (ref. 24). However, if relaminarization does exist, its effects are not apparent in the data farther downstream as will be seen later.

In a hypersonic nozzle, the flow is similar to that shown in figure 6 (ref. 9). Downstream of the contour point there are two separate regions of flow: the boundary layer and the uniform core. In this situation, the density distribution is like the one most commonly associated with boundary layer flow – that is, the density decreases smoothly from a constant outer edge value to the wall value. Upstream of the contour point, however, there is a nonuniform flow region between the boundary layer and the uniform core. This region is one of expanding hypersonic flow with significant Mach number variations across it. These Mach number variations cause inviscid density variations similar to those shown schematically in figure 7. In this situation, viscous effects act on a variable density inviscid flow field, rather than on the more common constant density flow field. The resulting density distribution is similar to that indicated by the dashed line in figure 7.

For nozzle flows, the inviscid density variation has not usually been considered, and the edge of the boundary layer has been defined as the point where density (or pitot pressure) is maximum. However, from figure 7, it is apparent that the maximum density can occur a significant distance from the point where density first deviates from the inviscid variation – that is, where viscous effects are first encountered. For most hypersonic nozzles, surveys are taken at or ahead of the contour point; thus, this variation would be typical of much of the nozzle wall data.

In the present tests two measurements have substantiated the above model. First, total temperature measurements indicated the existence of temperature and velocity gradients farther from the wall than the maximum density point. Second, hot wire surveys indicated the existence of strong intermittencies in the same area. Consequently, for the present tests the edge of the boundary layer was determined by using stagnation temperature, which is constant in the inviscid flow irrespective of variation in local Mach number. The data were plotted, a straight line was faired through the free-stream values, and a curve was fitted to the remaining data. The point of juncture between the straight line and the faired curve was taken as the edge of the boundary layer.

Temperature Pressure Variations Along Nozzle

Figure 8 shows typical temperature and pressure distributions measured on the nozzle wall and static pressure distributions for the outer edge of boundary layer. The static pressure was calculated from pitot pressure and reservoir pressure measurements assuming isentropic flow. The values are for nominal reservoir temperatures of 500° and 900° K. The nozzle has a hot throat, which is at very nearly recovery temperature during the tests. However, as can be seen, the temperature drops off rapidly with distance down the nozzle, so that even for the higher temperature conditions the wall temperature is nearly room temperature at all survey stations.

The reservoir temperature has no measurable effect on either the wall pressure or the free-stream static pressure. However, there is a marked difference between these pressures, indicating the existence of a pressure gradient across the boundary layer. This pressure difference appears to correlate with edge Mach number as shown in figure 9. Furthermore, from data of other investigations presented in figure 9, it appears that this phenomenon is not limited strictly to nozzle wall type flows.

The main reason for the high pressure ratios at the higher Mach numbers in figure 9 appears to be the relatively low value of p_e at these Mach numbers. If the pressure differences $p_w - p_e$ are normalized using the edge dynamic pressure $1/2\, \rho_e u_e^2$, the resulting ratios vary from about 1×10^{-2} at the lower Mach numbers to about 1×10^{-3} at the higher Mach numbers. Thus, although the pressure differences at the higher Mach numbers are very large relative to the static pressure, they are still small relative to dynamic pressure. An order-of-magnitude analysis of the time-averaged Navier-Stokes equations indicates that, as in the case of lower Mach numbers, the y momentum is small relative to the x momentum. So from this point of view, the y momentum equation need not be considered in the solution of the problem. However, the large relative pressure variations result in large density variations. Since density is involved directly in the continuity, x momentum, and energy equations, some way of accounting for these density variations is needed. Thus, it may be necessary to include the y momentum equation to properly describe the density variations in high Mach number flows.

Profile Measurements

The measured pitot pressure and uncorrected stagnation temperature for the five survey stations are presented in tables 1 through 5 with a representative plot presented in figure 10. The probe was traversed from near the wall to the free stream and back to the wall, with data being obtained going both directions. As can be seen, the repeatability of the pressure data was excellent; however, the temperature data show some hysteresis effects particularly in the region where low pressures exist. Since the hysteresis is undoubtedly due to the variations in support temperature, fairings of the data were weighted toward the measurements made on the outward traverse at the lower temperature ratios near the wall, and toward measurements on the inward traverse for higher temperature ratios farther from the wall. This procedure gives velocity values that vary as much as 5 percent from the value given by unweighted fairing; however, it is believed to be more accurate since it should minimize the effects of conduction losses into the supports.

Also shown on the temperature curve is the wall temperature slope as determined from heat-transfer measurements. As can be seen, within the accuracy of the data, the slope agrees with measured temperature profile. However, it is apparent that accurate determinations of the heat transfer from the temperature data alone would be very difficult.

Velocity and Density Profiles

Velocity and density profiles calculated using faired values from the pitot pressure and corrected stagnation temperature profiles are given in tables 6 to 10; table 11 is a summary of the more pertinent parameters associated with the data. In these tables, corrections have been made for real-gas effects (ref. 25). The reservoir pressure stated is that associated with the pitot pressure survey, and the total temperature is that associated with the temperature surveys. The viscosity law used in formulating some of the parameters was that of Akin (ref. 26). In some cases, there are differences between reservoir pressure and/or temperature for the pressure surveys and the corresponding values for the temperature survey. However, it will be shown later that the cross coupling between temperature and pressure is small; therefore, these differences should not significantly alter the accuracy of the data. The calculations for tables 6 through 10 required an assumption on static pressure p. Three possible assumptions were examined: $p = p_w$, $p = p_e$ and $p = p_w - (p_w - p_e)\, y/\delta$. Figure 11 shows typical velocity and density profiles resulting from each of the assumptions. As can be seen, the assumption $p = p_e$ results in a value for u/u_e near the wall that is too high. The other two assumptions, however, show little difference in either velocity or density ratio, thus it makes little difference which of these two assumptions are used. In this paper, the linear variation is used because it provides more accurate absolute values for pressure ratio and Mach number near the outer edge of the boundary layer. This assumption is not exact, but barring large excursions in p – values much larger than p_w or much smaller than p_e—it should not substantially affect the conclusions of this paper.

From figure 11, it appears that the boundary layer has a relatively thick inner region with linear velocity variations typical of those occurring in a viscous sublayer. In this region, the density is nearly constant. The outer region has small velocity variations and fairly full density profiles typical of profiles normally associated with a turbulent boundary layer. Furthermore, skin friction measurements suggest a velocity slope at the wall that is in reasonable agreement with the measured velocity profile. The deviation of velocity very near the wall is probably the result of either

wall-probe interference effects or rarefaction effects on the pitot probe. The data at $x = 3.56$ apparently have some end effects due to the close proximity of the open test section at $x = 3.61$, which affect the flow near the wall. Because of these effects these data are not included in the following discussions.

Effects of Wall Temperature Ratio

Stagnation temperature and pitot pressure variations across the boundary layer are shown in figure 12 for various wall temperature ratios T_w/T_{O_e}. Differences in T_w/T_{O_e} were obtained by varying the free-stream total temperature. These surveys were obtained at $x = 1.067$ where the edge Mach number was sufficiently low that wall temperature ratios near unity could be obtained without liquefaction problems.

For $T_w/T_{O_e} = 0.98$ there is an overshoot in the total temperature near the outer edge of the viscous sublayer ($y/\delta \approx 0.2$). Farther from the wall, the temperature drops to a value lower than $T_w (y/\delta \approx 0.4)$ and then rises uniformly to T_{O_e} at the edge of the boundary layer. The overshoot in total temperature is similar to that previously observed at wall temperature ratios close to unity and is attributed to viscous dissipation. It is of interest to note that in the present investigation these effects persist to much lower wall temperatures and cause some perturbation of the profile for values of T_w/T_{O_e} as low as 0.535.

Another point of interest is that in the outer region of the boundary layer there are essentially no significant differences in temperature or pressure profiles for a wide range of wall temperature ratios.

The effect of variation in temperature on computed velocity, density, and Mach number profiles is shown in figure 13. As might be expected from the variations in temperature and pressure, the temperature ratio affects the thickness of the viscous sublayer – the thickness increases as wall temperature ratio is decreased – but it has little effect on the computed values in the outer region of the boundary layer.

From figure 13(c), it is apparent that most of the boundary layer is hypersonic. For the probe measurements, one may obtain the energy relationship

$$\left(\frac{u}{u_e}\right)^2 \doteq \frac{M^2 \left\{ 1 + [(\gamma - 1)/2]\, M_e^2 \right\}}{M_e^2 \left\{ 1 + [(\gamma - 1)/2]\, M^2 \right\}} \frac{T_O}{T_{O_e}}$$

The hypersonic approximation $(M >> 1)$ to this relationship gives

$$\left(\frac{u}{u_e}\right)^2 \approx \frac{T_O}{T_{O_e}}$$

From this approximation

$$\frac{T_O - T_w}{T_{O_e} - T_w} = \frac{(u/u_e)^2 - (T_w/T_{O_e})}{1 - (T_w/T_{O_e})}$$

Examination of this equation (referred to hereafter as the "hypersonic approximation") reveals that as T_w/T_{Oe} approaches zero, the functional relationship between $(T_O - T_w)/(T_{Oe} - T_w)$ and u/u_e for the hypersonic portion of the boundary layer approaches the quadratic relationship recently noted by a number of investigators. However, if T_w/T_{Oe} is greater than zero the value of the temperature relationship will fall below the quadratic. Thus, it appears that as edge Mach number is increased, conditions may be encountered in the outer region of the boundary layer for flows on all types of bodies where the temperature-velocity relationship could vary substantially from the familiar Crocco (linear) relationship. Consequently, the recently observed deviation from a Crocco velocity-temperature relationship may not be strictly a pressure gradient phenomenon as has been suggested (refs. 27–28), but simply may be more evident in nozzle flows where the edge Mach number is generally higher and where the existence of a pressure gradient tends to augment the differences. Softley and Sullivan (ref. 29) have obtained data on a cone at M = 10.2 that agree very well with the hypersonic approximation. Furthermore the existence of hypersonic effects may explain why the data of Jones and Feller (ref. 27) show very little tendency to "relax" to the linear profile for as much as 100 boundary layer thicknesses downstream of the end of the nozzle.

Figure 14 replots data for two wall temperature ratios, 0.72 and 0.36 (fig. 12), on familiar Crocco energy type plots. Curves are given for the Crocco relationship, a quadratic relationship, and the hypersonic approximation just discussed. Excellent agreement is apparent between the data and the hypersonic approximation in the outer region of the boundary layer. Although this region appears small on this type of plot, the hypersonic data cover 60 to 75 percent of the boundary-layer thickness. In the viscous sublayer region the temperature-velocity relationship shows marked differences for the two temperature ratios presented in figure 14. The relationship for the higher wall temperature ratio is complicated by the temperature overshoot in the sublayer. The lower wall temperature data show a much simpler behavior. However, in either case it is evident that the temperature-velocity relationship is more complex than either the Crocco or the quadratic relationship indicates.

References 27 and 30, indicate that the velocity variation near the wall may be linear, even though the variation in the outer region is significantly different. The earlier discussion of the velocity profiles indicated that the measured u/u_e may be high in the region near the wall; thus, it appears that the present data is in basic agreement with this indication.

Effects of Nozzle Station

Typical variations in velocity, density, and Mach number profiles with nozzle station are shown in figure 15. It is apparent that there are significant changes with nozzle station. For the velocity profile, the effect seems to be limited to the sublayer region, with the relative thickness of the sublayer increasing with distance from the nozzle throat. This increase in sublayer thickness is probably associated with the increase in Mach number or, more exactly, the accompanying decrease in wall density (appendix B). The density and Mach number profiles show differences throughout the boundary layer, but most of these differences are probably associated with adjustments required to account for the changes in relative thickness in the sublayer.

Effects of Reservoir Pressure

Typical variations in velocity, density and Mach number profile with reservoir pressure are shown in figure 16. Again, all differences seem to be associated with changes in the sublayer thickness. In this case, the sublayer is relatively thicker at lower pressures.

Correlations of the Velocity Profile

A correlation of the velocity profiles using measured wall density and shear stress in law-of-the-wall parameters is presented in figure 17. The four cases shown are typical of the results for all cases and represent considerable ranges in tunnel pressure, temperature, and station. It can be seen that in the viscous sublayer the data are in excellent agreement with incompressible correlation values (ref. 31). However, above $y^+ = 10$, the data do not agree with the incompressible correlation. For this region, changes in pressure and station affect the y^+ value at the edge of the boundary layer, while changes in total temperature affect the relative level of u^+.

Correlations of the present data using the transformations of Coles (ref. 32) and Van Driest (ref. 33) are shown in figures 18 and 19. Coles' transformation stretches the y variable using a function of the density variation across the boundary layer. As can be seen, with this transformation, the data retain the approximate agreement with the incompressible profile in the viscous sublayer, while in the logarithmic region, the y variable is stretched to values comparable to those obtained in incompressible flows. Although this transformation seems to stretch the y^+ variable to proper proportions, it does not provide the changes in slope in the logarithmic region of the boundary layer required for complete agreement with incompressible data. It appears that the need for a slope change requires an operation on the velocity variable. Consequently, it is doubtful that other transformations that operate only on the y variable (refs. 34–36) will be successful in transforming the hypersonic turbulent boundary layer to the incompressible plane.

The transformation of Van Driest (ref. 33), which operates only on the u, variable, appears to be very successful in obtaining a consistent correlation of the data (fig. 19). Two ways of applying the Van Driest transformation are shown in figure 19. The first uses the measured density profile to compute u^+, while the second uses equation (54) from reference 33 to compute u^+. This equation was obtained assuming a Crocco temperature-velocity relationship. As indicated previously, the Crocco relationship is somewhat different than the measured temperature-velocity relationship. Therefore, the substantial agreement of both curves indicates that at least for the present conditions this transformation is not strongly affected by the assumed temperature-velocity relationship. In general, the transformation provides reasonable agreement between the present data and incompressible data. However, the present data terminate at lower y^+ values.

Velocity defect correlations using the Van Driest transformation on the data are shown in figure 20. The data below $y/\delta = 0.5$ are in the viscous sublayer, and, as might be expected, they are not correlated well. In the outer region, however, where flow conditions meet the requirements for correlation using the velocity defect law, the data agree very well with the incompressible correlation, indicating that the mixing length concept may be applicable to very high Mach number flows.

From the law of the wall correlations, it appears that the viscous sublayer thickness is adjusting very rapidly to the local density changes. Consequently, the sublayer is growing with distance down the nozzle. However, it is possible that the high Mach number of the outer, turbulent region of the boundary layer may restrict the rate of growth of turbulent bursts. As a consequence, the relationship between the sublayer thickness and the turbulent layer thickness may be affected. It appears from figure 21 that if such effects occur they are correlated by variations in M_e and R_θ. Figure 21 is basically the same as figure 19 of reference 37, except that additional data from tests on flat plates and cylinders have been added. This figure also shows that the relationship between δ_L/δ and $M_e/\sqrt{R_\theta}$, is the same for flat plates and cylinders, where there are no pressure gradient effects, as it is for nozzle walls where such effects may be present. This suggests that locally applied theories, developed for use with flat plates, which obtain their solution from M_e and R_θ , may provide reasonable agreement with values obtained on nozzle walls.

Wall Measurements

Measured recovery factor– The recovery factor for the present tests was determined by intermittently reading the heat-transfer rate as the reservoir temperature was slowly varied from room temperature to about twice room temperature and back again. The heat transfer versus temperature ratio was then plotted and the recovery factor taken as the temperature for which q is zero. The recovery factor determined by this procedure is about 0.8. This factor is somewhat lower than the 0.9 values previously measured at lower Mach numbers (ref. 38); in fact, it is near the value for laminar boundary layers. The reasons for this value are not understood, but they are probably associated with the fact that, as discussed later, the viscous sublayer is so thick that large turbulent fluctuations never reach the wall.

Skin-friction and heat-transfer measurements– Figure 22 shows the skin-friction and heat-transfer variations with R_θ for the different data stations. The variation with R_θ for each data station is approximately the 1/4 power relationship normally associated with a turbulent boundary layer. However, there is a marked difference in level of the coefficients at the various data stations, primiarily because of Mach number variations as shown in figure 23, where data with R_θ between 2000 and 3500 are plotted against Mach number. It is apparent that both skin friction (fig. 23(a)) and heat transfer (fig. 23(b)) show variations that agree in general with trends indicated by previous investigations at lower Mach numbers. In figure 23(a), the skin-friction data are also compared with values obtained from five commonly used turbulent skin-friction prediction techniques (refs. 32, 33, 39–41) and for reference purposes with the value predicted by the T' method (ref. 42) for laminar boundary layers. (The program used to make these comparisons is that developed by Hopkins and Inouye (ref. 43).) The turbulent prediction techniques were developed at lower Mach numbers (up to Mach number 10) for flows with no normal pressure gradient, and in this region the agreement with the data is reasonable. However, at the higher Mach numbers there is a very wide dispersion in the predicted values with most of the predictions being much lower than the data. Only the Van Driest *I* prediction technique (ref. 33) give a value that is close to the data. This might be expected, since this technique also provides a good transformation of the velocity profile data into the incompressible plane.

The reasons for the disagreements between data and theory are not fully understood at the present time; however, some of the more obvious possibilities are discussed here. First, the existence

of pressure gradients may introduce some disagreement between the data and the various predictions. However, there are two indications that this may not be so. The first is the close relationship between R_θ and the relative sublayer thickness as discussed previously. The second is shown in figure 24 by the comparisons between data and theory. The present data and those of reference 8 were obtained over a wide range of pressure gradients, and although both sets of data are somewhat higher than the predicted values, neither set shows trends associated with the variations in pressure gradient. Second, the actual temperature profiles differ from the Crocco profiles used in the theories. However, in the critical region near the wall, the temperature gradients appear to be nearly Crocco; therefore, the skin friction may not be strongly affected by the differences in temperature. Third, the transformed R_θ values are somewhat lower than any R_θ (fig. 24). Thus the value for incompressible flow at these R_θ is not known directly but can be obtained only from extrapolation of available incompressible data; such extrapolations, of course, could be in error.

Reynolds analogy factors $2C_H/C_f$ determined from the measured skin friction and heat transfer data are shown in figure 25. It is apparent that the Reynolds analogy factors are somewhat below the values measured by prior investigators at lower Mach numbers. The reasons for this are not clear at the present time. However, there is a tendency for the Reynolds analogy factor to decrease at the lower R_θ (fig. 25(a)) and at the higher Mach numbers (fig. 25(b)).

Figure 26 shows the variation of C_f, C_H, and $2C_H/C_f$ with wall temperature ratio. The open symbols are the data as measured, and the filled symbols represent data adjusted to a constant R_θ (equal to 3786) by means of the 1/4 power relationship between R_θ and C_f and C_H. It is apparent that all three coefficients C_f, C_H, and $2C_H/C_f$ vary with wall temperature with the value of the coefficients increasing as wall temperature ratio decreases.

Boundary-Layer Fluctuations

Figure 27 shows oscilloscope traces indicating the fluctuations in heat transfer to the cooled film probe. Of interest here is the intermittency at both the outer edge of the boundary layer and the edge of the viscous sublayer. The inner intermittency is similar to that reported by Corrsin (ref. 44) in incompressible flow and is as predominant as that at the outer edge of the boundary layer. The existence of this intermittency is not really surprising since such regions are common at turbulent boundaries. It is apparent that turbulence is being dissipated in the viscous sublayer, and it is unlikely that large fluctuations ever reach the wall – probably because of the large thickness of the sublayer.

The magnitude of the mass flow and temperature fluctuations are shown in figures 28 and 29. Figure 28(a), where the mass flow fluctuations are normalized by local mean mass flow, shows a variation similar to that reported in reference 2. Very large amplitude fluctuations on the order of 80 percent are observed near the edge of the viscous sublayer. (These fluctuations are sufficiently large that the linear assumptions used in deriving the equation for the data reduction may be violated. As a result, the magnitude of the fluctuations near the edge of the viscous sublayer may be different from those presented in this report. However, it is unlikely that the difference would be sufficiently large to alter the conclusions drawn from these data.) This type of plot gives the false impression that fluctuation amplitude is increasing as the edge of the sublayer is approached, when in fact there is a decrease in the amplitude as shown in figure 28(b), where the edge value of mass flow is used as the normalizing factor. The data show a maximum of around 15 percent at $y/\delta \simeq 0.8$ with consistent decrease from this point to the wall. Thus, the main reason for the large

relative amplitude of fluctuations is the small local mean mass flow near the edge of the viscous sublayer. From figure 29 it is apparent that the temperature fluctuations are nearly constant over the outer 70 percent of the boundary layer at a value between 1 percent and 2 percent, probably as a result of the very low temperature gradient throughout most of the turbulent region.

Flow Model

The present results suggest that a possible flow model for the origin and development of hypersonic turbulent boundary layers is that presented in figure 30. This model is essentially the same as the one presented by Maddalon and Henderson (ref. 45), except for the intermittent region near the outer edge of the viscous sublayer and the relative extent of each region. The main features incorporated into this model are: (1) breakdown to turbulence originates near the outer edge of the laminar boundary layer at hypersonic speeds (refs. 45–47); (2) the rate of growth of the turbulent bursts normal to the wall is restricted by high Mach number; (3) the viscous sublayer thickens with increasing Mach number due to the associated decreases in wall density; and (4) the existence of an intermittent region between the viscous sublayer, and the turbulent region, and at the outer edge of the boundary layer.

SUMMARY OF RESULTS

The nozzle wall boundary layer of the Ames M–50 helium tunnel has been thoroughly investigated with pitot pressure, total temperature, skin-friction, and wall heat-transfer measurements at five stations covering 85 percent of the nozzle length, and hot wire measurements at two stations near the exit of the nozzle. The resulting set of data is sufficiently complete and redundant that it should provide satisfactory tests of most available theories and prediction techniques.

In general, tests results are as follows:

1. The velocity and density profiles, the skin friction and heat transfer variations with R_θ, and the hot-wire measurements all indicate that the boundary layer is turbulent with a thick viscous sublayer.

2. The sublayer thickness, skin friction, and heat transfer vary substantially with nozzle position, and these variations were shown to be consistent with Mach number and Reynolds number trends previously observed in turbulent boundary layers at lower Mach numbers.

3. Observed pressure differences across the boundary layer were large relative to the static pressure but small relative to the dynamic pressure. In connection with these pressure differences, it was determined that the y momentum is still small relative to the x momentum. However, the variations in density caused by the pressure variations may be sufficiently large to affect the x momentum equation, and therefore they should be considered in theories applicable to high Mach number flows.

4. The temperature-velocity relationship in the outer region of the boundary layer was found to be accurately predicted by the hypersonic approximation obtained from a local energy relationship rather than either the Crocco or quadratic relationship more commonly associated with turbulent boundary layers.

5. Mass flow fluctuations were found to be as large as 80 percent of the local mean mass flow near the edge of the viscous sublayer with the maximum value relative to the edge mass flow being about 15 percent at $y/\delta \approx 0.8$.

Ames Research Center
National Aeronautics and Space Administration
Moffett Field, Calif., 94035, March 24, 1972

APPENDIX A

DERIVATION OF PARAMETERS USED TO CORRELATE TOTAL-TEMPERATURE-PROBE CALIBRATION DATA

If it is assumed that radiation losses are the major source of error and that the conduction losses can be neglected, then the relationship for determining recover factor of the probe is

$$rf = f\left(\frac{h}{To^4}\right)$$

where

$$h = \frac{k}{D} Nu_W$$

Furthermore, since the wire diameter is very small and the densities very low, it is reasonable to assume that the Nusselt number variation may be approximated by the free molecular value

$$Nu_W \propto R_W$$

For helium

$$R_W \approx \rho_W To^{-0.147} D$$

and

$$k \propto To^{0.647}$$

thus

$$\frac{h}{To^4} \propto \frac{\rho_W{}^{3.5}}{To} \propto \frac{p_2}{To^{4.5}}$$

or

$$rf = f\frac{p_2}{To^{4.5}}$$

APPENDIX B

EFFECT OF DENSITY ON SUBLAYER THICKNESS

To demonstrate the effect of density on the thickness of the sublayer one can take y^+ from the correlations in figures 17 and 19 and the definition for shear stress $\tau_w = \mu_w(\partial u/\partial y)_w \approx \mu_w(u_L/\delta_L)$, and arrive at the following relation for the laminar sublayer thickness

$$\delta_L = \frac{\mu_w}{\rho_w u_L} \text{const}$$

With the additional assumption $u_L \approx u_e$ (an assumption that gives only a first-order approximation but appears to be more accurate at higher Mach numbers), one obtains

$$\delta_L = \frac{\mu_w}{\rho_w u_e} \text{const}$$

It becomes apparent that for constant u_e and T_w, δ_L is primarily affected by the density and may become very large if the density is sufficiently low. Furthermore, in constant pressure and temperature flows the viscous sublayer will be of nearly constant thickness.

REFERENCES

1. Lee, Roland E.; Yanta, William J.; and Leonas, A. C.: Velocity Profile Skin Friction Balance and Heat Transfer Measurements of the Turbulent Layer at Mach 5. Proc. 1968 Heat Transfer and Fluid Mechanics Institute, Univ. of Washington, Seattle, Washington, June 17-18, 1968, Stanford Univ. Press, 1968, pp. 3-17.

2. Wallace, J. E.: Hypersonic Turbulent Boundary Layer Measurments Using an Electron Beam. Rep. AN-2112-Y-1, Cornell Aero. Lab., Buffalo, N.Y., Aug. 1968, NASA CR-96612.

3. Hopkins, Edward J.; Rubesin, Morris W.; Inouye, Mamoru; Keener, Earl; Mateer, George C.; Polek, Thomas E.: Summary and Correlation of Skin Friction and Heat Transfer Data for a Hypersonic Turbulent Boundary Layer on Simple Shapes. NASA SP-216, 1969, pp. 319-344.

4. Kemp, Joseph H., Jr.; and Owen, F. K.: Nozzle Wall Boundary Layers at Mach Numbers 20 to 47. AIAA Paper 71-161, 1971.

5. Bertram, M. H.; and Neal, L., Jr.: Recent Experiments in Hypersonic Turbulent Boundary Layers. NASA TM X-56,335, 1965.

6. Burke, A. F.: Turbulent Boundary Layers on Highly Cooled Surfaces at High Mach Numbers. Rep. 118, Cornell Aero. Lab., Buffalo, N.Y., Nov. 1961.

7. Kemp, J. H., Jr.; and Sreekanth, A. K.: Preliminary Results From an Experimental Investigation of Nozzle Wall Boundary Layer at Mach Numbers Ranging from 27 to 47. AIAA Paper 69-686, 1969.

8. Fischer, Michel C.; Maddalon, Dal V.; Weinstein, Leonard M.; and Wagner, Richard D., Jr.: Boundary-Layer Surveys on a Nozzle Wall at $M_\infty \approx 20$ Including Hot-Wire Fluctuation Measurements. AIAA Paper 70-746, 1970.

9. Kemp, J. H., Jr.: The Ames M-50 Helium Tunnel. NASA TN D-5788, 1970.

10. Thurtell, G. W.; and Tanner, C. B.: Momentum Transport Measurement in the Atmospheric Surface Layer With the Anemoclinometer. Final Rep. 1962-65, Dept. of Soil Science, Univ. of Wisconsin, 1965.

11. Arney, G. D., Jr.; and Bailey, A. B.: An Investigation of the Equilibrium Pressure Along Unequally Heated Tubes. AEDC-TDR-62-26, Feb. 1962.

12. Arney, G. D., Jr.; and Bailey, A. B.: Investigation of Equilibrium Pressures Along Unequally Heated Tubes, Addendum. AEDC-TDR-62-188, Oct. 1962.

13. Potter, J. L.; Kinslow, M.; and Boylan, D. E.: An Influence of the Orifice on Measured Pressures in Rarefied Flow. AEDC-TDR-64-175, Sept. 1964.

14. Potter, J. L.; and Bailey, A. B.: Pressures in the Stagnation Regions of Blunt Bodies in the Viscous-Layer to Merged-Layer Regimes of Rarefied Flow. AEDC-TDR-63-168, Sept. 1963.

15. Horstman, C. C.: Surface Pressures and Shock-Wave Shapes on Sharp Plates and Wedges in Low Density Hypersonic Flow. Proc. 6th International Symposium on Rarefied Gas Dynamics, Vol. 1, New York, Academic Press, Inc., 1969, pp. 593-605.

16. Winkler, E. M.: Stagnation Temperature Probes for Use at High Supersonic Speeds and Elevated Temperatures. NAVORD Rep. 3834, Oct. 1954.

17. Spangler, J. E.: A Sensitive Magnetic Balance for the Direct Measurement of Skin Friction Drag. LTV Rep. 0-71000/3R-39, Dec. 1963.

18. Coles, D.: Measurements in the Boundary Layer on a Smooth Flat Plate in Supersonic Flow. Ph.D. Thesis, Calif. Inst. of Tech., 1953.

19. Dhawan, Satish: Direct Measurements of Skin Friction. NACA Rep. 1121, 1953.

20. Fenter, Felix W.: Analyses and Direct Measurement of the Skin Friction of Uniformly Rough Surfaces at Supersonic Speeds. IAS Preprint 837, July 1958.

21. McCroskey, William J.: An Experimental Model for the Sharp Leading Edge Problem in Rarefied Hypersonic Flow. Ph.D. Thesis, Princeton Univ., Jan. 1966.

22. Kistler, Alan L.: Fluctuation Measurements in a Supersonic Turbulent Boundary Layer. Phys. Fluids, vol. 2, no. 3, May-June 1959, pp. 290-296.

23. Bach, L. H.; Massier, P. F.; and Cuffel, R. F.: Some Observations on Reduction of Turbulent Boundary-Layer Heat Transfer in Nozzles. AIAA, J., vol. 4, no. 12, Dec. 1966, pp. 2226-2229.

24. Bach, L. H.; Cuffel, R. F.; and Massier, P. F.: Laminarization of a Turbulent Boundary Layer in Nozzle Flow. AIAA J., vol. 7, no. 4, April 1969, pp. 730-733.

25. Erickson, Wayne D.: An Extension of Estimated Hypersonic Flow Parameters for Helium as a Real Gas. NASA TN D-1632, 1963.

26. Akin, S. W.: The Thermodynamic Properties of Helium. Trans. ASME, vol. 72, no. 6, Aug. 1950, pp. 751-757.

27. Jones, Robert A.; and Feller, William J.: Preliminary Surveys of the Wall Boundary Layer in a Mach 6 Axisymmetric Tunnel. NASA TN D-5620, 1970.

28. Bushnell, Dennis M.; Johnson, Charles B.; Harvey, William D.; and Feller, William V.: Comparison of Prediction Methods and Studies of Relaxation in Hypersonic Turbulent Boundary Layers. NASA SP-216, 1969, pp. 345-376.

29. Softley, Eric J.; and Sullivan, Robert J.: Theory and Experiment for the Structure of Some Hypersonic Boundary Layers. AGARD CP-30, May 1968, pp. 3-1-3-18.

30. Fiore, Anthony W.: Turbulent Boundary Layer Measurements at Hypersonic Mach Numbers. ARL 70-0166, 1970.

31. Coles, D. E.: Measurements in the Boundary Layer on a Smooth Flat Plate in Hypersonic Flow. III Measurements in a Flat Plate Boundary Layer at the Jet Propulsion Laboratory. JPL Rep. 20-71, 1953.

32. Coles, Donald: The Turbulent Boundary Layer in a Compressible Fluid. Phys. Fluids, vol. 7, no. 9, Sept. 1964, pp. 1403-1423.

33. Van Driest, E. R.: Turbulent Boundary Layers in Compressible Fluid. J. Aero. Sci., vol. 18, no. 3, March 1951, pp. 145-160, 216.

34. Mager, Artur: Transformation of the Compressible Turbulent Boundary Layer. J. Aero. Sci., vol. 25, no. 5, May 1958, pp. 305-311.

35. Baronti, Paslo O.; and Libby, Paul A.: Velocity Profile in Turbulent Compressible Boundary Layers. AIAA J., vol. 4, no. 2, Feb. 1966, pp. 193-202.

36. Laufer, John: Turbulent Shear Flows of Variable Density. AIAA J., vol. 7, no. 4, April 1969, pp. 706-713.

37. Beckwith, I. E.; Harvey, W. D.; and Clark, F. L.: Comparisons of Turbulent Boundary-Layer Measurements at Mach Number 19.5 With Theory and an Assessment of Probe Errors. NASA TN D-6192, 1971.

38. Rudy, David H.; and Weinstein, Leonard M.: Investigation of Turbulent Recovery Factor in Hypersonic Flow. AIAA J., vol. 8, no. 12, Dec. 1970, pp. 2286-2287.

39. Sommer, Simon C.; and Short, Barbara J.: An Experimental Study of Nozzle Wall Boundary Layers at Mach Numbers 20 to 47. NACA TN 3391, 1955 (also J. Aero. Sci., vol. 23, no. 6, June 1956, pp. 536-42).

40. Spalding, D. B.; and Chi, S. W.: The Drag of a Compressible Turbulent Boundary Layer on a Smooth Flat Plate With and Without Heat Transfer. J. Fluid Mech., vol. 18, pt. 1, Jan. 1964, pp. 117-143.

41. Van Driest, E. R.: Problem of Aerodynamic Heating. Aero Aspects Session, Nat'l Summer Meeting IAS, Los Angeles, 1956 (also Aeron. Engr. Rev., vol. 15, no. 10, Oct. 1956, pp. 26-41).

42. Rubesin, Morris W.; and Johnson, H. A.: A Critical Review of Skin Friction and Heat Transfer Solutions of the Laminar Boundary Layer of a Flat Plate. Trans. ASME 71, no. 4, 1949, 383-388.

43. Hopkins, E. J.; and Inouye, M.: An Evaluation of Theories for Predicting Turbulent Skin Friction and Heat Transfer on Flat Plates at Supersonic and Hypersonic Mach Numbers. AIAA J., vol. 9, no. 6, June 1971, pp. 993–1003.

44. Corrsin, S.: Some Current Problems in Turbulent Shear Flow. Proc. First Symp. Naval Hydrology, Nat. Acad. Sci., 1951.

45. Maddalon, D. V.; and Henderson, A., Jr.: Boundary-Layer Transition on Sharp Cones at Hypersonic Mach Numbers. AIAA J., vol. 6, no. 3, March 1968, pp. 424–431.

46. Nagamatsu, H. T.; Graber, B. C.; and Sheer, R. E.: Critical Layer Concept Relative to Hypersonic Boundary Layer Stability. GE Rep. 66-C-192, 1966.

47. Owen, F. K.: Fluctuation and Transition Measurements in Compressible Boundary Layers. AIAA Paper 70-745, 1970.

48. Scaggs, N. E.: Boundary Layer Profile Measurements in Hypersonic Nozzles. USAF ARL 66-0141, Aerospace Res. Lab., July 1966.

49. Speaker, W. V.; and Ailman, C. M.: Spectra and Space Time Correlations of the Fluctuating Pressures at a Wall Beneath a Supersonic Turbulent Boundary Layer Perturbed by Steps and Shock Waves. NASA CR-486, 1966.

50. Wagner, R. D., Jr.; Maddalon, D. V.; Weinstein, L. M.; and Henderson, A., Jr.: Influence of Measured Free-Stream Disturbances on Hypersonic Boundary Layer Transition. AIAA Paper 69-704, June 1969.

51. Matting, Fred W.; Chapman, Dean R.; Nyholm, Jack R.; and Thomas Andrew G.: Turbulent Skin Friction at High Mach Numbers and Reynolds Numbers in Air and Helium. NASA TR R-82, 1961.

52. Watson, Ralph D.; and Cary, Aubrey M., Jr.: The Transformation of Hypersonic Turbulent Boundary Layers to Incompressible Form. AIAA J. (Tech. Notes), vol. 5, no. 6, June 1967, pp. 1202-1203.

53. Shall, Paul Joseph, Jr.: A Boundary Layer Study on Hypersonic Nozzles. MS Thesis, U.S. Air Force Inst. Tech., March 1968. (Available from DDC as AD, 833 236.)

54. Perry, J. H.; and East, R. A.: Experimental Measurements of Cold Wall Turbulent Hypersonic Boundary Layers. AASU-275, Univ. Southampton, Feb. 1968.

55. Hill, F. K.: Turbulent Boundary Layer Measurements at Mach Numbers from 8 to 10. Phys. Fluids, vol. 2, no. 6, Nov. – Dec. 1959, pp. 668-680.

56. Lobbe, R. Kenneth; Winkler, Eva M.; and Persh, Jerome: Experimental Investigation of Turbulent Boundary Layers in Hypersonic Flow. J. Aero. Sci., vol. 22, no. 1, Jan. 1955, pp. 1-10.

57. Winkler, E. M.; and Cha, M. H.: Investigation of Flat Plate Hypersonic Turbulent Boundary Layers with Heat Transfer at a Mach Number of 5.2. NAVORD Rep. 6631, Sept. 1959.

58. Samuels, R. D.; Peterson, J. B., Jr.; and Adcock, J. B.: Experimental Investigation of the Turbulent Boundary Layer at a Mach Number of 6 with Heat Transfer at High Reynolds Numbers. NASA TN D-3858, 1967.

59. Owen, F. K.; and Horstman, C. C.: A Study of Turbulence Generation in a Hypersonic Boundary Layer. AIAA Paper 72-182, 1972.

60. Stalmach, Charles J., Jr.: Experimental Investigation of the Surface Impact Probe Method of Measuring Local Skin Friction at Supersonic Speeds. DRL-410 CF 2675, Univ. of Texas Research Lab., Austin, Texas, Jan. 1958.

TABLE 1. – MEASURED PRESSURES AND TEMPERATURES AT $\chi = 0.508$

$p_o = 66.1 \quad T_o = 514 \quad p_w = 5.26 \times 10^{-4}$					
y, cm	$\frac{p_{O_2}}{p_o}$	y, cm	$\frac{p_{O_2}}{p_o}$	y, cm	$\frac{p_{O_2}}{p_o}$
0.160	1.248×10^{-5}	2.446	3.149×10^{-3}	0.152	1.283×10^{-5}
0.193	1.295×10^{-5}	2.561	3.208×10^{-3}		
0.365	1.728×10^{-5}	2.979	2.984×10^{-3}		
0.496	2.214×10^{-5}	2.888	3.066×10^{-3}		
0.555	3.296×10^{-5}	2.676	3.227×10^{-3}		
0.734	6.387×10^{-5}	2.430	3.084×10^{-3}		
0.807	1.416×10^{-4}	2.528	3.183×10^{-3}		
0.930	3.719×10^{-4}	2.610	3.227×10^{-3}		
0.988	4.945×10^{-4}	2.643	3.234×10^{-3}		
1.070	6.090×10^{-4}	2.791	3.173×10^{-3}		
1.160	8.182×10^{-4}	1.864	2.163×10^{-3}		
1.397	1.293×10^{-3}	1.643	1.717×10^{-3}		
1.479	1.472×10^{-3}	1.389	1.247×10^{-3}		
1.635	1.777×10^{-3}	1.012	5.307×10^{-4}		
1.742	1.972×10^{-3}	0.889	2.182×10^{-4}		
1.840	2.181×10^{-3}	0.693	5.724×10^{-5}		
2.036	2.555×10^{-3}	0.611	3.206×10^{-5}		
2.184	2.839×10^{-3}	0.431	1.916×10^{-5}		
2.381	3.077×10^{-3}	0.250	1.458×10^{-5}		
$p_o = 66.2 \quad T_o = 916 \quad p_w = 5.26 \times 10^{-4}$					
0.119	1.281×10^{-5}	2.430	3.381×10^{-3}	0.701	3.363×10^{-5}
0.152	1.292×10^{-5}	2.832	3.247×10^{-3}	0.594	2.634×10^{-5}
0.218	1.381×10^{-5}	2.894	3.210×10^{-3}		
0.300	1.573×10^{-5}	2.773	3.343×10^{-3}		
0.373	1.787×10^{-5}	2.659	3.419×10^{-3}		
0.578	2.795×10^{-5}	2.504	3.379×10^{-3}		
0.758	4.633×10^{-5}	2.577	3.407×10^{-3}		
0.922	9.313×10^{-5}	2.389	3.294×10^{-3}		
1.053	1.861×10^{-4}	2.315	3.150×10^{-3}		
1.151	2.910×10^{-4}	1.934	2.687×10^{-3}		
1.217	5.554×10^{-4}	1.742	1.968×10^{-3}		
1.373	8.799×10^{-4}	1.479	1.170×10^{-3}		
1.447	1.116×10^{-3}	1.397	9.528×10^{-4}		
1.512	1.456×10^{-3}	1.340	8.485×10^{-4}		
1.659	1.678×10^{-3}	1.266	5.232×10^{-4}		
1.824	2.157×10^{-3}	1.102	1.972×10^{-4}		
1.963	2.499×10^{-3}	1.053	1.766×10^{-4}		
2.028	2.622×10^{-3}	0.914	8.504×10^{-5}		
2.184	2.990×10^{-3}	0.824	5.250×10^{-5}		

$p_o = 66.8 \quad T_o = 499 \quad T_w = 362$					
y, cm	$\frac{T_o}{T_{oe}}$	y, cm	$\frac{T_o}{T_{oe}}$	y, cm	$\frac{T_o}{T_{oe}}$
0.070	0.750	0.832	0.997		
0.156	0.767	0.671	0.944		
0.255	0.791	0.696	0.951		
0.692	0.939	0.338	0.809		
0.370	0.831	0.206	0.778		
1.081	0.987				
1.709	0.968				
2.042	0.972				
2.584	0.992				
3.257	1.001				
3.843	1.002				
3.504	0.999				
2.458	0.985				
1.910	0.971				
1.318	0.981				
1.824	0.970				
0.984	1.006				
1.075	0.994				
0.988	1.005				
$p_o = 66.8 \quad T_o = 820 \quad T_w = 397$					
0.177	0.553	2.944	0.999		
0.515	0.661	2.396	0.984		
0.928	0.838	2.190	0.970		
1.140	0.917	1.692	0.953		
1.725	0.940	1.564	0.949		
2.186	0.961	1.235	0.956		
2.437	0.979	0.893	0.878		
3.640	0.998	0.725	0.813		
0.058	0.530	0.539	0.728		
0.272	0.578	0.272	0.631		
0.515	0.662	0.107	0.579		
0.922	0.837				
1.297	0.954				
1.468	0.953				
1.927	0.960				
2.429	0.989				
2.851	0.996				
3.520	1.001				
3.862	0.999				

TABLE 1. – MEASURED PRESSURES AND TEMPERATURES AT χ = 0.508 – Continued

$p_o = 107.6$ $T_o = 315$ $p_w = 8.61 \times 10^{-4}$						$p_o = 108.9$ $T_o = 315$ $T_w = 333$					
y, cm	$\frac{p_{o_2}}{p_o}$	y, cm	$\frac{p_{o_2}}{p_o}$	y, cm	$\frac{p_{o_2}}{p_o}$	y, cm	$\frac{T_o}{T_{oe}}$	y, cm	$\frac{T_o}{T_{oe}}$	y, cm	$\frac{T_o}{T_{oe}}$
0.081	1.146×10^{-5}	2.865	2.799×10^{-3}	0.388	4.893×10^{-5}	0.115	1.066	1.824	0.977		
0.274	2.074×10^{-5}	2.738	2.918×10^{-3}	0.554	1.776×10^{-4}	0.243	1.080	1.363	0.981		
0.417	7.977×10^{-5}	2.654	2.998×10^{-3}	0.726	3.449×10^{-4}	0.383	1.110	0.864	1.010		
1.048	6.409×10^{-4}	2.484	3.048×10^{-3}	0.600	2.019×10^{-4}	0.618	1.059	0.395	1.110		
1.135	7.867×10^{-4}	2.065	2.562×10^{-3}	0.342	4.261×10^{-5}	1.243	0.985	0.272	1.074		
1.305	1.014×10^{-3}	1.936	2.261×10^{-3}	0.218	1.493×10^{-5}	1.536	0.980	0.099	1.057		
1.428	1.259×10^{-3}	1.726	1.888×10^{-3}	0.091	1.182×10^{-5}	1.783	0.979				
1.475	1.375×10^{-3}	1.515	1.360×10^{-3}			2.077	0.980				
1.600	1.586×10^{-3}	1.349	1.082×10^{-3}			2.289	0.986				
1.853	2.196×10^{-3}	1.168	7.563×10^{-4}			2.454	0.993				
2.322	2.973×10^{-3}	0.882	4.639×10^{-4}			2.746	1.000				
2.488	3.052×10^{-3}	0.666	2.393×10^{-4}			2.991	1.000				
2.784	2.880×10^{-3}	0.542	1.238×10^{-4}			3.631	1.000				
2.883	2.810×10^{-3}	0.334	2.869×10^{-5}			4.298	1.001				
2.194	2.799×10^{-3}	0.299	2.132×10^{-5}			3.293	1.002				
1.812	2.087×10^{-3}	0.467	1.095×10^{-4}			2.079	0.980				
1.898	2.231×10^{-3}	0.102	1.200×10^{-5}			2.495	0.994				
2.231	2.848×10^{-3}	0.251	1.767×10^{-5}			2.664	0.999				
2.318	2.986×10^{-3}	0.430	7.385×10^{-5}			2.326	0.986				
$p_o = 107.6$ $T_o = 395$ $p_w = 8.61 \times 10^{-4}$						$p_o = 108.9$ $T_o = 393$ $T_w = 339$					
0.102	1.174×10^{-5}	2.451	2.979×10^{-3}	1.357	1.174×10^{-3}	0.095	0.860	0.597	1.023		
0.185	1.435×10^{-5}	2.198	2.767×10^{-3}	0.977	5.349×10^{-4}	0.350	0.961	0.803	0.995		
0.392	3.406×10^{-5}	2.281	2.883×10^{-3}	0.672	2.501×10^{-4}	0.683	1.011	0.591	1.030		
0.508	1.067×10^{-4}	2.322	2.930×10^{-3}	0.554	1.353×10^{-4}	0.934	0.983	0.412	0.996		
0.550	1.326×10^{-4}	2.409	2.968×10^{-3}	0.344	2.562×10^{-5}	1.099	0.973	0.292	0.933		
0.595	1.827×10^{-4}	2.662	2.892×10^{-3}	0.089	1.207×10^{-5}	1.396	0.968	0.091	0.883		
0.724	3.077×10^{-4}	2.534	2.969×10^{-3}			1.772	0.974				
0.936	5.214×10^{-4}	2.189	2.747×10^{-3}			2.022	0.979				
0.977	5.893×10^{-4}	1.864	2.175×10^{-3}			2.520	0.996				
1.355	1.103×10^{-3}	1.612	1.596×10^{-3}			2.775	1.001				
1.567	1.540×10^{-3}	1.106	7.003×10^{-4}			3.071	0.999				
1.608	1.674×10^{-3}	1.054	6.073×10^{-4}			3.862	1.002				
1.778	1.977×10^{-3}	0.930	4.726×10^{-4}			3.528	1.003				
1.998	2.481×10^{-3}	0.259	1.779×10^{-5}			2.643	0.997				
2.306	2.912×10^{-3}	0.052	1.188×10^{-5}			1.684	0.970				
2.659	2.895×10^{-3}	0.517	1.107×10^{-4}			1.219	0.971				
2.862	2.746×10^{-3}	0.641	2.033×10^{-4}			0.725	1.011				
2.832	2.773×10^{-3}	0.720	2.781×10^{-4}			0.346	0.979				
2.621	2.917×10^{-3}	0.797	3.734×10^{-4}			0.428	1.007				

TABLE 1. – MEASURED PRESSURES AND TEMPERATURES AT χ = 0.508 – Continued

$p_o = 108.1$ $T_o = 518$ $p_w = 8.61 \times 10^{-4}$

y, cm	p_{o_2}/p_o	y, cm	p_{o_2}/p_o	y, cm	p_{o_2}/p_o
2.888	2.839×10^{-3}	1.250	1.140×10^{-3}		
2.462	3.090×10^{-3}	1.446	1.548×10^{-3}		
2.069	2.651×10^{-3}	1.561	1.793×10^{-3}		
1.750	2.048×10^{-3}	1.660	1.957×10^{-3}		
1.496	1.515×10^{-3}	1.905	2.424×10^{-3}		
1.135	8.649×10^{-4}	2.152	2.842×10^{-3}		
0.873	5.094×10^{-4}	2.389	3.066×10^{-3}		
0.537	4.077×10^{-5}	2.626	3.042×10^{-3}		
0.463	2.528×10^{-5}	2.807	2.915×10^{-3}		
0.299	1.426×10^{-5}	2.446	3.087×10^{-3}		
0.226	1.218×10^{-5}	2.069	2.619×10^{-3}		
0.136	1.184×10^{-5}	1.832	2.165×10^{-3}		
0.267	1.456×10^{-5}	1.348	1.194×10^{-3}		
0.455	3.152×10^{-5}	0.955	5.920×10^{-4}		
0.578	6.357×10^{-5}	0.496	3.452×10^{-5}		
0.742	3.035×10^{-4}	0.168	1.197×10^{-5}		
0.775	4.035×10^{-4}				
0.922	6.290×10^{-4}				
1.053	8.138×10^{-4}				

$p_o = 109.2$ $T_o = 930$ $p_w = 8.61 \times 10^{-4}$

y, cm	p_{o_2}/p_o	y, cm	p_{o_2}/p_o	y, cm	p_{o_2}/p_o
0.103	1.202×10^{-5}	2.282	3.009×10^{-3}		
0.480	2.544×10^{-5}	2.463	3.090×10^{-3}		
0.627	4.774×10^{-5}	2.561	3.032×10^{-3}		
0.693	9.246×10^{-5}	2.430	3.083×10^{-3}		
0.856	2.465×10^{-4}	2.290	3.033×10^{-3}		
0.939	3.692×10^{-4}	2.168	2.792×10^{-3}		
0.988	5.331×10^{-4}	1.799	2.163×10^{-3}		
1.086	7.330×10^{-4}	1.602	1.651×10^{-3}		
1.316	1.112×10^{-3}	1.324	1.135×10^{-3}		
1.488	1.560×10^{-3}	1.037	5.605×10^{-4}		
1.676	1.954×10^{-3}	0.889	3.028×10^{-4}		
1.856	2.293×10^{-3}	0.840	1.509×10^{-4}		
1.884	2.702×10^{-3}	0.709	7.444×10^{-5}		
2.167	2.912×10^{-3}	0.660	5.278×10^{-5}		
2.397	3.084×10^{-3}	0.545	3.128×10^{-5}		
2.544	3.046×10^{-3}	0.414	1.894×10^{-5}		
2.675	2.927×10^{-3}	0.332	1.563×10^{-5}		
2.586	3.013×10^{-3}	0.168	1.242×10^{-5}		
2.430	3.084×10^{-3}	0.136	1.208×10^{-5}		

$p_o = 109.4$ $T_o = 481$ $T_w = 339$

y, cm	T_o/T_{oe}	y, cm	T_o/T_{oe}	y, cm	T_o/T_{oe}
0.072	0.743	2.608	0.993		
0.259	0.825	2.898	0.997		
0.453	0.922	3.170	0.997		
0.782	0.990	3.759	1.000		
1.956	0.975	3.469	1.000		
1.495	0.963	2.833	0.995		
2.584	0.993	2.166	0.976		
3.088	0.996	1.700	0.968		
3.627	1.000	0.943	0.984		
2.285	0.979	0.700	0.996		
1.064	0.976	0.618	0.995		
0.445	0.933	0.366	0.891		
0.531	0.979	0.403	0.910		
0.613	0.992	0.185	0.820		
0.782	0.992				
1.031	0.972				
1.285	0.965				
1.577	0.965				
2.166	0.979				

$p_o = 105.0$ $T_o = 988$ $T_w = 400$

y, cm	T_o/T_{oe}	y, cm	T_o/T_{oe}	y, cm	T_o/T_{oe}
0.097	0.461	1.857	0.959		
0.126	0.495	1.103	0.939		
0.352	0.560	1.153	0.930		
0.634	0.659	0.898	0.862		
0.766	0.759	0.721	0.755		
0.889	0.840	0.440	0.654		
1.019	0.895	0.395	0.583		
1.482	0.940				
1.861	0.957				
2.404	0.985				
2.689	0.995				
2.870	0.996				
3.240	0.995				
3.615	1.000				
2.611	0.991				
3.149	1.000				
3.615	1.000				
3.489	1.002				
2.701	0.997				

TABLE 1. – MEASURED PRESSURES AND TEMPERATURES AT χ = 0.508 – Continued

p_o = 199 T_o = 523 $p_w = 13.4 \times 10^{-4}$						p_o = 200 T_o = 516 T_w = 352					
y, cm	$\frac{p_{O_2}}{p_o}$	y, cm	$\frac{p_{O_2}}{p_o}$	y, cm	$\frac{p_{O_2}}{p_o}$	y, cm	$\frac{T_o}{T_{oe}}$	y, cm	$\frac{T_o}{T_{oe}}$	y, cm	$\frac{T_o}{T_{oe}}$
0.111	1.186×10^{-5}	2.282	2.980×10^{-3}			0.049	0.747	2.322	0.997		
0.308	4.355×10^{-5}	2.372	2.941×10^{-3}			0.128	0.808	1.943	0.984		
0.389	1.141×10^{-4}	2.176	2.942×10^{-3}			0.226	0.854	1.647	0.977		
0.488	1.650×10^{-4}	1.782	2.412×10^{-3}			0.313	0.934	1.361	0.969		
0.570	3.726×10^{-4}	1.545	1.873×10^{-3}			0.440	0.978	1.186	0.967		
0.668	4.930×10^{-4}	1.348	1.579×10^{-3}			0.482	0.981	0.688	0.968		
0.750	5.640×10^{-4}	1.234	1.354×10^{-3}			0.786	0.968	0.440	0.975		
0.816	6.626×10^{-4}	1.086	1.016×10^{-3}			0.984	0.967	0.235	0.885		
0.938	8.540×10^{-4}	0.988	8.439×10^{-4}			1.235	0.965	0.486	0.982		
1.168	1.199×10^{-3}	0.766	5.868×10^{-4}			1.322	0.968	0.650	0.971		
1.307	1.471×10^{-3}	0.594	3.351×10^{-4}			1.696	0.978	0.984	0.965		
1.578	2.032×10^{-3}	0.537	2.383×10^{-4}			2.009	0.989	0.683	0.970		
1.922	2.704×10^{-3}	0.373	6.649×10^{-5}			2.157	0.992	0.325	0.932		
2.094	2.907×10^{-3}	0.308	3.836×10^{-5}			2.783	1.000	0.230	0.850		
2.274	2.973×10^{-3}	0.250	2.179×10^{-5}			3.710	0.999	0.152	0.795		
2.421	2.886×10^{-3}	0.144	1.193×10^{-5}			3.796	0.998				
2.487	2.827×10^{-3}	0.119	1.173×10^{-5}			3.372	1.001				
2.332	2.974×10^{-3}					3.036	1.000				
2.086	2.892×10^{-3}					2.450	1.000				
p_o = 199 T_o = 933 $p_w = 13.4 \times 10^{-4}$						p_o = 200 T_o = 942 T_w = 402					
0.135	1.135×10^{-5}	2.479	2.935×10^{-3}	0.095	1.154×10^{-5}	0.095	0.515	1.771	0.960		
0.357	2.543×10^{-5}	2.348	3.027×10^{-3}	0.258	1.713×10^{-5}	0.181	0.555	1.427	0.944		
0.431	5.683×10^{-5}	2.233	3.002×10^{-3}			0.286	0.606				
0.529	1.129×10^{-4}	2.069	2.796×10^{-3}			0.463	0.746				
0.660	2.897×10^{-4}	1.922	2.544×10^{-3}			0.536	0.813				
0.775	4.730×10^{-4}	1.824	2.396×10^{-3}			0.704	0.908				
0.922	6.897×10^{-4}	1.627	2.038×10^{-3}			1.149	0.945				
0.971	8.207×10^{-4}	1.561	1.861×10^{-3}			1.375	0.956				
1.086	9.855×10^{-4}	1.299	1.365×10^{-3}			1.713	0.964				
1.201	1.172×10^{-3}	1.119	1.014×10^{-3}			1.919	0.971				
1.307	1.430×10^{-3}	1.020	8.290×10^{-4}			2.211	0.985				
1.479	1.755×10^{-3}	0.824	5.160×10^{-4}			2.544	0.996				
1.651	2.056×10^{-3}	0.734	3.385×10^{-4}			2.637	0.999				
1.774	2.353×10^{-3}	0.660	2.045×10^{-4}			2.849	1.000				
2.004	2.736×10^{-3}	0.611	1.412×10^{-4}			3.265	1.000				
2.061	2.861×10^{-3}	0.480	5.677×10^{-5}			3.063	0.996				
2.233	3.003×10^{-3}	0.431	4.055×10^{-5}			2.685	0.997				
2.413	2.988×10^{-3}	0.398	2.583×10^{-5}			2.390	0.989				
2.564	2.860×10^{-3}	0.201	1.253×10^{-5}			2.016	0.974				

TABLE 1. – MEASURED PRESSURES AND TEMPERATURES AT χ = 0.508 – Concluded

y, cm	p_{O_2}/p_o	y, cm	p_{O_2}/p_o	y, cm	p_{O_2}/p_o
p_o = 270 T_o = 508 p_w = 18.1 × 10^{-4}					
0.185	1.377×10^{-5}	2.053	2.920×10^{-3}	0.283	1.789×10^{-5}
0.308	3.775×10^{-5}	2.176	2.967×10^{-3}	0.242	1.360×10^{-5}
0.357	6.001×10^{-5}	2.356	2.872×10^{-3}	0.201	1.318×10^{-5}
0.513	3.339×10^{-4}	2.143	2.960×10^{-3}		
0.633	4.875×10^{-4}	1.889	2.683×10^{-3}		
0.848	6.862×10^{-4}	1.610	2.101×10^{-3}		
0.906	7.736×10^{-4}	1.422	1.760×10^{-3}		
1.010	9.915×10^{-4}	1.332	1.537×10^{-3}		
1.168	1.262×10^{-3}	1.185	1.189×10^{-3}		
1.324	1.621×10^{-3}	1.037	9.372×10^{-4}		
1.504	2.001×10^{-3}	0.889	7.030×10^{-4}		
1.620	2.216×10^{-3}	0.701	4.944×10^{-4}		
1.766	2.534×10^{-3}	0.652	4.381×10^{-4}		
2.028	2.894×10^{-3}	0.570	3.480×10^{-4}		
2.290	2.900×10^{-3}	0.472	1.980×10^{-4}		
2.421	2.793×10^{-3}	0.423	8.301×10^{-5}		
2.323	2.899×10^{-3}	0.389	6.863×10^{-5}		
2.258	2.935×10^{-3}	0.373	4.190×10^{-5}		
2.036	2.862×10^{-3}	0.324	3.279×10^{-5}		
p_o = 268 T_o = 939 p_w = 18.2 × 10^{-4}					
0.201	1.186×10^{-5}	1.905	260.2×10		
0.209	1.485×10^{-5}	1.602	195.7×10		
0.398	8.747×10^{-5}	1.340	135.9×10		
0.545	22.63×10^{-5}	1.283	127.8×10		
0.570	28.12×10^{-5}	1.078	92.77×10		
0.677	45.36×10^{-5}	0.857	59.66×10		
0.939	77.98×10^{-5}	0.652	37.11×10		
1.127	108.8×10^{-5}	0.586	24.94×10		
1.340	150.4×10^{-5}	0.472	10.80×10		
1.479	183.4×10^{-5}	0.300	1.941×10		
1.651	215.1×10^{-5}	0.201	1.346×10		
1.856	258.4×10^{-5}	0.152	1.195×10		
2.053	278.9×10^{-5}				
2.233	289.9×10^{-5}				
2.315	286.0×10^{-5}				
2.438	278.9×10^{-5}				
2.565	272.0×10^{-5}				
2.315	288.4×10^{-5}				
2.143	288.7×10^{-5}				

y, cm	T_o/T_{oe}	y, cm	T_o/T_{oe}	y, cm	T_o/T_{oe}
p_o = 270 T_o = 513 T_w = 318					
0.105	0.838	3.281	1.000		
0.235	0.920	3.141	1.003		
0.361	0.952	2.901	1.000		
0.578	0.955	2.781	1.001		
0.739	0.955	2.561	1.001		
0.906	0.957	2.407	0.998		
1.070	0.960	2.244	0.996		
1.284	0.964	2.086	0.991		
1.451	0.969	1.863	0.981		
1.628	0.970	1.701	0.975		
1.760	0.975	1.242	0.964		
1.945	0.984	1.058	0.962		
2.209	0.995	0.939	0.961		
2.427	0.996	0.566	0.960		
2.633	0.998				
2.822	0.996				
3.045	0.998				
3.255	0.999				
3.419	1.000				
p_o = 269 T_o = 882 T_w = 361					
0.111	0.551	1.653	0.962	0.517	0.913
0.739	0.886	1.735	0.969	0.642	0.931
0.519	0.895	1.900	0.972	0.768	0.931
0.426	0.863	2.075	0.991	0.924	0.938
0.142	0.608	2.275	0.996	1.190	0.951
0.348	0.715	2.402	0.991	1.358	0.952
0.383	0.811	3.456	1.003	1.653	0.961
0.476	0.875	3.075	0.998	2.065	0.978
0.517	0.899	2.738	0.998	2.285	0.992
0.562	0.911	2.238	0.990	2.444	0.999
0.690	0.917	1.566	0.960	3.023	1.002
0.727	0.913	1.729	0.967	1.863	0.969
0.813	0.924	2.112	0.990	1.608	0.967
0.937	0.937	0.773	0.932	1.309	0.975
1.042	0.937	0.266	0.738	0.389	0.888
1.192	0.952	0.181	0.682	0.284	0.813
1.279	0.949	0.222	0.713		
1.357	0.958	0.307	0.810		
1.492	0.964	0.389	0.877		

TABLE 2. – MEASURED PRESSURES AND TEMPERATURES AT χ = 1.067

y, cm	p_{O_2}/p_o	y, cm	p_{O_2}/p_o	y, cm	p_{O_2}/p_o
p_o = 65.3 T_o = 490 p_w = 1.45 × 10^{-4}					
0.233	2.774 × 10^{-6}	6.807	1.102 × 10^{-3}		
0.513	2.871 × 10^{-6}	7.087	1.149 × 10^{-3}		
1.007	3.556 × 10^{-6}	7.501	1.173 × 10^{-3}		
1.553	4.411 × 10^{-6}	7.965	1.139 × 10^{-3}		
1.860	5.746 × 10^{-6}	8.547	1.056 × 10^{-3}		
2.060	8.690 × 10^{-6}	8.407	1.078 × 10^{-3}		
2.420	1.253 × 10^{-5}	8.100	1.121 × 10^{-3}		
2.926	3.919 × 10^{-5}	7.833	1.152 × 10^{-3}		
3.299	1.300 × 10^{-4}	7.526	1.171 × 10^{-3}		
3.566	2.028 × 10^{-4}	7.020	1.132 × 10^{-3}		
3.833	2.697 × 10^{-4}	6.192	9.746 × 10^{-4}		
4.260	4.065 × 10^{-4}	5.466	7.671 × 10^{-4}		
4.448	4.467 × 10^{-4}	4.539	4.843 × 10^{-4}		
4.686	5.327 × 10^{-4}	3.846	2.820 × 10^{-4}		
5.100	6.484 × 10^{-4}	3.226	1.029 × 10^{-4}		
5.260	7.077 × 10^{-4}	2.807	2.615 × 10^{-5}		
5.568	8.068 × 10^{-4}	2.493	1.391 × 10^{-5}		
6.101	9.476 × 10^{-4}	2.013	8.423 × 10^{-6}		
6.594	1.062 × 10^{-3}	1.187	4.692 × 10^{-6}		
p_o = 65 T_o = 914 p_w = 1.45 × 10^{-4}					
0.327	2.964 × 10^{-6}	7.381	1.262 × 10^{-3}		
0.733	3.506 × 10^{-6}	7.120	1.266 × 10^{-3}		
1.127	4.692 × 10^{-6}	6.126	1.078 × 10^{-3}		
1.793	7.291 × 10^{-6}	5.453	8.587 × 10^{-4}		
2.606	1.462 × 10^{-5}	4.966	6.579 × 10^{-4}		
3.134	4.263 × 10^{-5}	4.453	4.376 × 10^{-4}		
3.627	8.401 × 10^{-5}	3.967	2.214 × 10^{-4}		
4.420	4.023 × 10^{-4}	3.193	2.907 × 10^{-5}		
4.707	5.227 × 10^{-4}	2.593	1.547 × 10^{-5}		
5.461	8.154 × 10^{-4}	1.867	8.000 × 10^{-6}		
5.979	1.005 × 10^{-5}	1.060	4.700 × 10^{-6}		
6.528	1.176 × 10^{-3}	0.653	3.561 × 10^{-6}		
6.779	1.232 × 10^{-3}	0.233	3.053 × 10^{-6}		
7.153	1.268 × 10^{-3}				
7.488	1.260 × 10^{-3}				
7.932	1.200 × 10^{-3}				
8.372	1.121 × 10^{-3}				
8.133	1.148 × 10^{-3}				
7.587	1.238 × 10^{-3}				

y, cm	T_o/T_{oe}	y, cm	T_o/T_{oe}	y, cm	T_o/T_{oe}
p_o = 66.2 T_o = 500 T_w = 315					
0.411	0.663	8.192	1.001		
0.577	0.672	7.693	0.997		
0.958	0.693	6.144	0.969		
1.171	0.712	4.592	0.956		
1.780	0.784	3.134	0.977		
2.161	0.866	3.553	0.963		
2.573	0.941	2.672	0.971		
3.299	0.956	3.670	0.956		
3.975	0.955	4.221	0.954		
4.353	0.956	5.227	0.959		
5.179	0.960	2.720	0.972		
5.524	0.962	3.480	0.962		
5.855	0.966	1.897	0.849		
6.449	0.972	2.647	0.947		
6.728	0.980	1.814	0.819		
7.117	0.986	1.509	0.754		
7.559	0.995	0.940	0.690		
7.663	0.997	0.180	0.660		
9.175	0.999				
p_o = 66.3 T_o = 933 T_w = 358					
0.297	0.431	5.029	0.958		
0.297	0.406	4.272	0.942		
0.297	0.427	3.398	0.930		
0.627	0.444	2.944	0.855		
1.468	0.520	3.101	0.872		
1.979	0.592	2.819	0.808		
2.433	0.660	2.647	0.750		
2.845	0.763	2.357	0.682		
3.101	0.827	2.194	0.634		
3.398	0.888	0.792	0.449		
4.023	0.924	1.087	0.479		
4.775	0.940	1.681	0.556		
5.326	0.951	0.584	0.431		
6.038	0.966	0.576	0.445		
6.713	0.983	0.594	0.430		
7.546	1.000				
8.123	1.000				
7.092	0.989				
6.043	0.967				

TABLE 2. – MEASURED PRESSURES AND TEMPERATURES AT χ = 1.067 – Continued

p_o = 107.7 T_o = 306 p_w = 2.08 × 10^{-4}						p_o = 108.1 T_o = 305 T_w = 299					
y, cm	$\frac{p_{o_2}}{p_o}$	y, cm	$\frac{p_{o_2}}{p_o}$	y, cm	$\frac{p_{o_2}}{p_o}$	y, cm	$\frac{T_o}{T_{oe}}$	y, cm	$\frac{T_o}{T_{oe}}$	y, cm	$\frac{T_o}{T_{oe}}$
0 355	2.474 × 10^{-6}	6.738	1.176 × 10^{-3}			1 526	1.038	7.684	1.000		
0.882	2.698 × 10^{-6}	7.198	1.132 × 10^{-3}			7.701	1.002	5.756	0.979		
2.268	1.278 × 10^{-4}	7.364	1.102 × 10^{-3}			4.897	0.971	4.255	0.966		
2.614	1.809 × 10^{-4}	7.694	1.047 × 10^{-3}			4.288	0.969	2.786	0.984		
2.977	2.441 × 10^{-4}	6.738	1.176 × 10^{-3}			3.398	0.971	1.105	1.046		
3.356	3.198 × 10^{-4}	6.208	1.132 × 10^{-3}			2.433	0.997	0.312	0.995		
3.645	3.918 × 10^{-4}	5.534	9.762 × 10^{-4}			1.600	1.063	0.312	0.990		
3.851	4.646 × 10^{-4}	4.981	8.171 × 10^{-4}			0.841	1.025				
4.198	5.558 × 10^{-4}	4.757	7.510 × 10^{-4}			0.345	1.001				
4.445	6.443 × 10^{-4}	4.493	6.558 × 10^{-4}			0.826	1.006				
4.709	7.268 × 10^{-4}	4.231	5.781 × 10^{-4}			1.765	1.033				
4.940	8.117 × 10^{-4}	3.718	4.358 × 10^{-4}			2.606	0.984				
5.204	8.938 × 10^{-4}	2.317	1.426 × 10^{-4}			3.332	0.970				
5.352	9.301 × 10^{-4}	1.394	1.250 × 10^{-5}			3.843	0.968				
5.616	1.006 × 10^{-3}	0.668	6.723 × 10^{-6}			4.552	0.971				
5.730	1.042 × 10^{-3}	0.387	5.068 × 10^{-6}			5.425	0.976				
6.076	1.109 × 10^{-3}	0.305	3.275 × 10^{-6}			6.960	0.999				
6.309	1.150 × 10^{-3}					7.521	1.000				
6.606	1.172 × 10^{-3}					8.034	0.999				
p_o = 107.7 T_o = 416 p_w = 2.08 × 10^{-4}						p_o = 108.6 T_o = 418 T_w = 301					
0.338	2.485 × 10^{-6}	5.534	9.524 × 10^{-4}			2.408	0.962	2.507	0.984		
0.718	2.952 × 10^{-6}	5.088	8.236 × 10^{-4}			1.684	0.938	2.624	0.975		
1.262	4.180 × 10^{-6}	4.379	5.925 × 10^{-4}			1.024	0.814	1.864	0.997		
2.763	1.836 × 10^{-4}	3.950	4.583 × 10^{-4}			2.154	0.966	2.819	0.968		
2.977	2.237 × 10^{-4}	3.406	3.227 × 10^{-4}			2.705	0.955	2.954	0.968		
3.769	4.137 × 10^{-4}	2.894	2.086 × 10^{-4}			3.002	0.951	1.582	0.954		
4.056	4.924 × 10^{-4}	2.416	1.149 × 10^{-4}			3.708	0.947	1.915	0.983		
4.740	7.144 × 10^{-4}	1.822	2.057 × 10^{-5}			4.041	0.957	1.237	0.863		
4.989	7.936 × 10^{-4}	1.196	8.745 × 10^{-6}			4.331	0.968	0.907	0.812		
5.434	9.434 × 10^{-4}	0.618	4.354 × 10^{-6}			4.915	0.971	0.594	0.744		
5.863	1.053 × 10^{-3}	0.404	2.843 × 10^{-6}			5.720	0.978	0.576	0.739		
6.076	1.090 × 10^{-3}	0.371	2.603 × 10^{-6}			6.251	0.988				
6.622	1.152 × 10^{-3}					6.954	1.000				
7.033	1.132 × 10^{-3}					7.823	1.000				
7.480	1.061 × 10^{-3}					6.896	0.999				
7.661	1.034 × 10^{-3}					6.142	0.984				
7.117	1.130 × 10^{-3}					5.461	0.975				
6.309	1.126 × 10^{-3}					4.369	0.968				
5.896	1.052 × 10^{-3}					3.411	0.965				

TABLE 2. – MEASURED PRESSURES AND TEMPERATURES AT χ = 1.067 – Continued

p_o $p_o = 107.7$ $T_o = 572$ $p_w = 2.08 \times 10^{-4}$					
y, cm	$\frac{p_{O_2}}{p_o}$	y, cm	$\frac{p_{O_2}}{p_o}$	y, cm	$\frac{p_{O_2}}{p_o}$
0.256	2.483×10^{-6}	3.058	1.872×10^{-4}		
1.031	3.381×10^{-6}	2.598	8.923×10^{-5}		
1.822	8.465×10^{-6}	2.086	2.080×10^{-5}		
2.680	9.869×10^{-5}	1.592	9.738×10^{-6}		
3.785	3.565×10^{-4}	1.286	5.037×10^{-6}		
5.006	7.530×10^{-4}	0.833	4.083×10^{-6}		
5.796	1.000×10^{-3}	0.371	3.155×10^{-6}		
6.160	1.076×10^{-3}	0.338	2.664×10^{-6}		
6.640	1.115×10^{-3}				
7.099	1.082×10^{-3}				
7.892	9.585×10^{-4}				
7.645	9.940×10^{-4}				
7.132	1.077×10^{-3}				
6.391	1.108×10^{-3}				
5.517	9.188×10^{-4}				
4.890	7.180×10^{-4}				
4.346	5.285×10^{-4}				
4.148	4.716×10^{-4}				
3.421	2.811×10^{-4}				
$p_o = 109.8$ $T_o = 905$ $p_w = 1.12 \times 10^{-4}$					
0.492	2.570×10^{-6}	6.210	1.121×10^{-3}		
1.258	4.680×10^{-6}	6.847	1.134×10^{-3}		
1.997	1.018×10^{-5}	7.485	1.071×10^{-3}		
2.628	3.753×10^{-5}	6.842	1.163×10^{-3}		
3.294	2.092×10^{-4}	4.327	5.933×10^{-4}		
3.327	2.217×10^{-4}				
3.932	4.336×10^{-4}				
4.603	6.417×10^{-4}				
4.792	7.025×10^{-4}				
5.652	9.715×10^{-4}				
5.786	1.003×10^{-3}				
6.659	1.153×10^{-3}				
6.955	1.151×10^{-3}				
7.560	1.085×10^{-3}				
6.802	1.152×10^{-3}				
1.802	9.848×10^{-6}				
2.971	1.254×10^{-4}				
4 294	5.763×10^{-4}				
5.536	9.738×10^{-4}				

$p_o = 108.6$ $T_o = 577$ $T_w = 309$					
y, cm	$\frac{T_o}{T_{oe}}$	y, cm	$\frac{T_o}{T_{oe}}$	y, cm	$\frac{T_o}{T_{oe}}$
0.338	0.619	8.174	0.998	1.615	0.788
0.576	0.621	7.325	0.990	1.204	0.677
0.958	0.673	6.218	0.981	0.495	0.581
1.656	0.803	5.410	0.967		
1.946	0.881	4.702	0.957		
2.243	0.947	3.957	0.948		
2.819	0.956	3.366	0.947		
3.498	0.956	2.118	0.941		
4.254	0.958	2.243	0.892		
4.915	0.967	2.720	0.945		
5.245	0.972	3.068	0.940		
5.458	0.971	3.366	0.939		
6.053	0.979	3.876	0.939		
6.383	0.986	3.579	0.937		
6.894	0.994	3.150	0.938		
7.224	0.998	2.327	0.941		
7.884	0.998	2.819	0.936		
8.141	1.000	2.327	0.935		
8.585	1.001	1.780	0.845		
$p_o = 108.8$ $T_o = 920$ $T_w = 328$					
0.091	0.389	3.891	0.936		
0.536	0.453	3.553	0.934		
1.285	0.547	3.010	0.925		
1.666	0.621	2.408	0.888		
2.210	0.753	2.136	0.789		
2.555	0.830	1.880	0.708		
3.200	0.908	1.417	0.607		
3.388	0.917	0.709	0.506		
4.008	0.932	0.378	0.452		
4.592	0.949				
5.311	0.962				
6.071	0.987				
6.761	0.995				
7.480	0.999				
7.815	1.000				
6.728	1.000				
5.542	0.970				
4.922	0.956				
4.346	0.943				

TABLE 2. – MEASURED PRESSURES AND TEMPERATURES AT χ = 1.067 – Continued

y, cm	$\frac{p_{O_2}}{p_o}$	y, cm	$\frac{p_{O_2}}{p_o}$	y, cm	$\frac{p_{O_2}}{p_o}$
$p_o = 189$ $T_o = 509$ $p_w = 3.12 \times 10^{-4}$					
0.253	2.090×10^{-6}	6.566	9.700×10^{-4}		
0.907	2.449×10^{-6}	6.347	9.779×10^{-4}		
1.193	3.622×10^{-6}	5.959	9.608×10^{-4}		
1.606	1.436×10^{-5}	5.540	8.950×10^{-4}		
1.833	3.987×10^{-5}	5.088	7.735×10^{-4}		
2.240	1.015×10^{-4}	4.501	6.222×10^{-4}		
2.573	1.676×10^{-4}	4.087	5.075×10^{-4}		
2.906	2.261×10^{-4}	3.693	4.125×10^{-4}		
3.193	2.960×10^{-4}	3.167	2.938×10^{-4}		
3.533	3.607×10^{-4}	2.794	2.225×10^{-4}		
3.940	4.680×10^{-4}	2.273	1.324×10^{-4}		
4.386	5.808×10^{-4}	1.807	3.961×10^{-5}		
4.907	7.283×10^{-4}	1.447	9.542×10^{-6}		
5.314	8.312×10^{-4}	0.900	3.449×10^{-6}		
5.659	9.088×10^{-4}	0.307	3.219×10^{-6}		
5.994	9.550×10^{-4}				
6.327	9.875×10^{-4}				
7.013	9.250×10^{-4}				
6.713	9.540×10^{-4}				
$p_o = 189$ $T_o = 879$ $p_w = 3.12 \times 10^{-4}$					
0.287	2.239×10^{-6}	6.693	9.870×10^{-4}		
0.473	2.322×10^{-6}	6.919	9.716×10^{-4}		
0.720	2.652×10^{-6}	7.234	9.407×10^{-4}		
1.033	3.514×10^{-6}	7.361	9.228×10^{-4}		
1.347	5.492×10^{-6}	7.173	9.438×10^{-4}		
1.727	1.091×10^{-5}	6.660	9.908×10^{-4}		
2.273	5.058×10^{-5}	5.959	9.582×10^{-4}		
2.487	8.718×10^{-5}	5.179	7.804×10^{-4}		
2.741	1.384×10^{-4}	4.427	5.699×10^{-4}		
3.007	2.072×10^{-4}	4.006	4.671×10^{-4}		
3.553	3.272×10^{-4}	3.366	2.997×10^{-4}		
3.820	4.043×10^{-4}	2.860	1.806×10^{-4}		
4.112	4.807×10^{-4}	2.433	9.524×10^{-5}		
4.465	5.746×10^{-4}	2.066	2.916×10^{-5}		
4.793	6.593×10^{-4}	1.680	1.024×10^{-5}		
5.034	7.365×10^{-4}	1.220	5.148×10^{-6}		
5.339	8.217×10^{-4}	0.627	2.838×10^{-6}		
5.781	9.163×10^{-4}	0.260	2.315×10^{-6}		
6.114	9.720×10^{-4}				

y, cm	$\frac{T_O}{T_{Oe}}$	y, cm	$\frac{T_O}{T_{Oe}}$	y, cm	$\frac{T_O}{T_{Oe}}$
$p_o = 203$ $T_o = 534$ $T_w = 319$					
0.264	0.651	2.350	0.958		
0.594	0.705	1.979	0.962		
1.072	0.841	1.384	0.963		
1.057	0.846	1.681	0.962		
1.435	0.941	1.897	0.963		
2.144	0.956	2.441	0.953		
2.819	0.952	3.150	0.955		
3.447	0.959	4.122	0.963		
4.247	0.966	3.200	0.957		
4.999	0.973	2.276	0.961		
5.707	0.988	1.137	0.918		
6.269	0.995	1.351	0.948		
7.833	1.000	1.507	0.962		
7.844	1.000	1.897	0.959		
6.995	1.000	2.408	0.955		
4.867	0.972	1.351	0.952		
4.074	0.963	0.841	0.815		
3.200	0.955	0.676	0.764		
2.697	0.955	0.422	0.702		
$p_o = 205$ $T_o = 877$ $T_w = 348$					
0.048	0.451	5.674	0.983		
0.048	0.452	4.801	0.969		
0.462	0.547	4.089	0.960		
0.709	0.576	3.249	0.946		
1.039	0.667	2.456	0.941		
1.351	0.776	2.045	0.933		
2.118	0.909	1.501	0.869		
2.621	0.926	1.501	0.868		
3.249	0.936	1.153	0.790		
3.924	0.949	0.782	0.667		
4.636	0.963	0.792	0.668		
5.293	0.978				
5.938	0.991				
6.972	0.998				
7.849	1.000				
8.219	0.997				
8.214	1.002				
6.680	0.996				
6.556	0.991				

TABLE 2. – MEASURED PRESSURES AND TEMPERATURES AT χ = 1.067 – Concluded

p_o = 270 T_o = 487 p_w = 3.86 × 10^{-4}

y, cm	p_{o_2}/p_o	y, cm	p_{o_2}/p_o	y, cm	p_{o_2}/p_o
0.287	1.932 × 10^{-6}	6.327	9.232 × 10^{-4}	1.427	3.541 × 10^{-5}
1.100	2.852 × 10^{-6}	6.020	9.531 × 10^{-4}	1.380	2.540 × 10^{-5}
1.733	7.621 × 10^{-5}	5.553	9.347 × 10^{-4}	1.193	1.232 × 10^{-5}
2.167	1.284 × 10^{-4}	5.300	8.849 × 10^{-4}	1.007	5.631 × 10^{-6}
2.953	2.866 × 10^{-4}	4.953	8.094 × 10^{-4}	0.300	2.070 × 10^{-6}
3.113	3.222 × 10^{-4}	4.433	6.570 × 10^{-4}		
3.353	3.722 × 10^{-4}	4.187	5.886 × 10^{-4}		
3.593	4.343 × 10^{-4}	3.887	5.076 × 10^{-4}		
3.813	4.906 × 10^{-4}	3.606	4.373 × 10^{-4}		
3.940	5.310 × 10^{-4}	3.460	4.002 × 10^{-4}		
4.500	6.819 × 10^{-4}	3.140	3.364 × 10^{-4}		
4.953	7.931 × 10^{-4}	2.887	2.773 × 10^{-4}		
5.260	8.611 × 10^{-4}	2.540	2.035 × 10^{-4}		
5.447	9.074 × 10^{-4}	2.367	1.770 × 10^{-4}		
5.753	9.426 × 10^{-4}	2.173	1.457 × 10^{-4}		
5.979	9.548 × 10^{-4}	2.020	1.206 × 10^{-4}		
6.153	9.434 × 10^{-4}	1.913	1.111 × 10^{-4}		
6.500	8.963 × 10^{-4}	1.807	9.297 × 10^{-5}		
6.727	8.644 × 10^{-4}	1.593	5.772 × 10^{-5}		

p_o = 265 T_o = 502 T_w = 318

y, cm	T_o/T_{oe}	y, cm	T_o/T_{oe}	y, cm	T_o/T_{oe}
0.297	0.682	5.410	0.989		
0.709	0.801	3.818	0.967		
1.237	0.954	3.018	0.955		
1.732	0.959	2.441	0.954		
2.474	0.952	1.714	0.965		
3.035	0.960	1.204	0.975		
3.266	0.961	1.057	0.943		
3.678	0.965	1.344	0.969		
4.023	0.971	1.681	0.964		
4.618	0.977	2.111	0.955		
4.867	0.981	2.474	0.952		
5.377	0.988	3.101	0.969		
5.458	0.987	1.592	0.967		
6.004	0.993	1.046	0.947		
6.325	0.999	0.808	0.844		
6.845	1.000	0.554	0.755		
7.323	1.000				
7.176	0.999				
6.203	0.999				

p_o = 265 T_o = 883 p_w = 3.85 × 10^{-4}

y, cm	p_{o_2}/p_o	y, cm	p_{o_2}/p_o	y, cm	p_{o_2}/p_o
0.313	2.204 × 10^{-6}	5.673	9.189 × 10^{-4}		
0.740	2.402 × 10^{-6}	5.313	8.451 × 10^{-4}		
1.113	4.691 × 10^{-6}	4.993	7.663 × 10^{-4}		
1.380	7.136 × 10^{-6}	4.686	6.827 × 10^{-4}		
1.873	3.439 × 10^{-5}	4.287	5.833 × 10^{-4}		
2.407	1.270 × 10^{-4}	3.900	4.655 × 10^{-4}		
3.340	3.168 × 10^{-4}	3.540	3.781 × 10^{-4}		
3.887	4.507 × 10^{-4}	2.846	2.208 × 10^{-4}		
4.300	5.601 × 10^{-4}	2.033	6.619 × 10^{-5}		
4.807	7.071 × 10^{-4}	1.407	1.119 × 10^{-5}		
5.327	8.390 × 10^{-4}				
5.913	9.292 × 10^{-4}				
6.593	9.114 × 10^{-4}				
6.833	8.838 × 10^{-4}				
7.127	8.508 × 10^{-4}				
7.433	8.222 × 10^{-4}				
6.793	8.856 × 10^{-4}				
6.393	9.352 × 10^{-4}				
6.153	9.501 × 10^{-4}				

p_o = 276 T_o = 876 T_w = 339

y, cm	T_o/T_{oe}	y, cm	T_o/T_{oe}	y, cm	T_o/T_{oe}
0.355	0.454	4.163	0.970		
0.635	0.526	3.663	0.955		
0.973	0.614	3.150	0.945		
0.973	0.625	3.101	0.942		
1.382	0.786	2.487	0.933		
1.562	0.833	2.459	0.938		
1.674	0.873	1.943	0.928		
1.994	0.905	1.229	0.809		
2.007	0.908	1.016	0.671		
2.146	0.915	0.716	0.579		
2.634	0.927	0.350	0.478		
3.274	0.938				
3.927	0.955				
4.623	0.970				
5.530	0.990				
6.286	0.998				
7.046	1.000				
6.807	1.000				
5.715	0.991				

TABLE 3. – MEASURED PRESSURES AND TEMPERATURES AT χ = 1.625

$p_o = 66.9$ $T_o = 513$ $p_w = 0.698 \times 10^{-4}$						$p_o = 65.7$ $T_o = 515$ $T_w = 301$					
y, cm	$\frac{p_{o_2}}{p_o}$	y, cm	$\frac{p_{o_2}}{p_o}$	y, cm	$\frac{p_{o_2}}{p_o}$	y, cm	$\frac{T_o}{T_{oe}}$	y, cm	$\frac{T_o}{T_{oe}}$	y, cm	$\frac{T_o}{T_{oe}}$
0.262	1.471×10^{-6}	11.618	7.831×10^{-4}	1.316	2.032×10^{-6}	0.559	0.626	8.245	0.958		
1.707	2.130×10^{-6}	12.217	8.033×10^{-4}	0.691	1.716×10^{-6}	2.228	0.650	6.995	0.958		
2.647	3.313×10^{-6}	12.700	8.001×10^{-4}	0.081	1.521×10^{-6}	3.018	0.682	5.319	0.962		
4.234	8.087×10^{-6}	13.338	7.828×10^{-4}			3.691	0.717	5.154	0.946		
5.423	5.753×10^{-5}	12.835	8.013×10^{-4}			4.480	0.787	5.367	0.950		
6.510	2.148×10^{-4}	11.732	7.885×10^{-4}			5.154	0.879	5.697	0.957		
7.506	3.587×10^{-4}	10.160	6.893×10^{-4}			5.778	0.929	6.058	0.958		
8.534	4.935×10^{-4}	8.849	5.516×10^{-4}			6.601	0.946	6.568	0.958		
9.959	6.555×10^{-4}	7.935	4.416×10^{-4}			7.160	0.952	5.352	0.949		
11.194	7.567×10^{-4}	7.191	3.376×10^{-4}			8.903	0.956	4.430	0.871		
12.062	7.960×10^{-4}	6.256	2.033×10^{-4}			9.807	0.962	3.889	0.808		
13.238	7.799×10^{-4}	4.892	1.551×10^{-5}			10.990	0.974	2.705	0.714		
14.044	7.343×10^{-4}	5.738	9.730×10^{-5}			12.487	0.993	1.669	0.644		
13.060	7.894×10^{-4}	6.015	1.479×10^{-4}			13.769	1.000	0.254	0.613		
11.598	7.853×10^{-4}	5.047	2.121×10^{-5}			13.703	1.003				
10.168	6.823×10^{-4}	4.199	8.702×10^{-6}			11.943	0.987				
10.833	7.352×10^{-4}	2.916	4.004×10^{-6}			11.074	0.975				
11.422	7.731×10^{-4}	1.842	2.458×10^{-6}			9.825	0.965				
11.610	7.796×10^{-4}	1.793	2.149×10^{-6}			8.951	0.959				
$p_o = 65.3$ $T_o = 886$ $p_w = 0.698 \times 10^{-4}$						$p_o = 66.1$ $T_o = 890$ $T_w = 321$					
0.302	1.207×10^{-6}	12.814	8.220×10^{-4}	3.957	6.888×10^{-6}	0.272	0.351	11.542	0.981		
1.351	2.010×10^{-6}	13.459	7.961×10^{-4}	3.010	4.277×10^{-6}	1.143	0.376	10.046	0.959		
1.720	2.338×10^{-6}	14.031	7.611×10^{-4}	1.539	2.221×10^{-6}	1.816	0.408	8.334	0.938		
3.401	5.236×10^{-6}	12.687	8.305×10^{-4}	0.927	1.706×10^{-6}	2.738	0.464	7.226	0.933		
3.990	7.129×10^{-6}	12.405	8.339×10^{-4}	0.322	1.263×10^{-6}	3.947	0.552	6.208	0.901		
4.798	1.105×10^{-5}	12.189	8.325×10^{-4}			5.418	0.689	5.631	0.825		
6.182	5.317×10^{-5}	11.752	8.226×10^{-4}			6.370	0.848	4.742	0.673		
6.794	1.447×10^{-4}	11.013	7.775×10^{-4}			7.145	0.902	3.871	0.576		
7.102	2.018×10^{-4}	9.723	6.335×10^{-4}			8.260	0.933	2.319	0.468		
7.452	2.640×10^{-4}	8.877	5.205×10^{-4}			9.825	0.956	0.924	0.406		
7.930	3.400×10^{-4}	8.425	4.541×10^{-4}			11.303	0.974				
8.346	4.117×10^{-4}	8.326	4.320×10^{-4}			12.487	0.990				
8.870	4.937×10^{-4}	7.518	3.037×10^{-4}			13.637	0.996				
9.743	6.181×10^{-4}	7.325	2.695×10^{-4}			14.577	0.998				
10.193	6.793×10^{-4}	6.881	1.847×10^{-4}			15.560	1.000				
10.622	7.306×10^{-4}	6.551	1.229×10^{-4}			16.764	0.999				
11.255	7.930×10^{-4}	5.954	4.032×10^{-5}			16.599	1.001				
11.867	8.236×10^{-4}	5.758	2.678×10^{-5}			14.427	1.001				
12.276	8.289×10^{-4}	4.897	1.150×10^{-5}			12.840	0.995				

TABLE 3. – MEASURED PRESSURES AND TEMPERATURES AT χ = 1.625 – Continued

p_o = 107.3 T_o = 500 $p_w = 1.05 \times 10^{-4}$					
y, cm	$\frac{p_{O_2}}{p_o}$	y, cm	$\frac{p_{O_2}}{p_o}$	y, cm	$\frac{p_{O_2}}{p_o}$
0.239	1.114×10^{-6}	11.506	6.667×10^{-4}	5.067	5.628×10^{-5}
1.400	1.536×10^{-6}	12.167	6.663×10^{-4}	4.572	2.573×10^{-5}
2.073	2.182×10^{-6}	12.779	6.342×10^{-4}	4.249	1.368×10^{-5}
3.048	3.808×10^{-6}	13.261	5.856×10^{-4}	3.721	6.528×10^{-6}
3.721	6.335×10^{-6}	12.837	6.149×10^{-4}	3.134	4.206×10^{-6}
4.407	1.764×10^{-5}	12.456	6.501×10^{-4}	2.433	2.808×10^{-6}
4.849	3.809×10^{-5}	11.953	6.712×10^{-4}	1.734	1.936×10^{-6}
5.319	6.923×10^{-5}	11.626	6.716×10^{-4}	0.924	1.333×10^{-6}
5.844	1.205×10^{-4}	10.528	6.249×10^{-4}	0.244	1.072×10^{-6}
6.203	1.597×10^{-4}	9.500	5.417×10^{-4}		
6.675	2.039×10^{-4}	8.880	4.795×10^{-4}		
7.021	2.417×10^{-4}	8.458	4.312×10^{-4}		
7.356	2.855×10^{-4}	7.996	3.764×10^{-4}		
7.757	3.314×10^{-4}	7.653	3.340×10^{-4}		
8.153	3.826×10^{-4}	7.231	2.826×10^{-4}		
8.603	4.362×10^{-4}	6.939	2.512×10^{-4}		
9.012	4.846×10^{-4}	6.480	2.026×10^{-4}		
9.764	5.564×10^{-4}	6.017	1.574×10^{-4}		
10.726	6.296×10^{-4}	5.580	1.093×10^{-4}		
p_o = 107.6 T_o = 878 $p_w = 1.04 \times 10^{-4}$					
0.396	1.179×10^{-6}	11.321	6.829×10^{-4}	1.648	2.122×10^{-6}
1.168	1.558×10^{-6}	10.754	6.499×10^{-4}	0.363	1.155×10^{-6}
3.655	5.918×10^{-6}	11.176	6.563×10^{-4}		
5.568	3.988×10^{-5}	11.664	6.887×10^{-4}		
6.546	1.356×10^{-4}	12.299	6.905×10^{-4}		
6.835	1.787×10^{-4}	12.700	6.750×10^{-4}		
7.323	2.365×10^{-4}	11.320	6.838×10^{-4}		
8.446	3.816×10^{-4}	9.710	5.614×10^{-4}		
8.537	4.008×10^{-4}	8.867	4.705×10^{-4}		
9.012	4.640×10^{-4}	8.148	3.752×10^{-4}		
9.446	5.155×10^{-4}	7.533	2.905×10^{-4}		
9.804	5.542×10^{-4}	7.071	2.315×10^{-4}		
10.478	6.196×10^{-4}	6.624	1.732×10^{-4}		
10.805	6.443×10^{-4}	5.989	9.207×10^{-5}		
11.440	6.804×10^{-4}	5.423	3.985×10^{-5}		
11.979	6.904×10^{-4}	4.803	1.544×10^{-5}		
12.416	6.842×10^{-4}	4.262	9.114×10^{-6}		
12.126	6.894×10^{-4}	3.655	6.140×10^{-6}		
11.869	6.932×10^{-4}	2.553	3.341×10^{-6}		

p_o = 107 8 T_o = 495 T_w = 306					
y, cm	$\frac{T_o}{T_{oe}}$	y, cm	$\frac{T_o}{T_{oe}}$	y, cm	$\frac{T_o}{T_{oe}}$
0.287	0.628	9.987	0.973	1.405	0.673
1.077	0.646	9.134	0.965	1.669	0.680
1.915	0.693	8.458	0.963	0.584	0.636
1.405	0.668	7.308	0.954		
1.948	0.677	6.551	0.955		
3.066	0.772	3.378	0.917		
4.117	0.907	4.036	0.952		
3.363	0.848	4.874	0.958		
4.709	0.949	5.565	0.955		
5.926	0.952	6.337	0.955		
6.914	0.955	6.370	0.956		
8.047	0.959	5.334	0.961		
9.380	0.968	4.077	0.960		
11.008	0.982	3.790	0.938		
12.454	0.996	4.135	0.950		
14.115	1.001	3.459	0.898		
13.637	1.000	2.621	0.801		
12.700	1.000	1.824	0.733		
11.237	0.985	2.047	0.738		
p_o = 106.7 T_o = 886 T_w = 317					
0.155	0.353	13.310	0.995		
0.584	0.361	14.821	0.998		
0.698	0.384	16.114	0.997		
1.620	0.431	14.288	1.001		
2.664	0.513	12.288	1.001		
3.157	0.547	10.744	0.983		
3.823	0.621	9.380	0.964		
4.448	0.700	8.164	0.979		
5.286	0.820	6.998	0.934		
4.874	0.772	5.944	0.925		
5.385	0.839	4.859	0.851		
5.944	0.883	4.120	0.754		
6.665	0.915	2.870	0.570		
7.419	0.928	1.996	0.475		
8.146	0.938	0.533	0.406		
8.852	0.953				
10.104	0.970				
11.222	0.983				
12.225	0.992				

TABLE 3. – MEASURED PRESSURES AND TEMPERATURES AT χ = 1.625 – Continued

$p_o = 198$ $T_o = 520$ $p_w = 1.04 \times 10^{-4}$

y, cm	p_{o_2}/p_o	y, cm	p_{o_2}/p_o	y, cm	p_{o_2}/p_o
0.401	0.9460×10^{-6}	8.153	4.422×10^{-4}	8.352	4.680×10^{-4}
0.632	0.9956×10^{-6}	8.562	4.832×10^{-4}	8.036	4.458×10^{-4}
0.843	1.083×10^{-6}	9.012	5.228×10^{-4}	7.678	4.003×10^{-4}
1.466	1.497×10^{-6}	9.743	5.855×10^{-4}	7.336	3.622×10^{-4}
2.205	2.072×10^{-6}	10.503	6.048×10^{-4}	7.071	3.351×10^{-4}
2.500	3.186×10^{-6}	11.118	5.866×10^{-4}	6.716	2.895×10^{-4}
3.127	7.149×10^{-6}	11.730	5.429×10^{-4}	6.096	2.241×10^{-4}
3.510	1.738×10^{-5}	12.311	4.891×10^{-4}	5.674	1.893×10^{-4}
3.906	3.722×10^{-5}	12.852	4.502×10^{-4}	5.398	1.555×10^{-4}
4.275	5.831×10^{-5}	12.106	5.004×10^{-4}	5.001	1.280×10^{-4}
4.823	9.970×10^{-5}	11.692	5.428×10^{-4}	4.539	9.238×10^{-5}
5.055	1.189×10^{-4}	11.466	5.620×10^{-4}	4.117	5.961×10^{-5}
5.344	1.404×10^{-4}	11.163	5.879×10^{-4}	3.721	3.132×10^{-5}
5.878	1.904×10^{-4}	10.978	5.953×10^{-4}	3.233	1.066×10^{-5}
6.426	2.506×10^{-4}	10.363	6.061×10^{-4}	2.809	4.831×10^{-6}
6.703	2.768×10^{-4}	9.842	5.860×10^{-4}	2.545	3.545×10^{-6}
6.901	3.361×10^{-4}	9.497	5.695×10^{-4}	2.184	2.599×10^{-6}
7.468	3.659×10^{-4}	9.131	5.442×10^{-4}	1.384	1.550×10^{-6}
7.706	3.955×10^{-4}	8.603	4.994×10^{-4}	0.711	1.091×10^{-6}
				0.277	0.933×10^{-6}

$p_o = 203$ $T_o = 521$ $T_w = 317$

y, cm	T_o/T_{oe}	y, cm	T_o/T_{oe}	y, cm	T_o/T_{oe}
0.287	0.613	12.372	0.998	1.750	0.772
0.632	0.644	13.078	1.000	0.945	0.684
1.323	0.701	13.950	1.000		
1.577	0.716	14.379	1.002		
1.948	0.780	12.207	0.997		
2.753	0.902	9.428	0.981		
3.018	0.924	6.830	0.956		
3.708	0.943	5.550	0.951		
4.290	0.945	4.333	0.953		
4.958	0.945	2.047	0.880		
5.959	0.948	2.621	0.932		
6.789	0.957	3.246	0.950		
7.168	0.958	3.757	0.954		
7.506	0.961	4.117	0.950		
8.245	0.969	4.333	0.950		
9.002	0.975	3.624	0.956		
9.347	0.980	2.786	0.946		
10.744	0.993	2.029	0.832		
8.318	0.996	2.327	0.857		

$p_o = 200$ $T_o = 900$ $p_w = 1.45 \times 10^{-4}$

y, cm	p_{o_2}/p_o	y, cm	p_{o_2}/p_o	y, cm	p_{o_2}/p_o
0.251	9.495×10^{-7}	8.418	4.245×10^{-4}	7.257	3.187×10^{-4}
0.673	1.080×10^{-6}	8.854	4.720×10^{-4}	7.005	2.867×10^{-4}
1.107	1.312×10^{-6}	9.368	5.174×10^{-4}	6.624	2.406×10^{-4}
1.504	1.664×10^{-6}	10.119	5.670×10^{-4}	6.137	1.964×10^{-4}
1.900	2.142×10^{-6}	10.846	5.857×10^{-4}	5.812	1.576×10^{-4}
2.441	3.162×10^{-6}	11.494	5.656×10^{-4}	5.634	1.412×10^{-4}
2.875	4.319×10^{-6}	11.968	5.308×10^{-4}	5.344	1.160×10^{-4}
3.510	7.949×10^{-6}	12.441	4.992×10^{-4}	5.014	8.833×10^{-5}
3.833	1.288×10^{-5}	12.469	2.962×10^{-4}	4.638	5.872×10^{-5}
4.303	2.737×10^{-5}	11.953	5.295×10^{-4}	4.315	3.634×10^{-5}
4.552	4.152×10^{-5}	11.494	5.658×10^{-4}	3.906	1.714×10^{-5}
5.146	7.413×10^{-5}	11.283	5.790×10^{-4}	3.642	1.063×10^{-5}
5.212	8.704×10^{-5}	10.094	5.708×10^{-4}	3.272	6.629×10^{-6}
5.621	1.238×10^{-4}	9.342	5.284×10^{-4}	2.771	4.443×10^{-6}
6.017	1.584×10^{-4}	9.012	4.998×10^{-4}	2.520	3.500×10^{-6}
6.426	2.040×10^{-4}	8.590	4.609×10^{-4}	2.073	2.585×10^{-6}
6.723	2.368×10^{-4}	8.169	4.145×10^{-4}	1.504	1.775×10^{-6}
7.112	2.808×10^{-4}	7.864	3.841×10^{-4}	1.016	1.323×10^{-6}
7.534	3.266×10^{-4}	7.612	3.536×10^{-4}	0.382	0.969×10^{-6}
7.889	3.667×10^{-4}				

$p_o = 206$ $T_o = 888$ $T_w = 321$

y, cm	T_o/T_{oe}	y, cm	T_o/T_{oe}	y, cm	T_o/T_{oe}
0.231	0.377	8.920	0.970		
0.780	0.412	7.701	0.955		
1.372	0.462	5.878	0.934		
2.327	0.570	4.742	0.923		
3.066	0.657	4.069	0.891		
3.330	0.720	3.198	0.802		
3.995	0.823	2.705	0.712		
4.882	0.895	2.276	0.605		
5.550	0.920	1.110	0.473		
6.388	0.931	0.188	0.424		
6.914	0.941				
9.462	0.974				
10.726	0.992				
10.711	0.990				
11.895	0.998				
13.259	1.000				
13.259	0.999				
11.895	1.002				
10.546	0.989				

TABLE 3. – MEASURED PRESSURES AND TEMPERATURES AT χ = 1.625 – Concluded

y, cm	$\frac{p_{O_2}}{p_o}$	y, cm	$\frac{p_{O_2}}{p_o}$	y, cm	$\frac{p_{O_2}}{p_o}$
p_o = 268 T_o = 503 $p_w = 1.88 \times 10^{-4}$					
0.389	9.281×10^{-7}	8.103	4.644×10^{-4}	6.269	2.746×10^{-4}
1.016	1.159×10^{-6}	8.595	5.099×10^{-4}	5.740	2.175×10^{-4}
1.755	1.918×10^{-6}	8.946	5.414×10^{-4}	5.151	1.620×10^{-4}
2.256	3.302×10^{-6}	9.434	5.647×10^{-4}	4.737	1.280×10^{-4}
2.758	9.206×10^{-6}	9.883	5.709×10^{-4}	4.460	1.114×10^{-4}
3.127	2.235×10^{-5}	10.399	5.606×10^{-4}	4.196	9.424×10^{-5}
3.536	4.525×10^{-5}	10.846	5.268×10^{-4}	3.853	6.986×10^{-5}
3.906	6.701×10^{-5}	10.409	5.574×10^{-4}	3.523	4.856×10^{-5}
4.155	7.762×10^{-5}	10.068	5.691×10^{-4}	3.139	2.657×10^{-5}
4.460	9.816×10^{-5}	9.632	5.684×10^{-4}	2.652	1.196×10^{-5}
4.775	1.232×10^{-4}	9.210	5.578×10^{-4}	2 296	3.850×10^{-6}
5.080	1.483×10^{-4}	8.854	5.312×10^{-4}	1.768	2.190×10^{-6}
5.608	2.001×10^{-4}	8.471	5.056×10^{-4}	1 400	1.624×10^{-6}
6.071	2.459×10^{-4}	8.021	4.679×10^{-4}	0.884	1.233×10^{-6}
6.373	2.728×10^{-4}	7.732	4.395×10^{-4}	0.384	9.482×10^{-7}
6.822	3.295×10^{-4}	7.336	3.898×10^{-4}		
7.097	3.593×10^{-4}	7.071	3.589×10^{-4}		
7.323	3.887×10^{-4}	6.835	3.364×10^{-4}		
7.600	4.151×10^{-4}	6.596	3.104×10^{-4}		
p_o = 263 T_o = 887 $p_w = 1.87 \times 10^{-4}$					
0.264	9.212×10^{-7}	7.546	3.638×10^{-4}	7.099	3.263×10^{-4}
0.599	9.802×10^{-7}	7.904	3.998×10^{-4}	6.741	2.912×10^{-4}
1.107	1.255×10^{-6}	8.339	4.442×10^{-4}	6.347	2.471×10^{-4}
1.748	1.942×10^{-6}	8.628	4.758×10^{-4}		
2.334	3.226×10^{-6}	9.053	5.092×10^{-4}		
3.048	7.158×10^{-6}	9.474	5.610×10^{-4}		
3.437	1.309×10^{-5}	9.982	5.614×10^{-4}		
3.746	2.478×10^{-5}	10.549	5.674×10^{-4}		
4.155	4.697×10^{-5}	11.057	5.501×10^{-4}		
4.480	6.935×10^{-5}	11.532	5.180×10^{-4}		
4.790	9.233×10^{-5}	11.031	5.503×10^{-4}		
5.121	1.142×10^{-4}	10.610	5.670×10^{-4}		
5.398	1.380×10^{-4}	10.107	5.677×10^{-4}		
5.687	1.712×10^{-4}	9.594	5.477×10^{-4}		
5.989	1.979×10^{-4}	9.119	5.157×10^{-4}		
6.215	2.231×10^{-4}	8.788	4.921×10^{-4}		
6.624	2.606×10^{-4}	8.352	4.493×10^{-4}		
6.901	2.929×10^{-4}	7.930	4.134×10^{-4}		
7.231	3.278×10^{-4}	7.541	3.701×10^{-4}		

y, cm	$\frac{T_o}{T_{oe}}$	y, cm	$\frac{T_o}{T_{oe}}$	y, cm	$\frac{T_o}{T_{oe}}$
p_o = 274 T_o = 514 T_w = 302					
0.239	0.585	2.128	0.897		
1.209	0.716	1.890	0.919		
2.146	0.887	0.221	0.589		
2.179	0.920	2.146	0.883		
4.143	0.947				
5.138	0.952				
6.734	0.963				
7.572	0.972				
8.196	0.975				
10.366	0.993				
11.483	0.998				
12.784	1.000				
12.273	1.002				
10.942	0.999				
8.509	0.978				
7.226	0.967				
4.892	0.949				
0.231	0.609				
1.011	0.699				
p_o = 272 T_o = 893 T_w = 314					
0.485	0.380	3.970	0.923		
1.224	0.463	3.411	0.824		
1.356	0.497	4.333	0.908		
2.492	0.645	1.981	0.667		
2.639	0.685	1.250	0.499		
3.363	0.791				
4.529	0.887				
5.484	0.921				
7.028	0.951				
7.694	0.958				
8.491	0.970				
9.200	0.982				
10.284	0.991				
12.784	0.999				
11.814	1.000				
10.612	0.997				
6.436	0.946				
5.565	0.938				
4.727	0.933				

TABLE 4. – MEASURED PRESSURES AND TEMPERATURES AT χ = 2.793

$p_o = 108.2 \quad T_o = 500 \quad p_w = 0.395 \times 10^{-4}$

y, cm	$\frac{p_{O_2}}{p_o}$	y, cm	$\frac{p_{O_2}}{p_o}$	y, cm	$\frac{p_{O_2}}{p_o}$
4.595	0.1172×10^{-5}	20.157	3.722×10^{-4}	16.363	2.357×10^{-4}
4.999	0.1263×10^{-5}	20.828	3.949×10^{-4}	15.768	2.096×10^{-4}
5.811	0.1559×10^{-5}	21.587	4.106×10^{-4}	15.123	1.808×10^{-4}
6.576	0.1932×10^{-5}	22.070	4.169×10^{-4}	14.437	1.519×10^{-4}
7.737	0.2401×10^{-5}	23.152	4.248×10^{-4}	13.731	1.210×10^{-4}
8.153	0.3135×10^{-5}	23.866	4.217×10^{-4}	13.084	9.720×10^{-5}
8.956	0.4304×10^{-5}	24.544	4.208×10^{-4}	12.502	7.631×10^{-5}
9.799	0.7383×10^{-5}	24.958	4.220×10^{-4}	11.966	5.802×10^{-5}
10.780	2.269×10^{-5}	24.524	4.209×10^{-4}	11.394	4.013×10^{-5}
11.514	4.444×10^{-5}	23.978	4.219×10^{-4}	10.813	2.361×10^{-5}
12.116	6.237×10^{-5}	23.505	4.241×10^{-4}	10.267	1.465×10^{-5}
12.774	8.459×10^{-5}	23.022	4.251×10^{-4}	9.695	6.966×10^{-6}
13.477	1.105×10^{-4}	22.027	4.175×10^{-4}	9.124	4.777×10^{-6}
14.282	1.428×10^{-4}	21.468	4.098×10^{-4}	8.575	3.686×10^{-6}
15.240	1.817×10^{-4}	21.008	4.005×10^{-4}	8.067	3.048×10^{-6}
16.104	2.199×10^{-4}	20.325	3.809×10^{-4}	7.224	2.361×10^{-6}
16.916	2.536×10^{-4}	19.517	3.527×10^{-4}	6.515	1.932×10^{-6}
17.663	2.811×10^{-4}	18.872	3.314×10^{-4}	5.712	1.544×10^{-6}
18.412	3.096×10^{-4}	18.265	3.116×10^{-4}	4.628	1.161×10^{-6}
19.263	3.406×10^{-4}	17.109	2.666×10^{-4}		

$p_o = 110.2 \quad T_o = 934 \quad p_w = 0.395 \times 10^{-4}$

y, cm	$\frac{p_{O_2}}{p_o}$	y, cm	$\frac{p_{O_2}}{p_o}$	y, cm	$\frac{p_{O_2}}{p_o}$
0.460	1.481×10^{-6}	24.130	4.050×10^{-4}		
1.497	1.625×10^{-6}	23.677	4.157×10^{-4}		
2.864	1.931×10^{-6}	20.593	3.994×10^{-4}		
4.130	2.172×10^{-6}	18.034	3.151×10^{-4}		
5.268	2.602×10^{-6}	16.210	2.534×10^{-4}		
6.641	3.463×10^{-6}	12.903	1.155×10^{-4}		
7.813	4.338×10^{-6}	10.311	2.001×10^{-5}		
9.173	5.965×10^{-6}	7.820	6.176×10^{-6}		
10.372	1.558×10^{-5}	5.308	3.225×10^{-6}		
11.631	5.015×10^{-5}	2.864	2.172×10^{-6}		
12.971	1.053×10^{-4}	0.473	1.644×10^{-6}		
14.304	1.604×10^{-4}				
15.476	2.106×10^{-4}				
16.715	2.608×10^{-4}				
18.034	3.142×10^{-4}				
19.300	3.572×10^{-4}				
20.512	3.961×10^{-4}				
21.805	4.113×10^{-4}				
23.078	4.107×10^{-4}				

$p_o = 105.9 \quad T_o = 523 \quad T_w = 300$

y, cm	$\frac{T_O}{T_{Oe}}$	y, cm	$\frac{T_O}{T_{Oe}}$	y, cm	$\frac{T_O}{T_{Oe}}$
0.254	0.577	16.916	0.973	17.450	0.977
2.413	0.611	17.958	0.973	16.383	0.976
4.216	0.661	18.974	0.976	15.850	0.976
4.902	0.678	19.914	0.978	15.418	0.977
5.105	0.688	20.625	0.981	15.088	0.978
5.563	0.708	21.438	0.984	14.656	0.977
5.944	0.710	22.327	0.988	12.675	0.970
6.325	0.732	22.885	0.991	11.278	0.970
6.604	0.751	23.571	0.995	10.566	0.968
7.137	0.764	23.876	0.996	10.084	0.963
7.823	0.802	25.883	1.000	9.652	0.961
8.814	0.857	24.663	0.998	8.763	0.936
9.677	0.912	22.733	0.993	8.331	0.917
10.744	0.944	21.920	0.991	8.001	0.908
11.786	0.962	21.209	0.986	6.477	0.847
12.954	0 970	20.193	0.982	6.452	0.833
13.437	0.971	19.507	0.980		
14.605	0.971	18.745	0.978		
15.875	0.972	18.059	0.978		

$p_o = 110.6 \quad T_o = 967 \quad T_w = 300$

y, cm	$\frac{T_O}{T_{Oe}}$	y, cm	$\frac{T_O}{T_{Oe}}$	y, cm	$\frac{T_O}{T_{Oe}}$
0.203	0.345	16.820	0.957	17.232	0.967
1.494	0.366	17.297	0.962	16.129	0.958
1.354	0.366	17.747	0.966	15.014	0.951
2.606	0.384	18.232	0.970	14.188	0.945
4.750	0.433	18.522	0.970	13.673	0.946
4.554	0.432	18.786	0.973	13.505	0.944
5.672	0.474	19.322	0.977	12.954	0.938
5.339	0.470	19.708	0.981	12.512	0.930
8.250	0.576	20.328	0.985	11.925	0.919
9.832	0.663	20.907	0.987	12.093	0.925
9.416	0.641	21.463	0.990	11.608	0.907
11.361	0.786	22.235	0.994	11.105	0.874
12.024	0.834	23.726	0.999	10.983	0.881
12.210	0.855	24.397	1 001	10.815	0.860
12.611	0.873	25.461	1.001	10.698	0.838
13.170	0.896	25.483	0.996	8.766	0.735
13.586	0.908	23.927	0.999	9.126	0.744
14.034	0.918	23.114	0.996	8.158	0.709
14.653	0.929	22.050	0.994	7.866	0.681
15.291	0.939	20.864	0.988	7.744	0.661
15.819	0.948	19.230	0.978	4.486	0.586
16.360	0.954	18.212	0.971		

TABLE 4. – MEASURED PRESSURES AND TEMPERATURES AT χ = 2.793 –Continued

$p_o = 200$ $T_o = 514$ $p_w = 0.553 \times 10^{-4}$

y, cm	p_{O_2}/p_o	y, cm	p_{O_2}/p_o	y, cm	p_{O_2}/p_o
4.638	1.094×10^{-6}	17.785	3.118×10^{-4}	12.850	1.328×10^{-4}
5.118	1.222×10^{-6}	18.334	3.258×10^{-4}	12.235	1.120×10^{-4}
5.832	1.567×10^{-6}	19.400	3.360×10^{-4}	11.631	9.355×10^{-5}
6.477	2.120×10^{-6}	19.942	3.355×10^{-4}	10.836	7.013×10^{-5}
7.336	3.537×10^{-6}	20.556	3.289×10^{-4}	10.203	5.372×10^{-5}
8.174	9.413×10^{-6}	21.133	3.190×10^{-4}	9.606	3.854×10^{-5}
8.992	2.462×10^{-5}	21.605	3.095×10^{-4}	8.910	6.548×10^{-6}
9.700	4.076×10^{-5}	20.594	3.295×10^{-4}	8.166	9.222×10^{-6}
10.556	6.243×10^{-5}	19.954	3.351×10^{-4}	7.620	4.766×10^{-6}
11.234	8.248×10^{-5}	19.195	3.356×10^{-4}	7.142	3.047×10^{-6}
11.737	9.815×10^{-5}	18.550	3.296×10^{-4}	6.558	2.190×10^{-6}
12.334	1.176×10^{-4}	17.854	3.165×10^{-4}	6.055	1.767×10^{-6}
13.030	1.437×10^{-4}	17.114	2.937×10^{-4}	5.583	1.470×10^{-6}
13.823	1.747×10^{-4}	16.413	2.701×10^{-4}	4.994	1.207×10^{-6}
14.506	2.037×10^{-4}	15.842	2.505×10^{-4}	4.633	1.081×10^{-6}
15.154	2.290×10^{-4}	15.189	2.261×10^{-4}		
15.842	2.531×10^{-4}	14.587	2.012×10^{-4}		
16.345	2.710×10^{-4}	14.059	1.810×10^{-4}		
17.046	2.889×10^{-4}	13.358	1.537×10^{-4}		

$p_o = 200$ $T_o = 498$ $T_w = 297$

y, cm	T_o/T_{oe}	y, cm	T_o/T_{oe}	y, cm	T_o/T_{oe}
0.274	0.612	17.252	0.981	7.854	0.995
1.224	0.617	18.090	0.984	6.584	0.987
1.646	0.621	18.844	0.988	6.843	0.990
1.852	0.632	19.637	0.992	8.049	0.990
2.819	0.648	20.264	0.995	8.649	0.987
3.607	0.672	20.978	0.999	9.352	0.983
4.498	0.727	21.824	1.000	10.196	0.979
5.050	0.758	21.946	1.001	10.996	0.983
5.756	0.800	20.864	0.996	12.118	0.976
6.525	0.851	19.825	0.996	13.292	0.975
7.602	0.911	18.753	0.993	14.684	0.977
9.601	0.955	17.755	0.985	12.794	0.976
10.531	0.965	16.695	0.980	11.654	0.977
11.491	0.969	14.808	0.979	9.479	0.985
12.626	0.971	13.510	0.976	7.178	0.999
13.812	0.974	12.626	0.977	5.832	0.956
14.722	0.975	11.369	0.978	5.039	0.892
15.684	0.977	10.107	0.981	4.362	0.818
16.535	0.979	9.098	0.987		

$p_o = 201$ $T_o = 917$ $p_w = 0.553 \times 10^{-4}$

y, cm	p_{O_2}/p_o	y, cm	p_{O_2}/p_o	y, cm	p_{O_2}/p_o
4.564	1.220×10^{-6}	17.737	2.788×10^{-4}	14.625	1.704×10^{-4}
5.011	1.340×10^{-6}	18.270	2.934×10^{-4}	13.878	1.417×10^{-4}
5.626	1.630×10^{-6}	18.824	3.027×10^{-4}	13.246	1.183×10^{-4}
6.284	2.043×10^{-6}	19.388	3.140×10^{-4}	12.662	9.742×10^{-5}
6.695	2.359×10^{-6}	19.934	3.199×10^{-4}	12.111	7.901×10^{-5}
7.371	3.042×10^{-6}	20.594	3.227×10^{-4}	11.471	5.952×10^{-5}
8.446	5.171×10^{-6}	21.252	3.215×10^{-4}	10.955	4.279×10^{-5}
9.327	1.110×10^{-5}	21.935	3.125×10^{-4}	10.478	3.029×10^{-5}
10.284	2.660×10^{-5}	22.443	3.096×10^{-4}	9.967	2.022×10^{-5}
11.102	4.410×10^{-5}	22.232	3.090×10^{-4}	9.416	1.147×10^{-5}
11.575	6.027×10^{-5}	21.532	3.177×10^{-4}	8.956	7.489×10^{-6}
12.322	8.259×10^{-5}	20.810	3.228×10^{-4}	8.501	5.273×10^{-6}
12.830	1.014×10^{-4}	20.058	3.200×10^{-4}	7.894	3.883×10^{-6}
13.668	1.305×10^{-4}	19.301	3.131×10^{-4}	7.447	3.243×10^{-6}
14.506	1.752×10^{-4}	18.468	3.006×10^{-4}	7.023	2.703×10^{-6}
15.291	1.930×10^{-4}	17.887	2.845×10^{-4}	6.528	2.276×10^{-6}
15.898	2.166×10^{-4}	17.148	2.604×10^{-4}	6.104	2.011×10^{-6}
16.358	2.330×10^{-4}	16.754	2.477×10^{-4}	5.720	1.727×10^{-6}
16.817	2.476×10^{-4}	16.027	2.210×10^{-4}	5.187	1.454×10^{-6}
17.315	2.644×10^{-4}	15.433	1.984×10^{-4}	4.615	1.217×10^{-6}

$p_o = 200$ $T_o = 958$ $T_w = 340$

y, cm	T_o/T_{oe}	y, cm	T_o/T_{oe}	y, cm	T_o/T_{oe}
0.264	0.365	16.764	0.974	10.653	0.934
2.057	0.382	17.498	0.977	10.061	0.926
3.421	0.432	18.369	0.983	9.164	0.900
3.960	0.452	19.037	0.986	8.552	0.874
3.226	0.444	19.792	0.992	8.804	0.890
5.197	0.506	21.720	0.994	8.054	0.855
4.577	0.496	22.603	1.000	7.094	0.779
3.950	0.487	23.030	1.001	7.597	0.794
7.920	0.683	22.565	0.999	7.894	0.814
6.116	0.589	21.900	0.999	5.989	0.664
9.479	0.852	20.907	0.997	5.705	0.624
10.450	0.898	19.842	0.993		
9.764	0.872	18.722	0.988		
11.057	0.919	17.206	0.980		
12.194	0.939	16.192	0.976		
13.254	0.950	15.182	0.972		
14.470	0.961	13.368	0.960		
15.352	0.965	12.034	0.953		
16.154	0.970	11.171	0.940		

TABLE 4. – MEASURED PRESSURES AND TEMPERATURES AT χ = 2.793 – Concluded

$p_o = 270 \quad T_o = 506 \quad p_w = 0.658 \times 10^{-4}$

y, cm	p_{O_2}/p_o	y, cm	p_{O_2}/p_o	y, cm	p_{O_2}/p_o
4.602	1.127×10^{-6}	16.474	2.714×10^{-4}	15.748	2.449×10^{-4}
4.839	1.196×10^{-6}	16.934	2.841×10^{-4}	15.072	2.204×10^{-4}
5.819	1.942×10^{-6}	17.643	2.991×10^{-4}	14.214	1.920×10^{-4}
6.614	3.857×10^{-6}	18.214	3.040×10^{-4}	13.457	1.644×10^{-4}
7.775	1.545×10^{-5}	18.661	3.065×10^{-4}	12.817	1.402×10^{-4}
8.608	3.025×10^{-5}	19.185	3.046×10^{-4}	12.266	1.231×10^{-4}
9.129	4.076×10^{-5}	19.581	3.017×10^{-4}	11.730	1.066×10^{-4}
9.507	4.972×10^{-5}	20.053	2.943×10^{-4}	11.097	9.025×10^{-5}
9.974	5.966×10^{-5}	20.574	2.856×10^{-4}	10.500	7.422×10^{-5}
10.384	6.988×10^{-5}	21.059	2.739×10^{-4}	9.893	5.966×10^{-5}
10.861	8.148×10^{-5}	21.506	2.674×10^{-4}	9.395	4.909×10^{-5}
11.471	1.011×10^{-4}	20.985	2.761×10^{-4}	8.961	3.978×10^{-5}
12.179	1.232×10^{-4}	20.102	2.920×10^{-4}	8.613	3.357×10^{-5}
12.662	1.408×10^{-4}	19.370	3.027×10^{-4}	7.607	1.548×10^{-5}
13.172	1.578×10^{-4}	18.915	3.066×10^{-4}	7.186	9.206×10^{-6}
13.670	1.784×10^{-4}	18.476	3.071×10^{-4}	6.439	3.390×10^{-6}
14.376	2.030×10^{-4}	18.029	3.029×10^{-4}	5.931	2.132×10^{-6}
14.836	2.190×10^{-4}	17.544	2.962×10^{-4}	5.347	1.525×10^{-6}
15.283	2.322×10^{-4}	16.947	2.837×10^{-4}	4.628	1.137×10^{-6}
15.743	2.487×10^{-4}	16.307	2.644×10^{-4}		

$p_o = 265 \quad T_o = 523 \quad T_w = 300$

y, cm	T_o/T_{oe}	y, cm	T_o/T_{oe}	y, cm	T_o/T_{oe}
0.432	0.630	22.327	0.998	6.528	0.967
0.660	0.641	23.165	0.998	4.826	0.911
2.388	0.666	25.603	1.000	3.680	0.886
3.124	0.691	25.197	1.001		
5.080	0.811	24.613	1.000		
5.512	0.873	24.282	1.000		
6.299	0.898	23.520	1.000		
7.087	0.942	21.895	0.999		
8.230	0.956	20.168	0.994		
9.347	0.964	19.964	0.993		
10.465	0.966	18.009	0.985		
11.659	0.967	16.154	0.978		
12.573	0.967	14.529	0.974		
14.199	0.972	12.878	0.972		
16.053	0.976	11.049	0.973		
17.348	0.979	9.220	0.976		
18.846	0.987	7.112	0.980		
19.406	0.990	6.299	0.976		
21.311	0.996	5.283	0.955		

$p_o = 271 \quad T_o = 906 \quad p_w = 0.658 \times 10^{-4}$

y, cm	p_{O_2}/p_o	y, cm	p_{O_2}/p_o	y, cm	p_{O_2}/p_o
4.676	1.184×10^{-6}	16.474	2.429×10^{-4}	12.476	1.010×10^{-4}
5.309	1.450×10^{-6}	17.036	2.596×10^{-4}	11.732	7.797×10^{-5}
6.452	2.214×10^{-6}	17.419	2.711×10^{-4}	10.825	5.349×10^{-5}
6.800	2.614×10^{-6}	17.965	2.838×10^{-4}	10.005	3.320×10^{-5}
7.203	3.183×10^{-6}	18.537	2.930×10^{-4}	9.408	2.085×10^{-5}
7.882	4.785×10^{-6}	19.121	2.978×10^{-4}	8.743	1.093×10^{-5}
8.613	9.743×10^{-6}	19.891	2.986×10^{-4}	7.930	5.255×10^{-6}
9.309	2.012×10^{-5}	20.057	2.940×10^{-4}	7.173	3.165×10^{-6}
9.954	3.310×10^{-5}	19.766	2.988×10^{-4}	6.540	2.393×10^{-6}
10.427	4.311×10^{-5}	19.276	2.991×10^{-4}	6.091	2.005×10^{-6}
11.260	5.980×10^{-5}	18.600	2.944×10^{-4}	5.410	1.538×10^{-6}
11.819	7.933×10^{-5}	21.590	2.870×10^{-4}	4.663	1.181×10^{-6}
12.416	9.818×10^{-5}	17.840	2.832×10^{-4}		
12.974	1.172×10^{-4}	17.148	2.657×10^{-4}		
13.546	1.387×10^{-4}	16.457	2.448×10^{-4}		
13.972	1.568×10^{-4}	15.593	2.165×10^{-4}		
14.719	1.826×10^{-4}	14.712	1.872×10^{-4}		
15.347	2.069×10^{-4}	13.891	1.566×10^{-4}		
15.979	2.269×10^{-4}	13.185	1.290×10^{-4}		

$p_o = 272 \quad T_o = 913 \quad T_w = 297$

y, cm	T_o/T_{oe}	y, cm	T_o/T_{oe}	y, cm	T_o/T_{oe}
0.269	0.354	19.921	0.994	12.375	0.961
2.108	0.368	21.229	0.996	11.712	0.958
3.109	0.406	21.773	0.997	11.659	0.959
4.699	0.483	22.906	0.999	11.143	0.955
3.526	0.443	22.591	1.000	10.427	0.958
5.283	0.518	21.844	1.000	9.776	0.948
4.354	0.483	21.036	0.999	9.164	0.935
6.744	0.635	20.244	0.998	8.849	0.928
6.162	0.599	19.192	0.995	8.712	0.921
10.602	0.906	18.392	0.990	6.792	0.838
9.294	0.886	17.592	0.984	7.577	0.862
8.138	0.841	17.239	0.984	6.210	0.773
10.305	0.917	16.162	0.978	6.121	0.772
11.646	0.940	15.446	0.976	6.998	0.815
12.794	0.951	14.793	0.972	5.778	0.517
12.954	0.956	14.315	0.969	6.830	0.708
14.750	0.966	13.769	0.968	5.278	0.615
16.393	0.975	13.472	0.965	7.912	0.831
17.521	0.981	13.226	0.964	7.074	0.754
18.781	0.990	12.672	0.963	6.327	0.690

TABLE 5. – MEASURED PRESSURES AND TEMPERATURES AT $\chi = 3.56$

y, cm	p_{O_2}/p_o	y, cm	p_{O_2}/p_o	y, cm	p_{O_2}/p_o
$p_o = 201$ $T_o = 538$ $p_w = 0.504 \times 10^{-4}$					
3.213	3.393×10^{-7}	21.206	2.257×10^{-4}	15.781	8.894×10^{-5}
4.816	4.797×10^{-7}	22.177	2.396×10^{-4}	13.924	4.492×10^{-5}
5.804	6.208×10^{-7}	23.175	2.525×10^{-4}	12.200	1.499×10^{-5}
7.176	8.809×10^{-7}	24.879	2.663×10^{-4}	12.974	2.585×10^{-5}
8.212	1.183×10^{-6}	26.144	2.767×10^{-4}	12.395	1.759×10^{-5}
9.212	1.673×10^{-6}	27.635	2.815×10^{-4}	11.829	1.052×10^{-5}
9.761	2.130×10^{-6}	28.971	2.823×10^{-4}	11.082	5.528×10^{-6}
10.990	5.396×10^{-6}	28.971	3.498×10^{-4}	10.444	3.167×10^{-6}
12.179	1.445×10^{-5}	29.675	2.853×10^{-4}	9.304	1.708×10^{-6}
12.898	2.435×10^{-5}	28.461	2.831×10^{-4}	7.099	8.679×10^{-7}
12.873	2.296×10^{-5}	26.960	2.818×10^{-4}	4.958	5.046×10^{-7}
14.046	4.367×10^{-5}	25.644	2.722×10^{-4}	1.346	2.696×10^{-7}
15.067	6.575×10^{-5}	24.226	2.614×10^{-4}		
15.832	8.806×10^{-5}	23.084	2.527×10^{-4}		
16.794	1.130×10^{-4}	21.453	2.305×10^{-4}		
17.587	1.364×10^{-4}	20.228	2.080×10^{-4}		
18.504	1.604×10^{-4}	18.811	1.724×10^{-4}		
19.434	1.834×10^{-4}	17.892	1.486×10^{-4}		
20.513	2.131×10^{-4}	16.126	9.639×10^{-5}		
$p_o = 270$ $T_o = 519$ $p_w = 0.645 \times 10^{-4}$					
1.336	2.489×10^{-7}	18.717	1.745×10^{-4}	18.892	1.829×10^{-4}
3.734	3.694×10^{-7}	19.657	1.981×10^{-4}	18.316	1.689×10^{-4}
5.060	5.205×10^{-7}	20.952	2.240×10^{-4}	17.219	1.405×10^{-4}
6.027	7.227×10^{-7}	22.075	2.360×10^{-4}	15.822	1.044×10^{-4}
7.150	9.513×10^{-7}	23.320	2.419×10^{-4}	14.684	7.316×10^{-5}
8.344	1.532×10^{-6}	24.534	2.485×10^{-4}	15.494	9.308×10^{-5}
9.129	2.400×10^{-6}	25.583	2.508×10^{-4}	14.925	8.051×10^{-5}
9.906	4.043×10^{-6}	26.929	2.488×10^{-4}	13.363	4.403×10^{-5}
10.752	7.491×10^{-6}	28.349	2.426×10^{-4}	12.878	3.539×10^{-5}
11.587	1.315×10^{-5}	30.122	2.357×10^{-4}	11.844	2.032×10^{-5}
11.628	1.242×10^{-5}	31.189	2.285×10^{-4}	11.087	1.191×10^{-5}
12.004	1.711×10^{-5}	29.929	2.362×10^{-4}	10.528	7.609×10^{-6}
12.873	2.669×10^{-5}	28.766	2.410×10^{-4}	9.974	4.747×10^{-6}
13.843	4.391×10^{-5}	27.409	2.473×10^{-4}	9.119	2.481×10^{-6}
14.379	5.597×10^{-5}	26.098	2.518×10^{-4}	7.671	1.236×10^{-6}
15.588	8.549×10^{-5}	24.737	2.498×10^{-4}	6.599	8.630×10^{-7}
16.586	1.116×10^{-4}	23.350	2.429×10^{-4}	2.652	3.371×10^{-7}
17.361	1.371×10^{-4}	22.334	2.381×10^{-4}	1.336	2.715×10^{-7}
17.790	1.502×10^{-4}	20.513	2.181×10^{-4}	3.203	3.689×10^{-7}

y, cm	T_o/T_{oe}	y, cm	T_o/T_{oe}	y, cm	T_o/T_{oe}
$p_o = 201$ $T_o = 538$ $T_w = 297$					
2.075	0.679	20.843	0.976	14.981	0.970
3.658	0.675	22.029	0.979	14.640	0.967
4.663	0.675	23.734	0.984	12.781	0.961
6.035	0.679	24.996	0.990	11.834	0.944
7.066	0.687	26.487	0.995	11.252	0.928
8.067	0.706	27.821	0.997	10.686	0.902
8.623	0.718	25.342	0.998	9.944	0.879
9.848	0.767	29.434	0.999	9.306	0.853
10.330	0.794	29.118	0.998	8.164	0.819
11.034	0.836	28.524	1.001	5.959	0.783
11.730	0.871	27.313	0.996	3.818	0.755
12.903	0.906	25.809	0.992		
13.924	0.929	24.493	0.989		
14.691	0.946	23.081	0.983		
15.651	0.957	21.940	0.980		
16.439	0.960	20.307	0.978		
17.361	0.966	19.083	0.975		
19.368	0.973	17.663	0.970		
20.063	0.974	16.749	0.970		
$p_o = 270$ $T_o = 519$ $T_w = 297$					
2.596	0.635	19.804	0.975	15.291	0.966
3.932	0.637	20.297	0.981	14.679	0.965
4.890	0.646	22.172	0.983	13.543	0.966
6.010	0.656	23.383	0.986	14.315	0.961
7.203	0.683	24.435	0.963	13.782	0.960
7.991	0.715	25.784	0.996	12.220	0.958
8.763	0.754	27.196	0.998	11.737	0.951
9.609	0.807	28.976	1.000	10.698	0.946
10.485	0.844	30.922	0.998	9.936	0.928
10.866	0.867	28.783	1.000	9.383	0.905
11.730	0.890	27.615	0.999	8.821	0.889
12.697	0.929	26.261	0.997	8.435	0.879
13.233	0.938	24.950	0.992	7.978	0.859
14.445	0.949	23.592	0.989	6.533	0.832
15.446	0.958	22.205	0.984	5.461	0.812
16.220	0.960	21.186	0.981		
16.645	0.964	19.368	0.975		
17.574	0.968	17.747	0.969		
18.509	0.971	16.124	0.966		

TABLE 5. – MEASURED PRESSURES AND TEMPERATURES AT χ = 3.56 – Concluded

$p_o = 270$ $T_o = 892$ $p_w = 0.645 \times 10^{-4}$						$p_o = 270$ $T_o = 892$ $T_w = 297$					
y, cm	$\frac{p_{O_2}}{p_o}$	y, cm	$\frac{p_{O_2}}{p_o}$	y, cm	$\frac{p_{O_2}}{p_o}$	y, cm	$\frac{T_o}{T_{oe}}$	y, cm	$\frac{T_o}{T_{oe}}$	y, cm	$\frac{T_o}{T_{oe}}$
1.326	2.543×10^{-7}	27.531	2.571×10^{-4}	7.706	1.342×10^{-6}	2.619	0.407	28.466	0.995	13.007	0.892
3.754	4.241×10^{-7}	25.839	2.659×10^{-4}	7.120	1.082×10^{-6}	5.468	0.422	27.556	0.992	11.699	0.840
6.609	9.174×10^{-7}	24.359	2.576×10^{-4}	5.753	7.350×10^{-7}	6.624	0.451	26.383	0.994	10.693	0.768
7.762	1.273×10^{-6}	23.150	2.483×10^{-4}	3.891	4.532×10^{-7}	7.950	0.506	24.681	0.990	9.629	0.736
9.093	1.982×10^{-6}	22.166	2.411×10^{-4}	2.530	3.315×10^{-7}	9.383	0.571	23.210	0.983	8.075	0.680
10.528	3.942×10^{-6}	23.690	2.527×10^{-4}	1.326	2.762×10^{-7}	10.472	0.642	22.004	0.979	6.706	0.601
11.613	7.728×10^{-6}	24.864	2.619×10^{-4}			11.377	0.705	21.018	0.968	5.979	0.581
12.517	1.362×10^{-5}	26.271	2.661×10^{-4}			12.710	0.783	22.545	0.980	4.610	0.449
13.853	2.764×10^{-5}	27.970	2.566×10^{-4}			13.769	0.827	23.718	0.985		
14.912	4.569×10^{-5}	26.083	2.655×10^{-4}			14.851	0.869	25.126	0.995		
15.994	7.064×10^{-5}	23.574	2.526×10^{-4}			16.292	0.912	26.822	0.996		
17.447	1.096×10^{-4}	20.361	2.075×10^{-4}			17.282	0.935	28.395	1.000		
18.428	1.434×10^{-4}	17.983	1.373×10^{-4}			18.715	0.958	26.642	1.001		
19.860	1.857×10^{-4}	16.617	9.785×10^{-5}			20.894	0.971	24.933	0.985		
22.045	2.332×10^{-4}	15.270	6.512×10^{-5}			22.487	0.978	22.431	0.989		
24.143	2.498×10^{-4}	14.153	4.091×10^{-5}			24.544	0.984	19.213	0.960		
25.695	2.636×10^{-4}	12.842	1.939×10^{-5}			26.894	1.002	16.838	0.941		
28.042	2.549×10^{-4}	11.834	1.011×10^{-5}			29.238	1.002	15.471	0.931		
28.704	2.505×10^{-4}	9.218	2.130×10^{-6}			29.207	0.994	14.130	0.917		

TABLE 6. – COMPUTED PARAMETERS FOR χ = 0.508

p_{Oe} = 66.1 $p_w = 5.26 \times 10^{-4}$ $p_e = 3.74 \times 10^{-4}$ T_O = 499 T_w = 362 T_e = 394

u_e = 2668 M_e = 19.4 $\rho_e = 4.62 \times 10^{-3}$ $\frac{Re}{m} = 8.52 \times 10^{6}$ δ = 2.87

$\frac{\delta^*}{\delta}$ = 0.520 $\frac{\theta}{\delta}$ = 0.00568 $\frac{\Gamma}{\delta}$ = 0.0109 R_θ = 1381

$\frac{y}{\delta}$	$\frac{p_{O_2}}{p_{O_{2e}}}$	$\frac{T_O}{T_{Oe}}$	$\frac{u}{u_e}$	$\frac{\rho}{\rho_e}$	$\frac{T_O - T_w}{T_{Oe} - T_w}$	$\frac{T}{T_e}$	$\frac{M}{M_e}$
1.0000	1.0000	1.0000	1.0000	1.0000	1.0000	1.0	0.9989
0.9244	1.0385	0.9933	0.9967	1.0454	0.9757	1.0	1.0025
0.8889	1.0321	0.9866	0.9932	1.0461	0.9514	1.0	0.9924
0.8000	0.9551	0.9777	0.9883	0.9778	0.9190	1.1	0.9385
0.7111	0.8141	0.9699	0.9834	0.8416	0.8907	1.3	0.8522
0.6222	0.6603	0.9677	0.9808	0.6859	0.8826	1.7	0.7551
0.5333	0.4936	0.9699	0.9794	0.5140	0.8907	2.3	0.6427
0.4444	0.3365	0.9792	0.9793	0.3502	0.9245	3.5	0.5225
0.3556	0.1827	1.0065	0.9804	0.1892	1.0237	6.7	0.3789
0.3111	0.0913	1.0103	0.9564	0.0988	1.0373	13.0	0.2652
0.2667	0.0321	0.9912	0.8652	0.0414	0.9679	31.5	0.1543
0.1778	0.0076	0.8866	0.5769	0.0190	0.5879	70.4	0.0688
0.0889	0.0045	0.7960	0.4110	0.0173	0.2584	79.5	0.0461
0.0000	0.0026	0.7249	0.0027	0.0154	0.0000	91.7	0.0003

p_{Oe} = 66.2 $p_w = 5.26 \times 10^{-4}$ $p_e = 3.93 \times 10^{-4}$ T_O = 820 T_w = 397 T_e = 6.56

u_e = 2908 M_e = 19.2 $\rho_e = 2.92 \times 10^{-3}$ $\frac{Re}{m} = 4.89 \times 10^{6}$ δ = 2.87

$\frac{\delta^*}{\delta}$ = 0.544 $\frac{\theta}{\delta}$ = 0.00650 $\frac{\Gamma}{\delta}$ = 0.0122 R_θ = 913

$\frac{y}{\delta}$	$\frac{p_{O_2}}{p_{O_{2e}}}$	$\frac{T_O}{T_{Oe}}$	$\frac{u}{u_e}$	$\frac{\rho}{\rho_e}$	$\frac{T_O - T_w}{T_{Oe} - T_w}$	$\frac{T}{T_e}$	$\frac{M}{M_e}$
1.0000	1.0000	1.0000	1.0000	1.0001	1.0000	1.0	1.0000
0.9027	1.0685	0.9898	0.9950	1.0794	0.9802	1.0	1.0171
0.7965	0.9751	0.9798	0.9894	0.9960	0.9608	1.1	0.9551
0.7080	0.8224	0.9702	0.9836	0.8498	0.9424	1.3	0.8650
0.6195	0.6480	0.9596	0.9766	0.6790	0.9218	1.7	0.7575
0.5310	0.4455	0.9568	0.9718	0.4711	0.9163	2.5	0.6197
0.4425	0.1963	0.9595	0.9599	0.2121	0.9215	5.7	0.4055
0.3540	0.0467	0.9346	0.8797	0.0591	0.8734	20.9	0.1938
0.2655	0.0140	0.8549	0.6944	0.0268	0.7190	47.1	0.1018
0.1770	0.0070	0.7067	0.5051	0.0228	0.4320	56.7	0.0675
0.0885	0.0044	0.5827	0.3510	0.0230	0.1918	57.6	0.0465
0.0000	0.0025	0.4836	0.0075	0.0224	+0.0000	60.5	0.0010

p_{Oe} = 107.6 $p_w = 8.61 \times 10^{-4}$ $p_e = 5.41 \times 10^{-4}$ T_O = 315 T_w = 333 T_e = 2.36

u_e = 1803 M_e = 19.9 $\rho_e = 1.11 \times 10^{-2}$ $\frac{Re}{m} = 2.27 \times 10^{7}$ δ = 2.72

$\frac{\delta^*}{\delta}$ = 0.519 $\frac{\theta}{\delta}$ = 0.00430 $\frac{\Gamma}{\delta}$ = 0.00838 R_θ = 2662

$\frac{y}{\delta}$	$\frac{p_{O_2}}{p_{O_{2e}}}$	$\frac{T_O}{T_{Oe}}$	$\frac{u}{u_e}$	$\frac{\rho}{\rho_e}$	$\frac{T_O - T_w}{T_{Oe} - T_w}$	$\frac{T}{T_e}$	$\frac{M}{M_e}$
1.0000	1.0000	1.0000	1.0000	1.0000	1.0000	1.0	1.0000
0.9065	1.0411	0.9929	0.9964	1.0486	1.1212	1.0	0.9929
0.8411	1.0137	0.9877	0.9935	1.0269	1.2121	1.1	0.9620
0.7477	0.8733	0.9806	0.9891	0.8925	1.3333	1.3	0.8708
0.6542	0.6918	0.9788	0.9866	0.7103	1.3636	1.7	0.7567
0.5607	0.5034	0.9788	0.9838	0.5196	1.3636	2.4	0.6309
0.4673	0.3322	0.9859	0.9820	0.3437	1.2424	3.8	0.5012
0.3738	0.2123	0.9982	0.9791	0.2206	1.0303	6.3	0.3921
0.2804	0.1267	1.0282	0.9767	0.1318	0.5152	10.9	0.2963
0.1869	0.0404	1.0936	0.9256	0.0459	−0.6074	32.5	0.1625
0.0935	0.0061	1.0904	0.5587	0.0148	−0.5536	104.3	0.0548
0.0000	0.0027	1.0582	0.0119	0.0113	−0.0000	141.4	0.0010

TABLE 6. – COMPUTED PARAMETERS FOR x = 0.508 – Continued

p_{Oe} = 107.6 $p_w = 8.61 \times 10^{-4}$ $p_e = 5.09 \times 10^{-4}$ T_O = 393 T_w = 333 T_e = 2.88

u_e = 2014 M_e = 19.9 $\rho_e = 8.61 \times 10^{-3}$ $\frac{Re}{m} = 1.73 \times 10^7$ δ = 2.74

$\frac{\delta^*}{\delta}$ = 0.505 $\frac{\theta}{\delta}$ = 0.00550 $\frac{\Gamma}{\delta}$ = 0.0107 R_θ = 2608

$\frac{y}{\delta}$	$\frac{p_{O_2}}{p_{O_{2e}}}$	$\frac{T_O}{T_{Oe}}$	$\frac{u}{u_e}$	$\frac{\rho}{\rho_e}$	$\frac{T_O - T_w}{T_{Oe} - T_w}$	$\frac{T}{T_e}$	$\frac{M}{M_e}$
1.0000	1.0000	1.0000	1.0000	1.0000	1.0000	1.0	1.0000
0.9074	1.0567	0.9944	0.9971	1.0628	0.9630	1.0	0.9965
0.8333	1.0319	0.9887	0.9940	1.0443	0.9259	1.1	0.9618
0.7407	0.8936	0.9788	0.9882	0.9149	0.8611	1.3	0.8703
0.6481	0.7128	0.9718	0.9831	0.7371	0.8148	1.7	0.7568
0.5556	0.5284	0.9689	0.9790	0.5506	0.7963	2.4	0.6353
0.4630	0.3475	0.9703	0.9745	0.3651	0.8056	3.8	0.5028
0.3704	0.2163	0.9788	0.9694	0.2292	0.8611	6.3	0.3873
0.2778	0.1142	1.0042	0.9598	0.1228	1.0278	12.2	0.2746
0.1852	0.0333	1.0283	0.8729	0.0422	1.1857	37.1	0.1434
0.0926	0.0062	0.9380	0.5144	0.0177	0.5937	92.2	0.0536
0.0000	0.0028	0.8475	0.0107	0.0147	0.0000	115.7	0.0010

p_{Oe} = 108.1 $p_w = 8.61 \times 10^{-4}$ $p_e = 5.62 \times 10^{-4}$ T_O = 481 T_w = 339 T_e = 3.66

u_e = 2227 M_e = 19.8 $\rho_e = 7.49 \times 10^{-3}$ $\frac{Re}{m} = 1.42 \times 10^7$ δ = 2.72

$\frac{\delta^*}{\delta}$ = 0.511 $\frac{\theta}{\delta}$ = 0.00568 $\frac{\Gamma}{\delta}$ = 0.0109 R_θ = 2196

$\frac{y}{\delta}$	$\frac{p_{O_2}}{p_{O_{2e}}}$	$\frac{T_O}{T_{Oe}}$	$\frac{u}{u_e}$	$\frac{\rho}{\rho_e}$	$\frac{T_O - T_w}{T_{Oe} - T_w}$	$\frac{T}{T_e}$	$\frac{M}{M_e}$
1.0000	1.0000	1.0000	1.0000	1.0000	1.0000	1.0	1.0000
0.9159	1.0302	0.9908	0.9953	1.0399	0.9686	1.0	0.9930
0.8411	1.0034	0.9850	0.9921	1.0192	0.9490	1.1	0.9618
0.7477	0.8792	0.9780	0.9879	0.9007	0.9255	1.3	0.8802
0.6542	0.6980	0.9711	0.9828	0.7222	0.9020	1.6	0.7675
0.5607	0.5336	0.9688	0.9794	0.5557	0.8941	2.2	0.6572
0.4673	0.3792	0.9723	0.9771	0.3964	0.9059	3.2	0.5430
0.3738	0.2450	0.9792	0.9731	0.2578	0.9294	5.2	0.4279
0.2804	0.1218	1.0013	0.9630	0.1303	1.0043	10.6	0.2955
0.1869	0.0131	0.9858	0.7182	0.0231	0.9517	62.2	0.0911
0.0935	0.0043	0.8312	0.3949	0.0167	0.4274	88.8	0.0419
0.0000	0.0027	0.7052	0.0076	0.0166	0.0000	92.6	0.0008

p_{Oe} = 109.2 $p_w = 8.61 \times 10^{-4}$ $p_e = 5.51 \times 10^{-4}$ T_O = 988 T_w = 400 T_e = 7.39

u_e = 3193 $M_e \doteq 19.8$ $\rho_e = 3.63 \times 10^{-3}$ $\frac{Re}{m} = 6.15 \times 10^6$ δ = 2.69

$\frac{\delta^*}{\delta}$ = 0.518 $\frac{\theta}{\delta}$ = 0.00856 $\frac{\Gamma}{\delta}$ = *0.0161* R_θ = 1420

$\frac{y}{\delta}$	$\frac{p_{O_2}}{p_{O_{2e}}}$	$\frac{T_O}{T_{Oe}}$	$\frac{u}{u_e}$	$\frac{\rho}{\rho_e}$	$\frac{T_O - T_w}{T_{Oe} - T_w}$	$\frac{T}{T_e}$	$\frac{M}{M_e}$
1.0000	1.0000	1.0000	1.0000	1.0001	1.0000	1.0	1.0000
0.9434	1.0375	0.9928	0.9963	1.0452	0.9879	1.0	1.0027
0.8962	1.0546	0.9874	0.9936	1.0682	0.9789	1.0	0.9981
0.8491	1.0410	0.9822	0.9909	1.0602	0.9702	1.0	0.9794
0.7547	0.9113	0.9725	0.9852	0.9387	0.9538	1.2	0.8946
0.6604	0.7270	0.9621	0.9784	0.7590	0.9363	1.6	0.7808
0.5660	0.5358	0.9516	0.9706	0.5682	0.9187	2.2	0.6557
0.4717	0.3652	0.9436	0.9620	0.3938	0.9052	3.3	0.5298
0.4245	0.2901	0.9352	0.9541	0.3178	0.8911	4.2	0.4673
0.3774	0.1877	0.9156	0.9349	0.2137	0.8582	6.4	0.3718
0.2830	0.0379	0.7906	0.7852	0.0597	0.6481	23.9	0.1619
0.1887	0.0093	0.6429	0.5206	0.0296	0.4001	50.0	0.0742
0.0943	0.0045	0.5114	0.3166	0.0279	0.1792	55.0	0.0430
0.0000	0.0027	0.4048	0.0052	0.0294	0.0000	54.1	0.0007

TABLE 6. – COMPUTED PARAMETERS FOR x = 0.508 – Continued

p_{Oe} = 199 p_w = 13.4 X 10^{-4} p_e = 9.63 X 10^{-4} T_O = 516 T_w = 352 T_e = 3.80

u_e = 2308 M_e = 20.1 ρ_e = 1.24 X 10^{-2} $\frac{Re}{m}$ = 2.38 X 10^7 δ = 2.44

$\frac{\delta^*}{\delta}$ = 0.494 $\frac{\theta}{\delta}$ = 0.00577 $\frac{\Gamma}{\delta}$ = 0.0112 R_θ = 3343

$\frac{y}{\delta}$	$\frac{p_{O_2}}{p_{O_{2e}}}$	$\frac{T_O}{T_{Oe}}$	$\frac{u}{u_e}$	$\frac{\rho}{\rho_e}$	$\frac{T_O - T_W}{T_{Oe} - T_W}$	$\frac{T}{T_e}$	$\frac{M}{M_e}$
1.0000	1.0000	1.0000	1.0000	1.0000	1.0000	1.0	1.0000
0.9375	1.0313	0.9957	0.9979	1.0357	0.9865	1.0	1.0033
0.8333	0.9896	0.9882	0.9938	1.0020	0.9628	1.1	0.9637
0.7292	0.8437	0.9806	0.9891	0.8622	0.9392	1.3	0.8732
0.6250	0.6632	0.9720	0.9833	0.6856	0.9122	1.7	0.7601
0.5208	0.4861	0.9666	0.9780	0.5077	0.8953	2.3	0.6393
0.4167	0.3333	0.9656	0.9730	0.3514	0.8919	3.5	0.5202
0.3125	0.2188	0.9688	0.9672	0.2330	0.9020	5.5	0.4143
0.2083	0.0736	0.9864	0.9361	0.0829	0.9572	15.8	0.2355
0.1042	0.0075	0.8979	0.5909	0.0181	0.6795	74.9	0.0683
0.0000	0.0023	0.6814	0.0048	0.0151	0.0000	92.6	0.0005

p_{Oe} = 199.2 p_w = 13.4 X 10^{-4} p_e = 9.73 X 10^{-4} T_{Oe} = 942 T_w = 402 T_e = 6.94

u_e = 3118 M_e = 20.0 ρ_e = 6.84 X 10^{-3} $\frac{Re}{m}$ = 1.19 X 10^7 δ = 2.57

$\frac{\delta^*}{\delta}$ = 0.490 $\frac{\theta}{\delta}$ = 0.00882 $\frac{\Gamma}{\delta}$ = 0.0170 R_θ = 2688

$\frac{y}{\delta}$	$\frac{p_{O_2}}{p_{O_{2e}}}$	$\frac{T_O}{T_{Oe}}$	$\frac{u}{u_e}$	$\frac{\rho}{\rho_e}$	$\frac{T_O - T_W}{T_{Oe} - T_W}$	$\frac{T}{T_e}$	$\frac{M}{M_e}$
1.0000	1.0000	1.0000	1.0000	1.0001	1.0000	1.0	0.9988
0.8911	1.0470	0.9831	0.9915	1.0649	0.9706	1.0	1.0016
0.7921	0.9774	0.9701	0.9845	1.0082	0.9479	1.1	0.9507
0.6931	0.8174	0.9609	0.9789	0.8528	0.9318	1.3	0.8546
0.5941	0.6296	0.9533	0.9733	0.6641	0.9186	1.8	0.7376
0.4950	0.4591	0.9478	0.9678	0.4896	0.9088	2.5	0.6198
0.3960	0.3043	0.9438	0.9607	0.3290	0.9020	3.8	0.4966
0.2970	0.1426	0.9398	0.9420	0.1598	0.8949	8.0	0.3342
0.2475	0.0652	0.9337	0.9045	0.0786	0.8843	16.5	0.2234
0.1980	0.0278	0.9078	0.8188	0.0400	0.8391	32.9	0.1433
0.1485	0.0091	0.8207	0.6084	0.0217	0.6872	61.5	0.0779
0.0990	0.0056	0.6908	0.4591	0.0207	0.4605	65.4	0.0570
0.0495	0.0037	0.5631	0.3109	0.0217	0.2375	63.4	0.0392
0.0000	0.0023	0.4270	0.0086	0.0240	0.0000	58.0	0.0011

p_{Oe} = 270 p_w = 18.1 X 10^{-4} p_e = 12.8 X 10^{-4} T_{Oe} = 503 T_w = 318 T_e = 3.65

u_e = 2278 M_e = 20.3 ρ_e = 1.71 X 10^{-2} $\frac{Re}{m}$ = 3.34 X 10^7 δ = 2.36

$\frac{\delta^*}{\delta}$ = 0.492 $\frac{\theta}{\delta}$ = 0.00689 $\frac{\Gamma}{\delta}$ = 0.0134 R_θ = 5430

$\frac{y}{\delta}$	$\frac{p_{O_2}}{p_{O_{2e}}}$	$\frac{T_O}{T_{Oe}}$	$\frac{u}{u_e}$	$\frac{\rho}{\rho_e}$	$\frac{T_O - T_W}{T_{Oe} - T_W}$	$\frac{T}{T_e}$	$\frac{M}{M_e}$
1.0000	1.0000	1.0000	1.0000	1.0000	1.0000	1.0	1.0000
0.9677	1.0210	0.9956	0.9978	1.0255	0.9880	1.0	1.0037
0.9140	1.0385	0.9923	0.9961	1.0466	0.9790	1.0	1.0012
0.8602	1.0210	0.9867	0.9932	1.0350	0.9640	1.0	0.9821
0.7527	0.8776	0.9768	0.9874	0.9000	0.9369	1.2	0.8918
0.6452	0.7098	0.9691	0.9822	0.7354	0.9159	1.6	0.7860
0.5376	0.5105	0.9624	0.9763	0.5351	0.8979	2.2	0.6538
0.4301	0.3392	0.9591	0.9700	0.3597	0.8889	3.4	0.5229
0.3226	0.2308	0.9569	0.9623	0.2484	0.8829	5.2	0.4234
0.2151	0.0965	0.9547	0.9343	0.1095	0.8769	12.2	0.2683
0.1613	0.0245	0.9573	0.8238	0.0346	0.8840	39.1	0.1318
0.1075	0.0066	0.9352	0.5736	0.0164	0.8240	84.0	0.0627
0.0538	0.0034	0.8403	0.3503	0.0141	0.5661	99.1	0.0352
0.0000	0.0024	0.6298	0.0080	0.0163	−0.0060	86.9	0.0009

TABLE 6. – COMPUTED PARAMETERS FOR x = 0.508 – Concluded

p_{oe} = 268 p_w = 18.2 × 10^{-4} p_e = 12.6 × 10^{-4} T_o = 882 T_w = 361 T_e = 6.40

u_e = 3018 M_e = 20.2 ρ_e = 9.58 × 10^{-3} $\frac{Re}{m}$ = 1.71 × 10^7 δ = 2.41

$\frac{\delta^*}{\delta}$ = 0.500 $\frac{\theta}{\delta}$ = 0.00809 $\frac{\Gamma}{\delta}$ = 0.0157 R_θ = 3337

$\frac{y}{\delta}$	$\frac{p_{O_2}}{p_{O_{2e}}}$	$\frac{T_O}{T_{Oe}}$	$\frac{u}{u_e}$	$\frac{\rho}{\rho_e}$	$\frac{T_O - T_w}{T_{Oe} - T_w}$	$\frac{T}{T_e}$	$\frac{M}{M_e}$
1.0000	1.0000	1.0000	1.0000	1.0000	1.0000	1.0	0.9988
0.9474	1.0213	0.9946	0.9972	1.0269	0.9908	1.0	0.9978
0.9053	1.0284	0.9886	0.9942	1.0404	0.9806	1.0	0.9923
0.8421	1.0000	0.9829	0.9911	1.0179	0.9711	1.1	0.9656
0.7368	0.8723	0.9717	0.9847	0.8995	0.9521	1.2	0.8828
0.6316	0.6631	0.9602	0.9772	0.6941	0.9326	1.7	0.7539
0.5263	0.4716	0.9508	0.9696	0.5011	0.9168	2.4	0.6233
0.4211	0.3262	0.9426	0.9609	0.3526	0.9028	3.6	0.5084
0.3158	0.1879	0.9363	0.9472	0.2086	0.8921	6.3	0.3785
0.2632	0.1305	0.9335	0.9352	0.1482	0.8874	9.0	0.3122
0.2105	0.0621	0.9231	0.8944	0.0764	0.8699	17.8	0.2125
0.1579	0.0259	0.8868	0.7971	0.0391	0.8084	35.3	0.1344
0.1053	0.0058	0.8063	0.4986	0.0182	0.6723	77.1	0.0568
0.0000	0.0024	0.4060	0.0094	0.0259	−0.0053	56.0	0.0013

TABLE 7. – COMPUTED PARAMETERS FOR x = 1.067

p_{Oe} = 65 3 $p_w = 1.45 \times 10^{-4}$ $p_e = 0.682 \times 10^{-4}$ $T_O = 500$ $T_w = 315$ $T_e = 2.01$

$u_e = 2276$ M_e = 27 3 $\rho_e = 1.65 \times 10^{-3}$ $\frac{Re}{m} = 4.59 \times 10^6$ $\delta = 7.98$

$\frac{\delta^*}{\delta}$ = 0 587 $\frac{\theta}{\delta} = 0.00384$ $\frac{\Gamma}{\delta} = 0.00719$ $R_\theta = 1440$

$C_f = 3.62 \times 10^{-4}$ $C_H = 1.21 \times 10^{-4}$ $\frac{2C_H}{C_f}$ = 0 683 $\frac{M}{\sqrt{R\theta}} = 5.96$

$\frac{y}{\delta}$	$\frac{p_{O_2}}{p_{O_{2e}}}$	$\frac{T_O}{T_{Oe}}$	$\frac{u}{u_e}$	$\frac{\rho}{\rho_e}$	$\frac{T_O - T_w}{T_{Oe} - T_w}$	$\frac{T}{T_e}$	$\frac{M}{M_e}$
1 0000	1.0000	1.0000	1.0000	1.0000	1.0001	1 0	1.0000
0.9395	1.0319	0.9973	0.9986	1.0348	0.9928	1.0	0.9830
0.8758	0.9947	0.9884	0 9939	1.0069	0.9687	1.1	0.9344
0.7962	0.8848	0.9792	0 9888	0.9048	0.9437	1.4	0.8486
0.7166	0.7411	0.9705	0.9836	0.7658	0 9202	1.7	0.7498
0 6369	0.5656	0.9636	0.9787	0.5901	0.9015	2.4	0.6338
0 5573	0.3989	0.9650	0.9769	0.4175	0.9053	3.6	0.5160
0.4777	0.2358	0.9727	0 9750	0.2475	0.9262	6.4	0.3852
0.3981	0.0754	0.9923	0.9557	0.0818	0.9790	20.6	0 2112
0.3185	0.0133	1.0100	0.8038	0.0194	1.0271	91.2	0.0844
0.2389	0.0062	0.8785	0.6061	0.0146	0.6710	127.5	0.0538
0.1592	0.0039	0.7508	0.4498	0.0143	0.3252	136.6	0.0386
0.0796	0 0027	0 6595	0.2954	0.0143	0.0783	142.4	0.0248
0.0000	0.0020	0.6306	0.0000	0.0135	0.0000	156.9	0.0000

$p_{Oe} = 65$ $p_w = 1.45 \times 10^{-4}$ $p_e = 0.784 \times 10^{-4}$ $T_O = 933$ $T_w = 358$ $T_e = 3.91$

$u_e = 3109$ M_e = 26 4 $\rho_e = 9.79 \times 10^{-4}$ $\frac{Re}{m} = 2.41 \times 10^6$ $\delta = 7.67$

$\frac{\delta^*}{\delta}$ = 0 629 $\frac{\theta}{\delta} = 0.00496$ $\frac{\Gamma}{\delta}$ = 0 00909 $R_\theta = 916$

$C_f = 3.80 \times 10^{-4}$ C_H = 1 41 $\times 10^{-4}$ $\frac{2C_H}{C_f} = 0.742$ $\frac{M}{\sqrt{R_\theta}} = 0.875$

$\frac{y}{\delta}$	$\frac{p_{O_2}}{p_{O_{2e}}}$	$\frac{T_O}{T_{Oe}}$	$\frac{u}{u_e}$	$\frac{\rho}{\rho_e}$	$\frac{T_O - T_w}{T_{Oe} - T_w}$	$\frac{T}{T_e}$	$\frac{M}{M_e}$
1.0000	1.0000	1.0000	1.0000	1.0001	1.0000	1.0	1.0000
0.9404	1.0229	0.9947	0.9972	1.0286	0.9914	1.0	0.9869
0.8278	0.9100	0.9730	0.9858	0.9363	0.9562	1.3	0.8913
0.7450	0.7447	0.9598	0.9783	0.7779	0.9347	1.6	0.7827
0.6623	0.5532	0.9503	0.9720	0.5851	0.9194	2.2	0.6559
0.5795	0.3486	0.9477	0.9675	0.3720	0.9152	3.7	0.5069
0.4967	0.1187	0.9649	0.9598	0.1282	0.9430	11.4	0.2879
0.4139	0.0239	0.9790	0.8776	0.0302	0.9660	50.7	0.1247
0.3311	0.0115	0.7713	0.6901	0.0226	0.6288	71.0	0.0829
0.2483	0.0069	0.6208	0.5381	0.0211	0.3847	79.5	0.0611
0.1656	0.0043	0.5130	0.4025	0.0208	0.2096	84.1	0.0444
0.0828	0.0028	0.4369	0 2753	0.0210	0.0861	86.4	0.0300
0.0000	0.0018	0.3826	0.0000	0.0202	−0.0019	91.5	0.0000

$p_{Oe} = 107.7$ $p_w = 2.08 \times 10^{-4}$ $p_e = 1.12 \times 10^{-4}$ $T_O = 305$ $T_w = 299$ $T_e = 1.22$

$u_e = 1777$ $M_e = 27.3$ $\rho_e = 4.50 \times 10^{-3}$ $\frac{Re}{m}$ = 1 39 $\times 10^7$ δ = 7 11

$\frac{\delta^*}{\delta} = 0.557$ $\frac{\theta}{\delta}$ = 0 00383 $\frac{\Gamma}{\delta} = 0.00745$ $R_\theta = 3786$

$C_f = 2.33 \times 10^{-4}$ $C_H = 0.866 \times 10^{-4}$ $\frac{2C_H}{C_f} = 0.746$ $\frac{M}{\sqrt{R_\theta}}$ = 0 443

$\frac{y}{\delta}$	$\frac{p_{O_2}}{p_{O_{2e}}}$	$\frac{T_O}{T_{Oe}}$	$\frac{u}{u_e}$	$\frac{\rho}{\rho_e}$	$\frac{T_O - T_w}{T_{Oe} - T_w}$	$\frac{T}{T_e}$	$\frac{M}{M_e}$
1.0000	1.0000	1.0000	1.0000	1.0000	1.0000	1.0	0.9985
0.9357	1.0306	0.9945	0.9972	1.0364	0.7273	1.0	0.9871
0.8571	0.9799	0.9872	0.9933	0.9931	0 3636	1.1	0.9334
0.8036	0.9020	0.9800	0.9893	0.9214	−0.0000	1.3	0.8779
0.7143	0.7454	0.9709	0.9840	0.7696	−0.4545	1.6	0.7733
0.6250	0.5617	0.9672	0.9808	0.5835	−0.6364	2.3	0.6516
0.5357	0.3885	0.9672	0.9784	0.4054	−0.6364	3.4	0.5268
0.4464	0.2476	0.9727	0.9766	0 2591	−0.3636	5.7	0.4094
0.3571	0.1479	0 9927	0.9779	0.1540	0.6364	10.1	0.3082
0.2679	0.0604	1.0339	0.9674	0.0638	2.6929	25.5	0.1917
0.2232	0.0189	1.0548	0.8804	0.0235	3.7369	70.8	0.1046
0.1786	0.0066	1.0616	0.7028	0.0119	4.0759	142.6	0.0589
0.1339	0.0042	1.0408	0.5805	0.0099	3.0358	176.5	0.0437
0.0893	0.0030	1.0167	0.4677	0.0089	1.8358	200.0	0.0331
0.0000	0.0017	0.9891	0.0061	0.0075	0.4545	247.6	0.0004

TABLE 7. – COMPUTED PARAMETERS FOR x = 1.067 – Continued

p_{Oe} = 107.7 p_w = 2.08 X 10^{-4} p_e = 1.09 X 10^{-4} T_O = 418 T_w = 301 T_e = 1.66

u_e = 2080 M_e = 27.5 ρ_e = 3.23 X 10^{-3} $\frac{Re}{m}$ = 9.57 X 10^6 δ = 7.11

$\frac{\delta^*}{\delta}$ = 0.567 $\frac{\theta}{\delta}$ = 0.00408 $\frac{\Gamma}{\delta}$ = 0.00780 R_θ = 2767

C_f = 2.53 X 10^{-4} C_H = 0.967 X 10^{-4} $\frac{2C_H}{C_f}$ = 0.765 $\frac{M}{\sqrt{R_\theta}}$ = 0.523

$\frac{y}{\delta}$	$\frac{p_{O_2}}{p_{O_2e}}$	$\frac{T_O}{T_{Oe}}$	$\frac{u}{u_e}$	$\frac{\rho}{\rho_e}$	$\frac{T_O - T_w}{T_{Oe} - T_w}$	$\frac{T}{T_e}$	$\frac{M}{M_e}$
1.0000	1.0000	1.0000	1.0000	1.0000	1.0000	1.0	0.9985
0.9321	1.0276	0.9934	0.9966	1.0346	0.9763	1.0	0.9827
0.8571	0.9804	0.9854	0.9924	0.9955	0.9479	1.1	0.9307
0.8036	0.9029	0.9774	0.9880	0.9248	0.9194	1.3	0.8747
0.7143	0.7311	0.9721	0.9845	0.7540	0.9005	1.7	0.7614
0.6250	0.5503	0.9694	0.9818	0.5706	0.8910	2.4	0.6404
0.5357	0.3802	0.9668	0.9779	0.3971	0.8815	3.6	0.5169
0.4464	0.2413	0.9673	0.9735	0.2541	0.8833	5.9	0.4004
0.3571	0.1247	0.9880	0.9716	0.1314	0.9573	12.0	0.2800
0.2679	0.0196	0.9965	0.8610	0.0255	0.9874	65.2	0.1067
0.2232	0.0069	0.9675	0.6789	0.0133	0.8840	128.4	0.0599
0.1786	0.0048	0.8959	0.5738	0.0122	0.6291	143.5	0.0479
0.0893	0.0028	0.7620	0.3783	0.0117	0.1518	156.5	0.0302
0.0000	0.0017	0.7194	0.0052	0.0105	−0.0002	181.7	0.0004

p_{Oe} = 107.7 p_w = 2.08 X 10^{-4} p_e = 1.02 X 10^{-4} T_O = 577 T_w = 577 T_e = 2.22

u_e = 2444 M_e = 27.9 ρ_e = 2.23 X 10^{-3} $\frac{Re}{m}$ = 6.42 δ = 7.16

$\frac{\delta^*}{\delta}$ = 0.578 $\frac{\theta}{\delta}$ = 0.00392 $\frac{\Gamma}{\delta}$ = 0.00737 R_θ = 1801

C_f = 3.02 X 10^{-4} C_H = 1.161 X 10^{-4} $\frac{2C_H}{C_f}$ = 0 792 $\frac{M}{\sqrt{R_\theta}}$ = 0.655

1.0000	1.0000	1.0000	1.0000	1.0000	1.0001	1.0	0.9985
0.9113	1.0382	0.9956	0.9977	1.0430	0.9906	1.1	0.9733
0.8511	0.9953	0.9880	0.9937	1.0080	0.9741	1.2	0.9266
0.7979	0.9123	0.9818	0.9902	0.9303	0.9607	1.3	0.8665
0.7092	0.7211	0.9738	0.9853	0.7426	0.9435	1.8	0.7424
0.6206	0.5233	0.9702	0.9818	0.5425	0.9357	2.6	0.6110
0.5319	0 3451	0.9678	0.9775	0.3607	0.9306	4.2	0.4803
0.4433	0.1959	0.9669	0.9701	0.2076	0.9287	7.7	0.3509
0.3546	0.0662	0.9720	0.9423	0.0739	0.9396	22.8	0.1976
0.2660	0.0119	0.9201	0.7573	0.0196	0.8276	90.8	0.0796
0.1773	0.0050	0.7295	0.5172	0.0155	0.4168	120.6	0.0472
0.0887	0.0029	0.6021	0.3353	0.0154	0.1422	127.7	0.0297
0.0000	0.0018	0.5342	0.0045	0.0148	−0.0042	139.1	0.0004

p_{Oe} = 109.8 p_w = 2 04 X 10^{-4} p_e = 1.12 X 10^{-4} T_O = 920 T_w = 328 T_e = 3 61

u_e = 3087 M_e = 27.4 ρ_e = 1.51 X 10^{-3} $\frac{Re}{m}$ = 3.92 X 10^6 δ = 7.24

$\frac{\delta^*}{\delta}$ = 0.582 $\frac{\theta}{\delta}$ = 0.00594 $\frac{\Gamma}{\delta}$ = 0 0111 R_θ = 1685

C_f = 3.22 X 10^{-4} C_H = 1.22 X 10^{-4} $\frac{2C_H}{C_f}$ = 0.780 $\frac{M}{\sqrt{R_\theta}}$ = 0.671

1.0000	1.0000	1.0000	1.0000	1.0001	1.0000	1.0	1.0000
0.9298	0.0353	0.9940	0.9969	1.0417	0.9908	1.0	0.9893
0.8947	1.0193	0.9885	0.9940	1.0315	0.9821	1.1	0.9685
0.8421	0.9636	0.9787	0.9889	0.9853	0.9670	1.2	0.9235
0.7895	0.8824	0.9686	0.9835	0.9121	0.9512	1.3	0.8672
0.7368	0.7904	0.9586	0.9780	0.8262	0.9357	1.5	0 8060
0.6842	0.6898	0.9507	0.9734	0.7278	0.9235	1.8	0.7399
0.6316	0.5754	0.9439	0.9691	0.6124	0.9129	2.2	0.6643
0.5789	0.4599	0 9395	0.9655	0.4929	0.9061	2.8	0.5842
0.5263	0.3369	0.9402	0.9636	0 3624	0.9072	3.9	0.4921
0 4737	0.2139	0.9418	0.9595	0.2318	0.9096	6.3	0.3859
0.4211	0.1070	0.9381	0.9445	0.1193	0.9039	12.6	0.2685
0.3684	0.0401	0.8956	0.8826	0 0507	0.8379	30.6	0.1612
0.3158	0.0190	0.8224	0.7848	0.0299	0.7241	53.3	0.1085
0.2632	0.0080	0.6809	0.6033	0.0201	0.5045	81.3	0.0676
0.2105	0.0050	0.5669	0.4726	0 0191	0.3274	88.0	0.0509
0.1579	0.0033	0.4893	0.3604	0.0188	0.2070	92.0	0.0379
0.0702	0.0022	0.3943	0.2231	0 0204	0.0594	88.1	0 0240
0.0000	0.0017	0.3560	0.0000	0.0201	0.0000	90.9	0.0000

TABLE 7. – COMPUTED PARAMETERS FOR x = 1.067 – Continued

$p_{Oe} = 189$ $p_w = 3.12 \times 10^{-4}$ $p_e = 1.39 \times 10^{-4}$ $T_O = 534$ $T_w = 319$ $T_e = 1.85$

$u_e = 2352$ $M_e = 29.4$ $\rho_e = 3.68 \times 10^{-3}$ $\frac{Re}{m} = 1.15 \times 10^{7}$ $\delta = 6.96$

$\frac{\delta^*}{\delta} = 0.531$ $\frac{\theta}{\delta} = 0.00465$ $\frac{\Gamma}{\delta} = 0.00894$ $R_\theta = 3710$

$C_f = 2.73 \times 10^{-4}$ $C_H = 1.113 \times 10^{-4}$ $\frac{2C_H}{C_f} = 0.842$ $\frac{M}{\sqrt{R_\theta}} = 0.479$

$\frac{y}{\delta}$	$\frac{p_{O_2}}{p_{O_{2e}}}$	$\frac{T_O}{T_{Oe}}$	$\frac{u}{u_e}$	$\frac{\rho}{\rho_e}$	$\frac{T_O - T_w}{T_{Oe} - T_w}$	$\frac{T}{T_e}$	$\frac{M}{M_e}$
1.0000	1.0000	1.0000	1.0000	1.0000	1.0000	1.0	1.0000
0.9051	1.0522	0.9948	0.9973	1.0580	0.9870	1.1	0.9704
0.8212	0.9888	0.9865	0.9928	1.0031	0.9663	1.2	0.8998
0.7299	0.8246	0.9761	0.9869	0.8465	0.9404	1.6	0.7862
0.6387	0.6418	0.9657	0.9805	0.6672	0.9145	2.2	0.6659
0.5474	0.4664	0.9570	0.9743	0.4910	0.8929	3.2	0.5467
0.4562	0.3172	0.9540	0.9696	0.3369	0.8856	5.0	0.4352
0.3650	0.1679	0.9605	0.9640	0.1801	0.9016	9.9	0.3062
0.2737	0.0560	0.9747	0.9347	0.0633	0.9370	30.1	0.1707
0.1825	0.0046	0.9659	0.5839	0.0112	0.9151	180.9	0.0435
0.1369	0.0030	0.8826	0.4354	0.0104	0.7077	200.3	0.0308
0.0730	0.0026	0.7526	0.3459	0.0118	0.3842	182.9	0.0256
0.0000	0.0018	0.5963	0.0000	0.0130	−0.0052	172.2	0.0000

$p_{Oe} = 189$ $p_w = 3.12 \times 10^{-4}$ $p_e = 1.48 \times 10^{-4}$ $T_O = 877$ $T_w = 348$ $T_e = 3.09$

$u_e = 3015$ $M_e = 29.0$ $\rho_e = 2.33 \times 10^{-3}$ $\frac{Re}{m} = 6.56 \times 10^{6}$ $\delta = 6.99$

$\frac{\delta^*}{\delta} = 0.562$ $\frac{\theta}{\delta} = 0.00520$ $\frac{\Gamma}{\delta} = 0.00989$ $R_\theta = 2380$

$C_f = 3.01 \times 10^{-4}$ $C_H = 1.02 \times 10^{-4}$ $\frac{2C_H}{C_f} = 0.690$ $\frac{M}{\sqrt{R_\theta}} = 0.594$

$\frac{y}{\delta}$	$\frac{p_{O_2}}{p_{O_{2e}}}$	$\frac{T_O}{T_{Oe}}$	$\frac{u}{u_e}$	$\frac{\rho}{\rho_e}$	$\frac{T_O - T_w}{T_{Oe} - T_w}$	$\frac{T}{T_e}$	$\frac{M}{M_e}$
1.0000	1.0000	1.0000	1.0000	1.0000	1.0000	1.0	1.0000
0.9600	1.0217	0.9946	0.9972	1.0274	0.9911	1.0	0.9891
0.9164	1.0326	0.9899	0.9948	1.0433	0.9833	1.1	0.9721
0.8182	0.9457	0.9786	0.9887	0.9672	0.9646	1.3	0.8871
0.7273	0.7790	0.9672	0.9823	0.8072	0.9457	1.6	0.7733
0.6364	0.5942	0.9583	0.9765	0.6228	0.9310	2.3	0.6506
0.5455	0.4239	0.9533	0.9719	0.4483	0.9227	3.4	0.5307
0.4545	0.2609	0.9534	0.9675	0.2782	0.9228	5.9	0.4028
0.3636	0.1014	0.9587	0.9524	0.1112	0.9316	15.6	0.2432
0.3182	0.0471	0.9523	0.9174	0.0552	0.9210	32.3	0.1627
0.2727	0.0185	0.9223	0.8238	0.0263	0.8714	69.9	0.0993
0.2455	0.0112	0.8516	0.7251	0.0200	0.7541	93.1	0.0758
0.1818	0.0051	0.7393	0.5373	0.0151	0.5682	128.3	0.0478
0.0909	0.0024	0.4928	0.2641	0.0170	0.1598	120.2	0.0243
0.0000	0.0017	0.3925	0.0000	0.0187	−0.0063	111.5	0.0000

TABLE 7. – COMPUTED PARAMETERS FOR x = 1.067 Concluded

$p_{Oe} = 270$ $p_w = 3.86 \times 10^{-4}$ $p_e = 1.86 \times 10^{-4}$ $T_O = 502$ $T_w = 318$ $T_e = 1\ 68$

$u_e = 2281$ $M_e = 29.9$ $\rho_e = 5.40 \times 10^{-3}$ $\dfrac{Re}{m} = 1.74 \times 10^{-7}$ $\delta = 6\ 47$

$\dfrac{\delta^*}{\delta} = 0\ 528$ $\dfrac{\theta}{\delta} = 0.00423$ $\dfrac{\Gamma}{\delta} = 0.00820$ $R_\theta = 4756$

$C_f = 2.03 \times 10^{-4}$ $C_H = 0.957 \times 10^{-4}$ $\dfrac{2C_H}{C_f} = 0.938$ $\dfrac{M}{\sqrt{R_\theta}} = 0.439$

$\frac{y}{\delta}$	$\frac{p_{O_2}}{p_{O_{2e}}}$	$\frac{T_O}{T_{Oe}}$	$\frac{u}{u_e}$	$\frac{\rho}{\rho_e}$	$\frac{T_O - T_w}{T_{Oe} - T_w}$	$\frac{T}{T_e}$	$\frac{M}{M_e}$
1.0000	1.0000	1.0000	1.0000	1.0000	1.0000	1.0	0.9984
0.9608	1.0432	0.9978	0.9989	1.0456	0.9940	1.0	0.9991
0.9098	1.0595	0.9945	0.9972	1.0655	0.9849	1.0	0.9814
0.8824	1.0486	0.9923	0.9960	1.0571	0.9789	1.1	0.9636
0.7843	0.9189	0.9845	0.9917	0.9343	0.9577	1.3	0.8627
0.6863	0.7270	0.9768	0.9869	0.7462	0.9366	1.8	0.7366
0.5882	0.5351	0.9690	0.9816	0.5551	0.9154	2.6	0.6084
0.4902	0.3676	0.9613	0.9752	0.3861	0.8943	4.0	0.4867
0.3922	0.2243	0.9601	0.9695	0.2381	0.8910	7.0	0.3677
0.2941	0.1216	0.9671	0.9618	0.1309	0.9100	13.5	0.2622
0.2647	0.0838	0.9737	0.9548	0.0913	0.9281	19.6	0.2155
0.1961	0.9157	0.9262	0.8098	0.0229	0.7985	81.4	0.0898
0.1765	0.0081	0.9884	0.7314	0.0139	0.9682	135.9	0.0627
0.1471	0.0042	0.9351	0.5721	0.0106	0.8226	181 7	0.0424
0.0980	0.0026	0.7919	0.4013	0.0105	0.4316	188.4	0.0292
0.0000	0.0016	0.6338	0.0000	0.0109	0.0000	189.2	0.0000

$p_{Oe} = 265$ $p_w = 3\ 85 \times 10^{-4}$ $p_e = 1\ 89 \times 10^{-4}$ $T_O = 876$ $T_w = 339$ $T_e = 2.96$

$u_e = 3013$ $M_e = 29.6$ $\rho_e = 3.09 \times 10^{-3}$ $\dfrac{Re}{m} = 8.96 \times 10^{6}$ $\delta = 6.60$

$\dfrac{\delta^*}{\delta} = 0\ 557$ $\dfrac{\theta}{\delta} = 0.00484$ $\dfrac{\Gamma}{\delta} = 0.00924$ $R_\theta = 2870$

$C_f = 2.58 \times 10^{-4}$ $C_H = 1.02 \times 10^{-4}$ $\dfrac{2C_H}{C_f} = 0.813$ $\dfrac{M}{\sqrt{R_\theta}} = 0\ 552$

1.0000	1.0000	1.0000	1.0000	1.0000	1.0000	1.0	1.0000
0.9615	1.0328	0.9972	0.9986	1.0358	0.9954	1.0	0.9962
0.9231	1.0437	0.9945	0.9972	1.0497	0.9910	1.0	0.9825
0.8654	1.0164	0.9900	0.9948	1.0271	0.9838	1.1	0.9433
0.7692	0.8333	0.9794	0.9888	0.8522	0.9663	1.5	0.8185
0.6731	0.6721	0.9681	0.9822	0.6965	0.9479	2.0	0.7067
0.5769	0.4836	0.9575	0.9752	0.5082	0.9306	2.9	0.5779
0.4808	0.3142	0.9490	0.9676	0.3351	0.9168	4.7	0.4501
0.3846	0.1656	0.9498	0.9599	0.1791	0.9181	9.3	0.3163
0.3365	0.0956	0.9495	0.9474	0.1059	0.9177	16.3	0.2364
0.2885	0.0415	0.9460	0.9098	0.0495	0.9120	35.9	0.1529
0.2404	0.0158	0.9124	0.8068	0.0234	0.8572	78.2	0.0919
0.1923	0.0071	0.7900	0.6309	0.0161	0.6575	116.6	0.0588
0.0962	0.0027	0.5130	0.3278	0.0165	0.2057	120.4	0.0301
0.0000	0.0016	0.3855	0.0000	0.0173	−0.0021	114.3	0.0000

TABLE 8. – COMPUTED PARAMETERS FOR $x = 1.625$

$p_{Oe} = 66.9$ $p_w = 0.698 \times 10^{-4}$ $p_e = 0.372 \times 10^{-4}$ $T_O = 515$ $T_w = 301$ $T_e = 1.60$

$u_e = 2310$ $M_e = 30.9$ $\rho_e = 1.13 \times 10^{-3}$ $\frac{R_e}{m} = 3.78 \times 10^6$ $\delta = 13.34$

$\frac{\delta^*}{\delta} = 0.563$ $\frac{\theta}{\delta} = 0.00434$ $\frac{\Gamma}{\delta} = 0.00820$ $R_\theta = 2190$

$C_f = 2.66 \times 10^{-4}$ $C_H = 0.758 \times 10^{-4}$ $\frac{2C_H}{C_f} = 0.552$ $\frac{M}{\sqrt{R_\theta}} = 0.660$

$\frac{y}{\delta}$	$\frac{p_{O_2}}{p_{O_{2e}}}$	$\frac{T_O}{T_{Oe}}$	$\frac{u}{u_e}$	$\frac{\rho}{\rho_e}$	$\frac{T_O - T_w}{T_{Oe} - T_w}$	$\frac{T}{T_e}$	$\frac{M}{M_e}$
1.0000	1.0000	1.0000	1.0000	1.0000	1.0001	1.0	1.0000
0.9714	1.0192	0.9931	0.9965	1.0263	0.9834	1.0	0.9972
0.9238	1.0321	0.9874	0.9936	1.0454	0.9696	1.0	0.9837
0.9048	1.0244	0.9852	0.9925	1.0399	0.9643	1.1	0.9725
0.8571	0.9949	0.9776	0.9885	1.0181	0.9460	1.1	0.9405
0.8095	0.9462	0.9701	0.9846	0.9760	0.9280	1.2	0.9007
0.7619	0.8782	0.9651	0.9818	0.9110	0.9159	1.3	0.8527
0.7143	0.7987	0.9602	0.9790	0.8332	0.9041	1.5	0.7995
0.6667	0.7077	0.9566	0.9768	0.7415	0.8955	1.8	0.7403
0.6190	0.6077	0.9565	0.9762	0.6375	0.8953	2.1	0.6752
0.5714	0.5000	0.9578	0.9760	0.5246	0.8983	2.6	0.6031
0.5238	0.3846	0.9593	0.9753	0.4040	0.9019	3.5	0.5210
0.4762	0.2654	0.9625	0.9742	0.2792	0.9096	5.3	0.4265
0.4286	0.1278	0.9682	0.9678	0.1360	0.9235	11.1	0.2915
0.3810	0.0317	0.9620	0.9139	0.0373	0.9085	41.6	0.1423
0.3333	0.0133	0.9026	0.8076	0.0197	0.7654	81.1	0.0900
0.2857	0.0081	0.8067	0.6945	0.0156	0.5344	104.7	0.0681
0.2381	0.0056	0.7385	0.6032	0.0139	0.3702	120.8	0.0551
0.1905	0.0041	0.6882	0.5202	0.0128	0.2489	134.5	0.0450
0.1429	0.0030	0.6520	0.4375	0.0119	0.1617	148.2	0.0361
0.0952	0.0022	0.6216	0.3496	0.0112	0.0886	160.6	0.0277
0.0476	0.0017	0.6003	0.2323	0.0105	0.0372	175.6	0.0176
0.0000	0.0013	0.5827	0.0083	0.0101	−0.0052	187.3	0.0006

$p_{Oe} = 65.3$ $p_w = 0.698 \times 10^{-4}$ $p_e = 0.379 \times 10^{-4}$ $T_O = 890$ $T_w = 321$ $T_e = 2.77$

$u_e = 3036$ $M_e = 30.6$ $\rho_e = 6.66 \times 10^{-4}$ $\frac{R_e}{m} = 1.99 \times 10^6$ $\delta = 13.46$

$\frac{\delta^*}{\delta} = 0.593$ $\frac{\theta}{\delta} = 0.00484$ $\frac{\Gamma}{\delta} = 0.00885$ $R_\theta = 1296$

$C_f = 3.00 \times 10^{-4}$ $C_H = 1.00 \times 10^{-4}$ $\frac{2C_H}{C_f} = 0.668$ $\frac{M}{\sqrt{R_\theta}} = 0.839$

$\frac{y}{\delta}$	$\frac{p_{O_2}}{p_{O_{2e}}}$	$\frac{T_O}{T_{Oe}}$	$\frac{u}{u_e}$	$\frac{\rho}{\rho_e}$	$\frac{T_O - T_w}{T_{Oe} - T_w}$	$\frac{T}{T_e}$	$\frac{M}{M_e}$
1.0000	1.0000	1.0000	1.0000	1.0000	1.0001	1.0	1.0000
0.9434	1.0376	0.9935	0.9967	1.0445	0.9899	1.0	0.9952
0.9057	1.0439	0.9881	0.9939	1.0566	0.9814	1.0	0.9835
0.8491	1.0100	0.9791	0.9893	1.0320	0.9673	1.1	0.9467
0.8019	0.9436	0.9704	0.9847	0.9731	0.9537	1.2	0.8994
0.7547	0.8559	0.9614	0.9798	0.8913	0.9397	1.4	0.8423
0.7075	0.7531	0.9528	0.9751	0.7920	0.9262	1.6	0.7775
0.6604	0.6391	0.9460	0.9710	0.6776	0.9156	1.9	0.7050
0.6132	0.5125	0.9422	0.9682	0.5465	0.9096	2.5	0.6218
0.5660	0.3810	0.9421	0.9666	0.4074	0.9094	3.4	0.5281
0.5189	0.2387	0.9421	0.9631	0.2570	0.9094	5.6	0.4120
0.4717	0.0996	0.9461	0.9522	0.1094	0.9156	13.6	0.2621
0.4245	0.0326	0.8911	0.8823	0.0412	0.8296	36.9	0.1471
0.3774	0.0172	0.7457	0.7608	0.0288	0.6021	54.2	0.1047
0.3302	0.0107	0.6548	0.6632	0.0231	0.4598	69.5	0.0806
0.2830	0.0080	0.5701	0.5812	0.0219	0.3274	75.0	0.0680
0.2358	0.0058	0.5104	0.5057	0.0205	0.2340	82.1	0.0566
0.1887	0.0043	0.4603	0.4339	0.0197	0.1555	87.6	0.0470
0.1415	0.0032	0.4221	0.3632	0.0189	0.0958	93.3	0.0381
0.0943	0.0023	0.3918	0.2846	0.0181	0.0483	99.9	0.0288
0.0472	0.0017	0.3699	0.1873	0.0172	0.0140	107.6	0.0183
0.0000	0.0013	0.3609	0.0078	0.0163	0.0000	115.9	0.0007

TABLE 8. – COMPUTED PARAMETERS FOR x = 1.625 – Continued

$p_{o_e} = 107.3$ $p_w = 1.05 \times 10^{-4}$ $p_e = 0.432 \times 10^{-4}$ $T_o = 495$ $T_w = 306$ $T_e = 1.36$

$u_e = 2876$ $M_e = 33.1$ $\rho_e = 1.55 \times 10^{-3}$ $\frac{Re}{m} = 5.70 \times 10^{6}$ $\delta = 12.57$

$\frac{\delta^*}{\delta} = 0.582$ $\frac{\theta}{\delta} = 0.00390$ $\frac{\Gamma}{\delta} = 0.00739$ $R_\theta = 2800$

$C_f = 2.38 \times 10^{-4}$ $C_H = 0.797 \times 10^{-4}$ $\frac{2C_H}{C_f} = 0.650$ $\frac{M}{\sqrt{R_\theta}} = 0.625$

$\frac{y}{\delta}$	$\frac{p_{o_2}}{p_{o_{2e}}}$	$\frac{T_o}{T_{oe}}$	$\frac{u}{u_e}$	$\frac{\rho}{\rho_e}$	$\frac{T_o - T_w}{T_{oe} - T_w}$	$\frac{T}{T_e}$	$\frac{M}{M_e}$
1.0000	1.0000	1.0000	1.0000	1.0000	1.0001	1.0	1.0000
0.9798	1.0311	0.9950	0.9975	1.0363	0.9869	1.0	1.0010
0.9394	1.0388	0.9902	0.9950	1.0492	0.9744	1.0	0.9775
0.9091	1.0295	0.9868	0.9932	1.0436	0.9655	1.1	0.9542
0.8586	0.9907	0.9789	0.9891	1.0125	0.9451	1.2	0.9073
0.8081	0.9255	0.9726	0.9857	0.9524	0.9286	1.3	0.8516
0.7576	0.8478	0.9688	0.9835	0.8764	0.9187	1.5	0.7929
0.7071	0.7360	0.9655	0.9814	0.7641	0.9101	1.9	0.7196
0.6566	0.6196	0.9624	0.9791	0.6460	0.9019	2.3	0.6439
0.6061	0.5016	0.9606	0.9772	0.5249	0.8972	3.0	0.5657
0.5556	0.3866	0.9612	0.9761	0.4055	0.8989	4.1	0.4855
0.5051	0.2764	0.9633	0.9745	0.2906	0.9042	5.9	0.4016
0.4545	0.1733	0.9670	0.9710	0.1833	0.9139	9.8	0.3113
0.4040	0.0845	0.9737	0.9593	0.0913	0.9313	20.4	0.2127
0.3535	0.0320	0.9822	0.9180	0.0373	0.9537	51.9	0.1277
0.3030	0.0126	0.9714	0.8171	0.0180	0.9253	111.8	0.0775
0.2525	0.0066	0.9064	0.6819	0.0129	0.7559	162.0	0.0537
0.2020	0.0044	0.7978	0.5550	0.0120	0.4726	179.5	0.0415
0.1515	0.0032	0.7176	0.4503	0.0118	0.2634	188.6	0.0329
0.1010	0.0023	0.6630	0.3408	0.0115	0.1209	200.2	0.0241
0.0505	0.0018	0.6290	0.2050	0.0111	0.0322	214.8	0.0140
0.0000	0.0015	0.6155	0.0099	0.0109	−0.0029	225.2	0.0007

$p_{o_e} = 107.6$ $p_w = 1.04 \times 10^{-4}$ $p_e = 0.471 \times 10^{-4}$ $T_o = 886$ $T_w = 317$ $T_e = 2.47$

$u_e = 3032$ $M_e = 32.5$ $\rho_e = 9.29 \times 10^{-4}$ $\frac{Re}{m} = 3.00 \times 10^{6}$ $\delta = 12.70$

$\frac{\delta^*}{\delta} = 0.606$ $\frac{\theta}{\delta} = 0.00440$ $\frac{\Gamma}{\delta} = 0.00808$ $R_\theta = 1680$

$C_f = 2.68 \times 10^{-4}$ $C_H = 0.931 \times 10^{-4}$ $\frac{2C_H}{C_f} = 0.695$ $\frac{M}{\sqrt{R_\theta}} = 0.792$

1.0000	1.0000	1.0000	1.0000	1.0000	1.0000	1.0	1.0000
0.9300	1.0252	0.9925	0.9961	1.0332	0.9883	1.1	0.9722
0.9000	1.0148	0.9892	0.9944	1.0262	0.9833	1.1	0.9515
0.8500	0.9600	0.9824	0.9908	0.9778	0.9727	1.2	0.9015
0.8000	0.8815	0.9759	0.9873	0.9043	0.9625	1.4	0.8425
0.7500	0.7881	0.9676	0.9827	0.8159	0.9497	1.6	0.7780
0.7000	0.6815	0.9604	0.9786	0.7115	0.9384	2.0	0.7072
0.6500	0.5630	0.9517	0.9734	0.5939	0.9249	2.5	0.6289
0.6000	0.4370	0.9453	0.9689	0.4652	0.9149	3.3	0.5426
0.5500	0.3111	0.9433	0.9658	0.3332	0.9118	4.7	0.4487
0.5000	0.1970	0.9452	0.9624	0.2123	0.9148	7.7	0.3501
0.4450	0.1022	0.9478	0.9529	0.1121	0.9189	15.2	0.2468
0.4000	0.0329	0.9249	0.8973	0.0402	0.8833	43.8	0.1371
0.3500	0.0163	0.8241	0.7903	0.0253	0.7265	72.3	0.0940
0.3000	0.0096	0.7074	0.6700	0.0202	0.5450	93.4	0.0701
0.2500	0.0068	0.6036	0.5687	0.0193	0.3836	101.0	0.0572
0.2000	0.0049	0.5215	0.4745	0.0189	0.2559	106.7	0.0465
0.1500	0.0034	0.4593	0.3846	0.0185	0.1591	112.0	0.0368
0.1000	0.0025	0.4103	0.2972	0.0184	0.0830	115.8	0.0279
0.0500	0.0018	0.3751	0.1989	0.0182	0.0283	120.6	0.0183
0.0000	0.0014	0.3570	0.0058	0.0176	0.0000	128.2	0.0005

TABLE 8. – COMPUTED PARAMETERS FOR x = 1.625 – Continued

$p_{O_e} = 198$ $p_w = 1.45 \times 10^{-4}$ $p_e = 0.655 \times 10^{-4}$ $T_O = 515$ $T_w = 304$ $T_e = 1.29$

$u_e = 2312$ $M_e = 34.5$ $\rho_e = 2.47 \times 10^{-3}$ $\frac{Re}{m} = 9.52 \times 10^6$ $\delta = 11.42$

$\frac{\delta^*}{\delta} = 0.561$ $\frac{\theta}{\delta} = 0.00376$ $\frac{\Gamma}{\delta} = 0.00722$ $R_\theta = 4096$

$C_f = 1.96 \times 10^{-4}$ $C_H = 0.679 \times 10^{-4}$ $\frac{2C_H}{C_f} = 0.672$ $\frac{M}{\sqrt{R_\theta}} = 0.539$

$\frac{y}{\delta}$	$\frac{p_{O_2}}{p_{O_{2e}}}$	$\frac{T_O}{T_{O_e}}$	$\frac{u}{u_e}$	$\frac{\rho}{\rho_e}$	$\frac{T_O - T_w}{T_{O_e} - T_w}$	$\frac{T}{T_e}$	$\frac{M}{M_e}$
1.0000	1.0000	1.0000	1.0000	1.0000	1.0000	1.0	1.0000
0.9222	1.0503	0.9935	0.9967	1.0572	0.9843	1.0	0.9798
0.8889	1.0416	0.9903	0.9950	1.0520	0.9764	1.1	0.9582
0.8333	0.9844	0.9849	0.9921	1.0000	0.9633	1.2	0.9051
0.7778	0.8648	0.9784	0.9886	0.8848	0.9475	1.4	0.8256
0.7222	0.7938	0.9709	0.9845	0.8188	0.9291	1.6	0.7708
0.6667	0.6794	0.9634	0.9802	0.7069	0.9108	2.0	0.6958
0.6111	0.5546	0.9620	0.9788	0.5786	0.9076	2.5	0.6141
0.5556	0.4298	0.9610	0.9771	0.4499	0.9049	3.4	0.5286
0.5000	0.3154	0.9611	0.9753	0.3312	0.9052	4.9	0.4431
0.4444	0.2166	0.9646	0.9739	0.2280	0.9137	7.4	0.3597
0.3889	0.1334	0.9683	0.9694	0.1416	0.9228	12.3	0.2766
0.3333	0.0572	0.9756	0.9514	0.0627	0.9405	28.9	0.1773
0.2778	0.0146	0.9809	0.8579	0.0191	0.9535	98.3	0.0867
0.2222	0.0059	0.9582	0.7073	0.0107	0.8982	182.8	0.0524
0.1667	0.0035	0.8264	0.5474	0.0096	0.5772	210.0	0.0378
0.1111	0.0023	0.7095	0.4107	0.0097	0.2924	215.5	0.0280
0.0556	0.0017	0.6334	0.2859	0.0098	0.1070	219.7	0.0193
0.0000	0.0013	0.5894	0.0058	0.0094	0.0000	234.7	0.0004

$p_{O_e} = 200$ $p_w = 1.45 \times 10^{-4}$ $p_e = 0.618 \times 10^{-4}$ $T_O = 888$ $T_w = 321$ $T_e = 2.15$

$u_e = 3036$ $M_e = 34.9$ $\rho_e = 1.40 \times 10^{-3}$ $\frac{Re}{m} = 4.99 \times 10^6$ $\delta = 11.68$

$\frac{\delta^*}{\delta} = 3036$ $\frac{\theta}{\delta} = 0.00501$ $\frac{\Gamma}{\delta} = 0.00945$ $R_\theta = 2916$

$C_f = 2.45 \times 10^{-4}$ $C_H = 0.920 \times 10^{-4}$ $\frac{2C_H}{C_f} = 0.752$ $\frac{M}{\sqrt{R_\theta}} = 0.646$

1.0000	1.0000	1.0000	1.0000	1.0000	1.0000	1.0	1.0000
0.9783	1.0327	0.9965	0.9982	1.0363	0.9945	1.0	1.0017
0.9239	1.0672	0.9891	0.9944	1.0791	0.9829	1.0	0.9840
0.8696	1.0363	0.9827	0.9911	1.0549	0.9729	1.1	0.9391
0.8152	0.9691	0.9753	0.9872	0.9944	0.9613	1.3	0.8813
0.7609	0.8784	0.9662	0.9823	0.9102	0.9470	1.5	0.8155
0.7065	0.7623	0.9586	0.9781	0.7966	0.9353	1.8	0.7395
0.6522	0.6334	0.9528	0.9745	0.6667	0.9262	2.2	0.6571
0.5978	0.5009	0.9476	0.9709	0.5311	0.9179	3.0	0.5703
0.5435	0.3684	0.9447	0.9679	0.3929	0.9133	4.2	0.4778
0.4891	0.2505	0.9440	0.9648	0.2687	0.9124	6.4	0.3853
0.4348	0.1488	0.9470	0.9604	0.1609	0.9170	11.1	0.2906
0.3804	0.0715	0.9453	0.9438	0.0798	0.9143	23.4	0.1970
0.3261	0.0229	0.9204	0.8732	0.0294	0.8754	66.1	0.1085
0.2717	0.0109	0.8351	0.7545	0.0182	0.7418	110.5	0.0725
0.2174	0.0063	0.6707	0.5988	0.0161	0.4844	129.4	0.0531
0.1630	0.0040	0.5389	0.4621	0.0161	0.2781	134.8	0.0402
0.1087	0.0027	0.4609	0.3532	0.0161	0.1559	139.1	0.0302
0.0543	0.0019	0.4024	0.2370	0.0161	0.0643	143.2	0.0200
0.0000	0.0013	0.3613	0.0080	0.0160	0.0000	149.4	0.0007

TABLE 8. – COMPUTED PARAMETERS FOR x = 1.625 – Continued

$p_{Oe} = 268$ $p_w = 1.88 \times 10^{-4}$ $p_e = 0.742 \times 10^{-4}$ $T_O = 514$ $T_w = 302$ $T_e = 1.20$

$u_e = 2310$ $M_e = 35.8$ $\rho_e = 3.03 \times 10^{-3}$ $\frac{Re}{m} = 1.23 \times 10^{7}$ $\delta = 11.04$

$\frac{\delta^*}{\delta} = 0.521$ $\frac{\theta}{\delta} = 0.00411$ $\frac{\Gamma}{\delta} = 0.00794$ $R_\theta = 5582$

$C_f = 1.88 \times 10^{-4}$ $C_H = 0.794 \times 10^{-4}$ $\frac{2C_H}{C_f} = 0.827$ $\frac{M}{\sqrt{R_\theta}} = 0.478$

$\frac{y}{\delta}$	$\frac{p_{O_2}}{p_{O_{2e}}}$	$\frac{T_O}{T_{Oe}}$	$\frac{u}{u_e}$	$\frac{\rho}{\rho_e}$	$\frac{T_O - T_W}{T_{Oe} - T_W}$	$\frac{T}{T_e}$	$\frac{M}{M_e}$
1.0000	1.0000	1.0000	1.0000	1.0000	1.0000	1.0	1.0000
0.9425	1.0729	0.9946	0.9973	1.0788	0.9869	1.0	0.9929
0.8736	1.0979	0.9892	0.9945	1.1101	0.9739	1.1	0.9588
0.8046	1.0345	0.9838	0.9916	1.0522	0.9608	1.2	0.8920
0.7471	0.9290	0.9773	0.9880	0.9515	0.9452	1.5	0.8179
0.6897	0.8119	0.9708	0.9844	0.8377	0.9295	1.8	0.7414
0.6322	0.6737	0.9665	0.9816	0.6990	0.9191	2.2	0.6560
0.5747	0.5278	0.9626	0.9787	0.5508	0.9095	3.0	0.5649
0.5172	0.3954	0.9620	0.9769	0.4139	0.9082	4.2	0.4763
0.4598	0.2841	0.9602	0.9737	0.2992	0.9038	6.1	0.3938
0.4023	0.2015	0.9602	0.9703	0.2136	0.9038	9.0	0.3238
0.3448	0.1209	0.9619	0.9633	0.1298	0.9079	15.5	0.2450
0.2874	0.0512	0.9665	0.9400	0.0575	0.9191	36.6	0.1557
0.2299	0.0119	0.9692	0.8189	0.0170	0.9256	129.2	0.0722
0.1724	0.0045	0.9170	0.6254	0.0101	0.7993	226.6	0.0416
0.1149	0.0026	0.7776	0.4494	0.0096	0.4622	247.9	0.0286
0.0575	0.0017	0.6425	0.2684	0.0100	0.1356	245.5	0.0172
0.0000	0.0013	0.5864	0.0026	0.0101	0.0000	252.3	0.0002

$p_{Oe} = 263$ $p_w = 1.87 \times 10^{-4}$ $p_e = 0.794 \times 10^{-4}$ $T_O = 893$ $T_w = 314$ $T_e = 2.14$

$u_e = 3277$ $M_e = 35.1$ $\rho_e = 1.81 \times 10^{-3}$ $\frac{Re}{m} = 6.50 \times 10^{6}$ $\delta = 11.17$

$\frac{\delta^*}{\delta} = 0.570$ $\frac{\theta}{\delta} = 0.00465$ $\frac{\Gamma}{\delta} = 0.00879$ $R_\theta = 3378$

$C_f = 2.17 \times 10^{-4}$ $C_H = 0.782 \times 10^{-4}$ $\frac{2C_H}{C_f} = 0.721$ $\frac{M}{\sqrt{R_\theta}} = 0.603$

1.0000	1.0000	1.0000	1.0000	1.0000	1.0000	1.0	0.9983
0.9205	1.0422	0.9913	0.9955	1.0515	0.9866	1.1	0.9684
0.8523	0.9982	0.9844	0.9919	1.0144	0.9760	1.2	0.9106
0.7955	0.9101	0.9818	0.9904	0.9278	0.9719	1.4	0.8429
0.7386	0.8055	0.9670	0.9825	0.8343	0.9491	1.7	0.7701
0.6818	0.6917	0.9602	0.9786	0.7221	0.9386	2.0	0.6942
0.6250	0.5670	0.9545	0.9750	0.5962	0.9298	2.6	0.6122
0.5682	0.4404	0.9513	0.9722	0.4656	0.9248	3.5	0.5262
0.5114	0.3138	0.9492	0.9692	0.3337	0.9217	5.1	0.4337
0.4545	0.2128	0.9492	0.9658	0.2278	0.9216	7.8	0.3491
0.3977	0.1262	0.9484	0.9583	0.1370	0.9204	13.5	0.2629
0.3409	0.0494	0.9244	0.9202	0.0578	0.8834	33.3	0.1605
0.2841	0.0158	0.8543	0.8072	0.0235	0.7752	85.4	0.0880
0.2273	0.0071	0.7392	0.6485	0.0156	0.5977	133.6	0.0565
0.1705	0.0040	0.6124	0.4953	0.0140	0.4022	153.8	0.0402
0.1136	0.0026	0.4782	0.3518	0.0151	0.1950	148.3	0.0291
0.0568	0.0017	0.4023	0.2216	0.0157	0.0780	147.7	0.0184
0.0000	0.0013	0.3517	0.0000	0.0164	0.0000	147.1	0.0000

TABLE 8. – COMPUTED PARAMETERS FOR x = 1.625 – Concluded

p_{Oe} = 108.2 p_w = 0.395 X 10^{-4} p_e = 0.212 X 10^{-4} T_O = 523 T_W = 300 T_e = 1.07

u_e = 2331 M_e = 38.1 ρ_e = 9.68 X 10^{-4} $\frac{Re}{m}$ = 4.22 X 10^6 δ = 25.0

$\frac{\delta^*}{\delta}$ = 0.616 $\frac{\theta}{\delta}$ = 0.00196 $\frac{\Gamma}{\delta}$ = 0.00368 R_θ = 2074

C_f = 1.64 X 10^{-4} C_H = 0.493 X 10^{-4} $\frac{2C_H}{C_f}$ = 0.609 $\frac{M}{\sqrt{R_\theta}}$ = 0.835

$\frac{y}{\delta}$	$\frac{p_{O_2}}{p_{O_{2e}}}$	$\frac{T_O}{T_{Oe}}$	$\frac{u}{u_e}$	$\frac{\rho}{\rho_e}$	$\frac{T_O - T_W}{T_{Oe} - T_W}$	$\frac{T}{T_e}$	$\frac{M}{M_e}$
1.0000	1.0000	1.0000	1.0000	1.0000	1.0001	1.0	0.9982
0.9543	1.0096	0.9989	0.9994	1.0108	0.9973	1.0	0.9838
0.9036	1.0144	0.9944	0.9971	1.0202	0.9869	1.1	0.9660
0.8629	0.9856	0.9891	0.9944	0.9968	0.9745	1.1	0.9371
0.8122	0.9067	0.9842	0.9918	0.9218	0.9629	1.3	0.8817
0.7614	0.7990	0.9806	0.9897	0.8156	0.9546	1.5	0.8125
0.7107	0.7392	0.9800	0.9893	0.7553	0.9532	1.7	0.7677
0.6599	0.5742	0.9783	0.9878	0.5883	0.9492	2.2	0.6650
0.6091	0.4402	0.9798	0.9878	0.4510	0.9528	3.0	0.5726
0.5584	0.3086	0.9830	0.9879	0.3160	0.9603	4.4	0.4717
0.5076	0.1986	0.9860	0.9867	0.2037	0.9672	7.1	0.3724
0.4569	0.0971	0.9915	0.9815	0.1005	0.9801	14.8	0.2563
0.4061	0.0301	0.9984	0.9517	0.0329	0.9962	46.4	0.1402
0.3553	0.0101	0.9910	0.8646	0.0131	0.9790	120.3	0.0791
0.3046	0.0063	0.9328	0.7748	0.0099	0.8426	163.9	0.0607
0.2538	0.0043	0.8186	0.6650	0.0090	0.5751	185.2	0.0490
0.2030	0.0030	0.7238	0.5598	0.0085	0.3530	201.8	0.0395
0.1523	0.0022	0.6606	0.4664	0.0080	0.2050	217.7	0.0317
0.1015	0.0015	0.6209	0.3543	0.0074	0.1121	243.4	0.0228
0.0508	0.0010	0.5877	0.1800	0.0067	0.0343	272.7	0.0109
0.0000	0.0009	0.5730	0.0036	0.0067	0.0000	281.3	0.0035

p_{Oe} = 110.2 p_w = 0.395 X 10^{-4} p_e = 0.224 X 10^{-4} T_O = 967 T_W = 300 T_e = 1.96

u_e = 3167 M_e = 37.9 ρ_e = 5.57 X 10^{-4} $\frac{Re}{m}$ = 2.14 X 10^6 δ = 24.1

$\frac{\delta^*}{\delta}$ = 0.604 $\frac{\theta}{\delta}$ = 0.00280 $\frac{\Gamma}{\delta}$ = 0.00508 R_θ = 1450

C_f = 1.90 X 10^{-4} C_H = 0.680 X 10^{-4} $\frac{2C_H}{C_f}$ = 0.715 $\frac{M}{\sqrt{R_\theta}}$ = 0.975

$\frac{y}{\delta}$	$\frac{p_{O_2}}{p_{O_{2e}}}$	$\frac{T_O}{T_{Oe}}$	$\frac{u}{u_e}$	$\frac{\rho}{\rho_e}$	$\frac{T_O - T_W}{T_{Oe} - T_W}$	$\frac{T}{T_e}$	$\frac{M}{M_e}$
1.0000	1.0000	1.0001	1.0000	1.0000	1.0001	1.0	1.0000
0.9474	1.0028	0.9975	0.9987	1.0055	0.9963	1.1	0.9819
0.8684	0.9804	0.9902	0.9949	0.9904	0.9858	1.1	0.9439
0.8421	0.9580	0.9880	0.9938	0.9700	0.9827	1.2	0.9246
0.7895	0.8824	0.9817	0.9905	0.8994	0.9735	1.3	0.8718
0.7368	0.7675	0.9758	0.9872	0.7874	0.9649	1.6	0.7994
0.6842	0.6695	0.9693	0.9836	0.6918	0.9555	1.9	0.7344
0.6316	0.5210	0.9645	0.9806	0.5417	0.9485	2.4	0.6376
0.5789	0.3922	0.9630	0.9789	0.4091	0.9464	3.3	0.5446
0.5263	0.2570	0.9596	0.9751	0.2700	0.9414	5.2	0.4343
0.4737	0.1450	0.9351	0.9583	0.1576	0.9060	9.2	0.3213
0.4211	0.0329	0.8667	0.8914	0.0410	0.8067	36.3	0.1504
0.3684	0.0127	0.7542	0.7774	0.0206	0.6437	74.5	0.0916
0.3158	0.0080	0.6386	0.6719	0.0170	0.4761	92.8	0.0709
0.2632	0.0053	0.5468	0.5746	0.0151	0.3429	107.2	0.0564
0.2105	0.0041	0.4760	0.4997	0.0148	0.2403	111.9	0.0480
0.1579	0.0028	0.4235	0.4178	0.0138	0.1641	123.0	0.0383
0.1053	0.0018	0.3787	0.3224	0.0128	0.0992	135.6	0.0281
0.0526	0.0011	0.3365	0.2058	0.0123	0.0380	145.1	0.0174
0.0000	0.0008	0.3102	0.0000	0.0115	0.0000	153.0	0.0000

TABLE 9. – COMPUTED PARAMETERS FOR x = 2.793

p_{Oe} = 200 p_w = 0.553 X 10^{-4} p_e = 0.242 X 10^{-4} T_O = 498 T_W = 297 T_e = 0.83

u_e = 2273 M_e = 42.2 ρ_e = 1.41 X 10^{-3} $\frac{Re}{m}$ = 7.11 X 10^6 δ = 21.3

$\frac{\delta^*}{\delta}$ = 0.600 $\frac{\theta}{\delta}$ = 0.00218 $\frac{\Gamma}{\delta}$ = 0.00415 R_θ = 3308

C_f = 1.47 X 10^{-4} C_H = 0.418 X 10^{-4} $\frac{2C_H}{C_f}$ = 0.561 $\frac{M}{\sqrt{R_\theta}}$ = 0.730

$\frac{y}{\delta}$	$\frac{p_{O_2}}{p_{O_{2e}}}$	$\frac{T_O}{T_{Oe}}$	$\frac{u}{u_e}$	$\frac{\rho}{\rho_e}$	$\frac{T_O - T_W}{T_{Oe} - T_W}$	$\frac{T}{T_e}$	$\frac{M}{M_e}$
1.0000	1.0000	1.0000	1.0000	1.0000	1.0001	1.0	1.0000
0.9524	1.0522	0.9948	0.9974	1.0577	0.9872	1.0	0.9958
0.9107	1.0665	0.9912	0.9955	1.0760	0.9781	1.0	0.9782
0.8929	1.0570	0.9901	0.9950	1.0677	0.9754	1.1	0.9640
0.8333	0.9905	0.9814	0.9905	1.0096	0.9539	1.2	0.9034
0.7738	0.8703	0.9757	0.9874	0.8926	0.9397	1.5	0.8213
0.7143	0.7278	0.9738	0.9861	0.7484	0.9350	1.8	0.7298
0.6548	0.5728	0.9746	0.9860	0.5891	0.9369	2.5	0.6300
0.5952	0.4146	0.9768	0.9861	0.4261	0.9425	3.6	0.5223
0.5357	0.2769	0.9804	0.9862	0.2845	0.9513	5.6	0.4164
0.4762	0.1646	0.9857	0.9853	0.1693	0.9646	9.9	0.3135
0.4167	0.0658	0.9964	0.9773	0.0686	0.9912	25.6	0.1936
0.3571	0.0152	1.0235	0.9216	0.0175	1.0582	104.8	0.0903
0.2976	0.0063	1.0276	0.8173	0.0089	1.0685	215.3	0.0559
0.2381	0.0039	0.9475	0.7000	0.0073	0.8696	273.5	0.0425
0.1786	0.0026	0.7678	0.5462	0.0074	0.4237	280.5	0.0327
0.1190	0.0017	0.6764	0.4120	0.0071	0.1968	302.6	0.0238
0.0595	0.0011	0.6261	0.2657	0.0067	0.0718	331.6	0.0146
0.0000	0.0009	0.5971	0.0094	0.0064	0.0000	356.1	0.0005

p_{Oe} = 201 p_w = 0.553 X 10^{-4} p_e = 0.244 X 10^{-4} T_O = 958 T_W = 300 T_e = 1.58

u_e = 3154 M_e = 42.1 ρ_e = 7.52 X 10^{-4} $\frac{Re}{m}$ = 3.34 X 10^6 δ = 21.8

$\frac{\delta^*}{\delta}$ = 0.632 $\frac{\theta}{\delta}$ = 0.00226 $\frac{\Gamma}{\delta}$ = 0.00410 R_θ = 1645

C_f = 1.79 X 10^{-4} C_H = 0.576 X 10^{-4} $\frac{2C_H}{C_f}$ = 0.658 $\frac{M}{\sqrt{R_\theta}}$ = 1.030

1.0000	1.0000	1.0000	1.0000	1.0000	1.0001	1.0	1.0000
0.9419	1.0287	0.9946	0.9973	1.0343	0.9922	1.1	0.9788
0.9070	1.0159	0.9904	0.9951	1.0260	0.9860	1.1	0.9533
0.8721	0.9904	0.9888	0.9942	1.0019	0.9838	1.2	0.9232
0.8140	0.8917	0.9858	0.9925	0.9051	0.9793	1.4	0.8494
0.7558	0.7580	0.9786	0.9886	0.7754	0.9688	1.7	0.7608
0.6977	0.6146	0.9761	0.9869	0.6309	0.9652	2.3	0.6666
0.6395	0.4650	0.9733	0.9847	0.4793	0.9611	3.1	0.5649
0.5814	0.3121	0.9732	0.9832	0.3226	0.9610	4.9	0.4514
0.5233	0.1783	0.9743	0.9804	0.1853	0.9625	8.9	0.3332
0.4651	0.0777	0.9847	0.9754	0.0814	0.9778	21.2	0.2148
0.4070	0.0232	0.9993	0.9413	0.0259	0.9989	69.6	0.1145
0.3488	0.0109	0.8730	0.8223	0.0156	0.8151	120.1	0.0761
0.2907	0.0067	0.7146	0.6884	0.0133	0.5846	146.5	0.0577
0.2326	0.0044	0.5850	0.5668	0.0127	0.3960	160.3	0.0454
0.1744	0.0031	0.4888	0.4642	0.0127	0.2559	166.0	0.0365
0.1163	0.0019	0.4181	0.3475	0.0121	0.1530	180.5	0.0262
0.0581	0.0012	0.3611	0.2270	0.0120	0.0700	187.8	0.0168
0.0000	0.0009	0.3132	0.0021	0.0123	0.0000	189.9	0.0002

TABLE 9. – COMPUTED PARAMETERS FOR x = 2.793 – Concluded

$p_{Oe} = 270$ $p_w = 0.658 \times 10^{-4}$ $p_e = 0.251 \times 10^{-4}$ $T_O = 523$ $T_w = 300$ $T_e = 0.78$

$u_e = 2330$ $M_e = 44.6$ $\rho_e = 1.60 \times 10^{-3}$ $\frac{Re}{m} = 8.49 \times 10^6$ $\delta = 21.3$

$\frac{\delta^*}{\delta} = 0.549$ $\frac{\theta}{\delta} = 0.00248$ $\frac{\Gamma}{\delta} = 0.00476$ $R_\theta = 4412$

$C_f = 1.44 \times 10^{-4}$ $C_H = 0.501 \times 10^{-4}$ $\frac{2C_H}{C_f} = 0.696$ $\frac{M}{\sqrt{R_\theta}} = 0.672$

$\frac{y}{\delta}$	$\frac{p_{O_2}}{p_{O_2e}}$	$\frac{T_O}{T_{Oe}}$	$\frac{u}{u_e}$	$\frac{\rho}{\rho_e}$	$\frac{T_O - T_w}{T_{Oe} - T_w}$	$\frac{T}{T_e}$	$\frac{M}{M_e}$
1.0000	1.0000	1.0000	1.0000	1.0000	1.0001	1.0	1.0000
0.9286	1.1033	0.9935	0.9967	1.1106	0.9847	1.0	0.9943
0.8690	1.1292	0.9888	0.9943	1.1421	0.9737	1.1	0.9649
0.8333	1.1144	0.9822	0.9910	1.1348	0.9584	1.1	0.9364
0.7738	1.0037	0.9789	0.9891	1.0259	0.9505	1.3	0.8567
0.7143	0.8413	0.9761	0.9874	0.8628	0.9440	1.7	0.7580
0.6548	0.6863	0.9745	0.9862	0.7055	0.9402	2.2	0.6630
0.5952	0.5240	0.9743	0.9854	0.5394	0.9397	3.1	0.5621
0.5357	0.3616	0.9755	0.9848	0.3726	0.9427	4.7	0.4539
0.4762	0.2325	0.9781	0.9838	0.2399	0.9486	7.8	0.3542
0.4167	0.1365	0.9802	0.9803	0.1418	0.9536	13.8	0.2645
0.3571	0.0572	0.9877	0.9687	0.0606	0.9713	33.9	0.1668
0.2976	0.0111	1.0065	0.8802	0.0139	1.0153	155.5	0.0708
0.2381	0.0041	0.9746	0.7139	0.0072	0.9404	310.8	0.0406
0.1786	0.0028	0.8596	0.5907	0.0069	0.6709	341.2	0.0321
0.1190	0.0018	0.7374	0.4436	0.0068	0.3844	361.0	0.0234
0.0595	0.0011	0.6390	0.2442	0.0066	0.1538	386.7	0.0125
0.0000	0.0009	0.5734	0.0096	0.0069	0.0000	382.6	0.0005

$p_{Oe} = 271$ $p_w = 0.658 \times 10^{-4}$ $p_e = 0.281 \times 10^{-4}$ $T_O = 913$ $T_w = 297$ $T_e = 1.42$

$u_e = 3078$ $M_e = 43.5$ $\rho_e = 9.67 \times 10^{-4}$ $\frac{Re}{m} = 4.54 \times 10^6$ $\delta = 21.6$

$\frac{\delta^*}{\delta} = 0.606$ $\frac{\theta}{\delta} = 0.00238$ $\frac{\Gamma}{\delta} = 0.00432$ $R_\theta = 2330$

$C_f = 1.65 \times 10^{-4}$ $C_H = 0.666 \times 10^{-4}$ $\frac{2C_H}{C_f} = 0.810$ $\frac{M}{\sqrt{R_\theta}} = 0.895$

1.0000	1.0000	1.0000	1.0000	1.0000	1.0001	1.0	1.0000
0.9412	1.0348	0.9971	0.9985	1.0380	0.9957	1.1	0.9793
0.8941	1.0383	0.9932	0.9965	1.0456	0.9899	1.1	0.9534
0.8588	1.0209	0.9888	0.9942	1.0327	0.9834	1.2	0.9263
0.8235	0.9791	0.9873	0.9934	0.9921	0.9811	1.3	0.8895
0.7647	0.8502	0.9815	0.9903	0.8669	0.9726	1.6	0.8036
0.7059	0.7108	0.9782	0.9883	0.7276	0.9677	2.0	0.7136
0.6471	0.5505	0.9728	0.9850	0.5673	0.9597	2.7	0.6109
0.5882	0.3798	0.9696	0.9823	0.3934	0.9549	4.0	0.4943
0.5294	0.2334	0.9706	0.9805	0.2426	0.9565	6.9	0.3779
0.4706	0.1307	0.9740	0.9775	0.1365	0.9615	12.8	0.2760
0.4118	0.0449	0.9818	0.9615	0.0483	0.9731	38.0	0.1579
0.3529	0.0139	0.9616	0.8893	0.0172	0.9431	111.1	0.0854
0.2941	0.0075	0.8018	0.7489	0.0128	0.7060	156.1	0.0607
0.2353	0.0046	0.5248	0.5469	0.0142	0.2953	146.0	0.0458
0.1765	0.0029	0.4418	0.4357	0.0133	0.1722	162.8	0.0346
0.1176	0.0018	0.3932	0.3307	0.0122	0.1001	183.3	0.0247
0.0588	0.0013	0.3546	0.2433	0.0122	0.0428	190.7	0.0178
0.0000	0.0008	0.3287	0.0067	0.0113	0.0045	212.1	0.0005

TABLE 10. – COMPUTED PARAMETERS FOR χ = 3.56

$p_{O_e} = 201$ $p_w = 0.504 \times 10^{-4}$ $p_e = 0.203 \times 10^{-4}$ $T_O = 538$ $T_W = 297$ $T_e = 0.83$

$u_e = 2363$ $M_e = 43.8$ $\rho_e = 1.18 \times 10^{-3}$ $\frac{Re}{m} = 6.14 \times 10^{6}$ $\delta = 29.0$

$\frac{\delta^*}{\delta} = 0.601$ $\frac{\theta}{\delta} = 0.00210$ $\frac{\Gamma}{\delta} = 0.00395$ $R_\theta = 3732$ $C_f = 0.92 \times 10^{-4}$

$\frac{y}{\delta}$	$\frac{p_{O_2}}{p_{O_{2e}}}$	$\frac{T_O}{T_{Oe}}$	$\frac{u}{u_e}$	$\frac{\rho}{\rho_e}$	$\frac{T_O - T_W}{T_{Oe} - T_W}$	$\frac{T}{T_e}$	$\frac{M}{M_e}$
1.0000	1.0000	1.0000	1.0000	1.0000	1.0001	1.0	1.0000
0.9561	1.0042	0.9946	0.9973	1.0098	0.9880	1.1	0.9710
0.9211	0.9922	0.9915	0.9956	1.0009	0.9810	1.1	0.9424
0.8772	0.9625	0.9874	0.9935	0.9751	0.9719	1.2	0.9023
0.8333	0.9226	0.9835	0.9914	0.9386	0.9630	1.3	0.8600
0.7895	0.8812	0.9806	0.9898	0.8993	0.9566	1.5	0.8194
0.7456	0.8232	0.9768	0.9878	0.8436	0.9481	1.6	0.7730
0.7018	0.7422	0.9753	0.9869	0.7620	0.9449	1.9	0.7172
0.6579	0.6365	0.9731	0.9854	0.6553	0.9400	2.3	0.6497
0.6140	0.5092	0.9713	0.9839	0.5258	0.9359	3.0	0.5689
0.5702	0.3812	0.9708	0.9828	0.3945	0.9348	4.2	0.4823
0.5263	0.2550	0.9721	0.9816	0.2644	0.9377	6.5	0.3867
0.4825	0.1531	0.9745	0.9791	0.1595	0.9430	11.2	0.2940
0.4386	0.0753	0.9679	0.9662	0.0804	0.9284	23.0	0.2023
0.3947	0.0274	0.9585	0.9300	0.0313	0.9074	61.2	0.1195
0.3509	0.0094	0.9236	0.8315	0.0132	0.8293	150.2	0.0682
0.3070	0.0054	0.8658	0.7289	0.0095	0.7002	216.0	0.0498
0.2632	0.0036	0.8050	0.6322	0.0081	0.5645	261.5	0.0393
0.2193	0.0025	0.7494	0.5392	0.0074	0.4404	295.8	0.0315
0.1754	0.0018	0.6988	0.4445	0.0069	0.3273	323.1	0.0248
0.1316	0.0014	0.6482	0.3508	0.0068	0.2144	338.4	0.0192
0.0877	0.0011	0.6065	0.2469	0.0068	0.1211	351.5	0.0132
0.0439	0.0009	0.5745	0.1435	0.0068	0.0499	356.9	0.0076
0.0000	0.0009	0.5522	0.0080	0.0071	0.0000	355.7	0.0004

$p_{O_e} = 270$ $p_w = 0.645 \times 10^{-4}$ $p_e = 0.218 \times 10^{-4}$ $T_O = 519$ $T_W = 297$ $T_e = 0.73$

$u_e = 2321$ $M_e = 45.9$ $\rho_e = 1.44 \times 10^{-3}$ $\frac{Re}{m} = 8.03 \times 10^{6}$ $\delta = 27.2$

$\frac{\delta^*}{\delta} = 0.599$ $\frac{\theta}{\delta} = 0.00227$ $\frac{\Gamma}{\delta} = 0.00427$ $R_\theta = 4944$ $C_f = 0.56 \times 10^{-4}$

1.0000	1.0000	1.0000	1.0000	1.0000	1.0001	1.0	1.0000
0.9720	1.0104	0.9977	0.9988	1.0128	0.9946	1.0	0.9787
0.9486	1.0148	0.9954	0.9976	1.0196	0.9893	1.1	0.9602
0.9252	1.0112	0.9932	0.9965	1.0183	0.9841	1.1	0.9392
0.8879	0.9976	0.9900	0.9948	1.0080	0.9765	1.2	0.9044
0.8411	0.9691	0.9847	0.9920	0.9847	0.9641	1.3	0.8597
0.7944	0.9294	0.9806	0.9899	0.9485	0.9545	1.5	0.8140
0.7477	0.8600	0.9779	0.9884	0.8803	0.9483	1.7	0.7586
0.7009	0.7501	0.9746	0.9864	0.7708	0.9406	2.1	0.6877
0.6542	0.6169	0.9717	0.9845	0.6363	0.9337	2.7	0.6064
0.6075	0.4817	0.9711	0.9836	0.4978	0.9324	3.6	0.5218
0.5607	0.3454	0.9698	0.9817	0.3581	0.9294	5.2	0.4307
0.5140	0.2110	0.9704	0.9793	0.2197	0.9308	8.9	0.3286
0.4673	0.1063	0.9726	0.9736	0.1118	0.9360	18.4	0.2278
0.4206	0.0485	0.9732	0.9574	0.0526	0.9374	40.9	0.1503
0.3738	0.0216	0.9642	0.9166	0.0254	0.9162	88.4	0.0978
0.3271	0.0082	0.9220	0.8063	0.0121	0.8175	192.6	0.0583
0.2804	0.0047	0.8600	0.6940	0.0091	0.6724	267.7	0.0426
0.2336	0.0031	0.8001	0.5860	0.0078	0.5320	322.8	0.0327
0.1869	0.0022	0.7433	0.4891	0.0073	0.3991	356.1	0.0260
0.1402	0.0016	0.6901	0.3928	0.0071	0.2746	378.4	0.0203
0.0935	0.0013	0.6397	0.2864	0.0071	0.1566	393.8	0.0145
0.0467	0.0010	0.6015	0.1646	0.0071	0.0672	405.6	0.0082
0.0000	0.0010	0.5727	0.0075	0.0074	0.0000	404.4	0.0004

TABLE 10. – COMPUTED PARAMETERS FOR x = 3.56 – Concluded

$p_{Oe} = 270$ $p_w = 0.645 \times 10^{-4}$ $p_e = 0.233 \times 10^{-4}$ $T_O = 892$ $T_W = 297$ $T_e = 1.29$

$u_e = 3044$ $M_e = 45.1$ $\rho_e = 8.84 \times 10^{-4}$ $\frac{R_e}{m} = 4.37 \times 10^6$ $\delta = 27.7$

$\frac{\delta^*}{\delta} = 0.621$ $\frac{\theta}{\delta} = 0.00309$ $\frac{\Gamma}{\delta} = 0.00572$ $R_\theta = 3731$ $C_f = 0.61 \times 10^{-4}$

$\frac{y}{\delta}$	$\frac{p_{O_2}}{p_{O_2 e}}$	$\frac{T_O}{T_{Oe}}$	$\frac{u}{u_e}$	$\frac{\rho}{\rho_e}$	$\frac{T_O - T_W}{T_{Oe} - T_W}$	$\frac{T}{T_e}$	$\frac{M}{M_e}$
1.0000	1.0000	1.0000	1.0000	1.0000	1.0001	1.0	1.0000
0.9633	1.0217	0.9972	0.9985	1.0247	0.9958	1.1	0.9796
0.9404	1.0271	0.9951	0.9975	1.0323	0.9927	1.1	0.9641
0.9147	1.0233	0.9932	0.9965	1.0305	0.9898	1.1	0.9451
0.8716	0.9957	0.9888	0.9942	1.0074	0.9832	1.2	0.9011
0.8028	0.9271	0.9762	0.9877	0.9503	0.9644	1.5	0.8294
0.7339	0.7876	0.9659	0.9822	0.8164	0.9489	1.8	0.7322
0.6881	0.6469	0.9593	0.9784	0.6756	0.9390	2.3	0.6460
0.6422	0.5039	0.9516	0.9739	0.5311	0.9274	3.1	0.5558
0.5963	0.3620	0.9453	0.9696	0.3849	0.9181	4.6	0.4598
0.5505	0.2240	0.9406	0.9648	0.2404	0.9109	7.6	0.3534
0.5046	0.1279	0.9317	0.9556	0.1398	0.8976	13.7	0.2611
0.4587	0.0632	0.9129	0.9349	0.0720	0.8694	27.8	0.1794
0.4128	0.0245	0.8792	0.8849	0.0309	0.8189	67.6	0.1090
0.3670	0.0127	0.8081	0.8039	0.0192	0.7123	113.0	0.0765
0.3211	0.0073	0.7284	0.7051	0.0140	0.5928	160.9	0.0563
0.2752	0.0049	0.6485	0.6095	0.0121	0.4731	192.6	0.0444
0.2294	0.0033	0.5746	0.5132	0.0112	0.3624	216.4	0.0353
0.1835	0.0023	0.5093	0.4213	0.0108	0.2644	230.5	0.0281
0.1376	0.0017	0.4530	0.3347	0.0109	0.1801	236.8	0.0220
0.0917	0.0013	0.4012	0.2448	0.0112	0.1024	237.0	0.0161
0.0459	0.0010	0.3626	0.1462	0.0116	0.0445	236.9	0.0096
0.0000	0.0009	0.3329	0.0037	0.0122	−0.0000	231.1	0.0002

TABLE 11. – TEST PARAMETERS

x	M_C	p_{0e}	T_{0e}	δ	$p_w \times 10^4$	T_w	$C_f \times 10^4$	$C_H \times 10^4$	$\rho_w \times 10^5$	$\frac{\delta_L}{\delta}$	$\frac{U_L}{U_e}$	$\frac{M_L}{Me}$	R_θ
0.508	19.4	66.1	499	2.87	5.26	362	4.87		7.4	0.3	0.95	0.24	1381
	19.2	66.2	820	2.87	5.26	397	4.84*		6.54	0.39	0.94	0.28	913
	19.9	107.6	315	2.72	8.61	333	4.06*		12.55	0.19	0.94	0.16	2662
	19.9	107.6	393	2.74	8.61	333	4.28*		12.65	0.20	0.93	0.16	2608
	19.8	108.1	481	2.72	8.61	339	3.78*		12.43	0.25	0.94	0.13	2196
	19.8	109.2	988	2.69	8.61	400	4.38*		10.67	0.29	0.91	0.18	1420
	20.1	199	516	2.44	13.4	352	3.37*		18.73	0.17	0.90	0.09	3343
	20.0	199	942	2.57	13.4	402	3.71*		16.40	0.28	0.88	0.18	2688
	20.3	270	503	2.36	18.1	318	2.39*		27.9	0.18	0.92	0.18	5430
	20.2	268	882	2.41	18.2	361	3.42*		24.8	0.21	0.91	0.21	3337
1.067	27.3	65.3	500	7.98	1.45	315	3.62	1.21	2.23	0.39	0.93	0.20	1440
	26.4	65	933	7.67	1.45	358	3.80	1.41	1.98	0.16	0.93	0.22	916
	27.3	107.7	305	7.11	2.08	299	2.33	0.866	3.37	0.25	0.94	0.18	3786
	27.5	107.7	418	7.11	2.08	301	2.53	0.967	3.39	0.31	0.94	0.18	2767
	27.9	107.7	577	7.16	2.08	309	3.02	1.16	3.30	0.33	0.92	0.17	1801
	27.4	109.8	920	7.24	2.04	328	3.22	1.22	3.04	0.38	0.92	0.19	1685
	29.4	189	534	6.96	3.12	319	2.73	1.11	4.78	0.28	0.94	0.18	3710
	29.0	189	877	6.99	3.12	348	3.01	1.02	4.36	0.32	0.93	0.17	2380
	29.9	270	502	6.47	3.86	318	2.03	0.957	5.89	0.23	0.93	0.15	4756
	29.6	265	876	6.60	3.85	339	2.58	1.02	5.35	0.29	0.92	0.16	2870
1.625	30.9	66.9	515	13.34	0.698	301	2.66	0.758	1.14	0.40	0.94	0.20	2190
	30.6	65.3	890	13.46	0.698	321	3.00	1.00	1.085	0.46	0.94	0.21	1296
	33.1	107.3	495	12.57	1.05	306	2.38	0.797	1.72	0.36	0.93	0.14	2800
	32.5	107.6	886	12.70	1.04	317	2.68	0.931	1.634	0.42	0.93	0.18	1680
	34.5	198	515	11.42	1.45	304	1.96	0.679	2.32	0.31	0.93	0.14	4096
	34.9	200	888	11.68	1.45	321	2.45	0.920	2.24	0.35	0.93	0.15	2916
	35.8	268	514	11.04	1.88	302	1.88	0.794	3.06	0.26	0.92	0.12	5582
	35.1	263	893	11.17	1.87	314	2.17	0.782	2.97	0.34	0.92	0.17	3378
2.793	38.1	108.2	523	25	0.395	300	1.64	0.493	0.658	0.40	0.94	0.14	2074
	37.9	110.2	967	24.1	0.395	300	1.90	0.680	0.640	0.46	0.94	0.25	1450
	42.2	200	498	21.3	0.553	297	1.47	0.418	0.902	0.35	0.92	0.09	3308
	42.1	201	958	21.8	0.553	300	1.79	0.576	0.925	0.41	0.94	0.12	1645
	44.6	270	523	21.3	0.658	300	1.44	0.501	1.103	0.33	0.94	0.13	4412
	43.5	271	913	21.6	0.658	297	1.65	0.666	1.092	0.38	0.94	0.12	2330

*These values estimated from velocity profiles.

TABLE 11

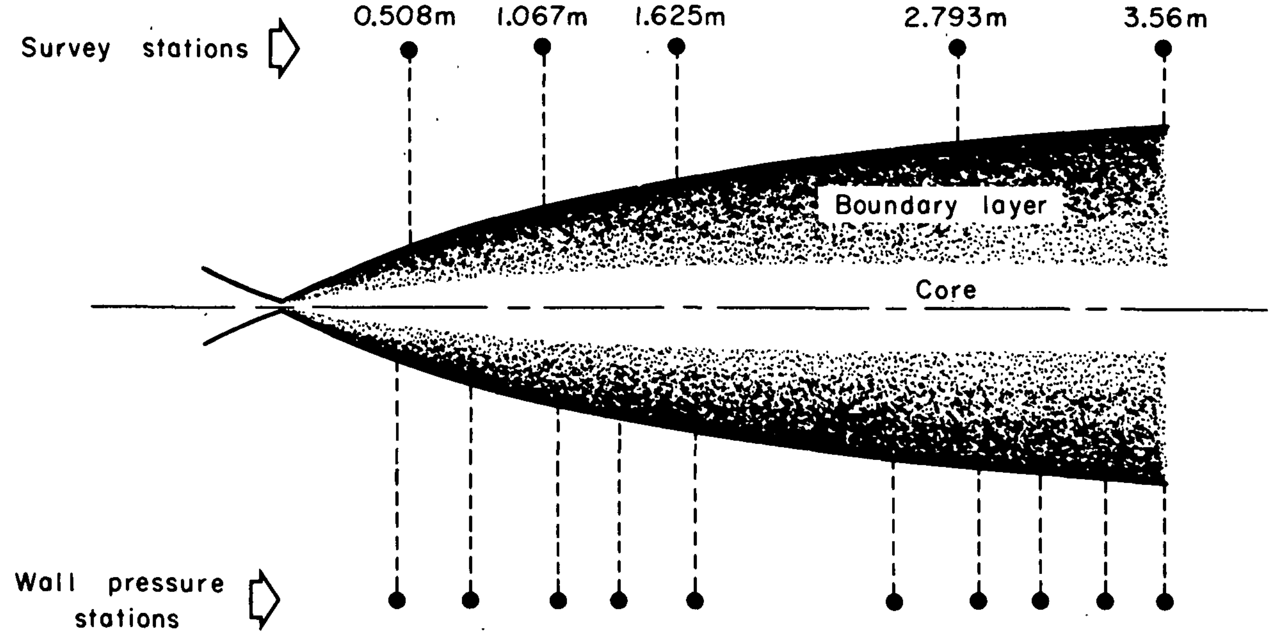

Figure 1.– Schematic of the M–50 nozzle.

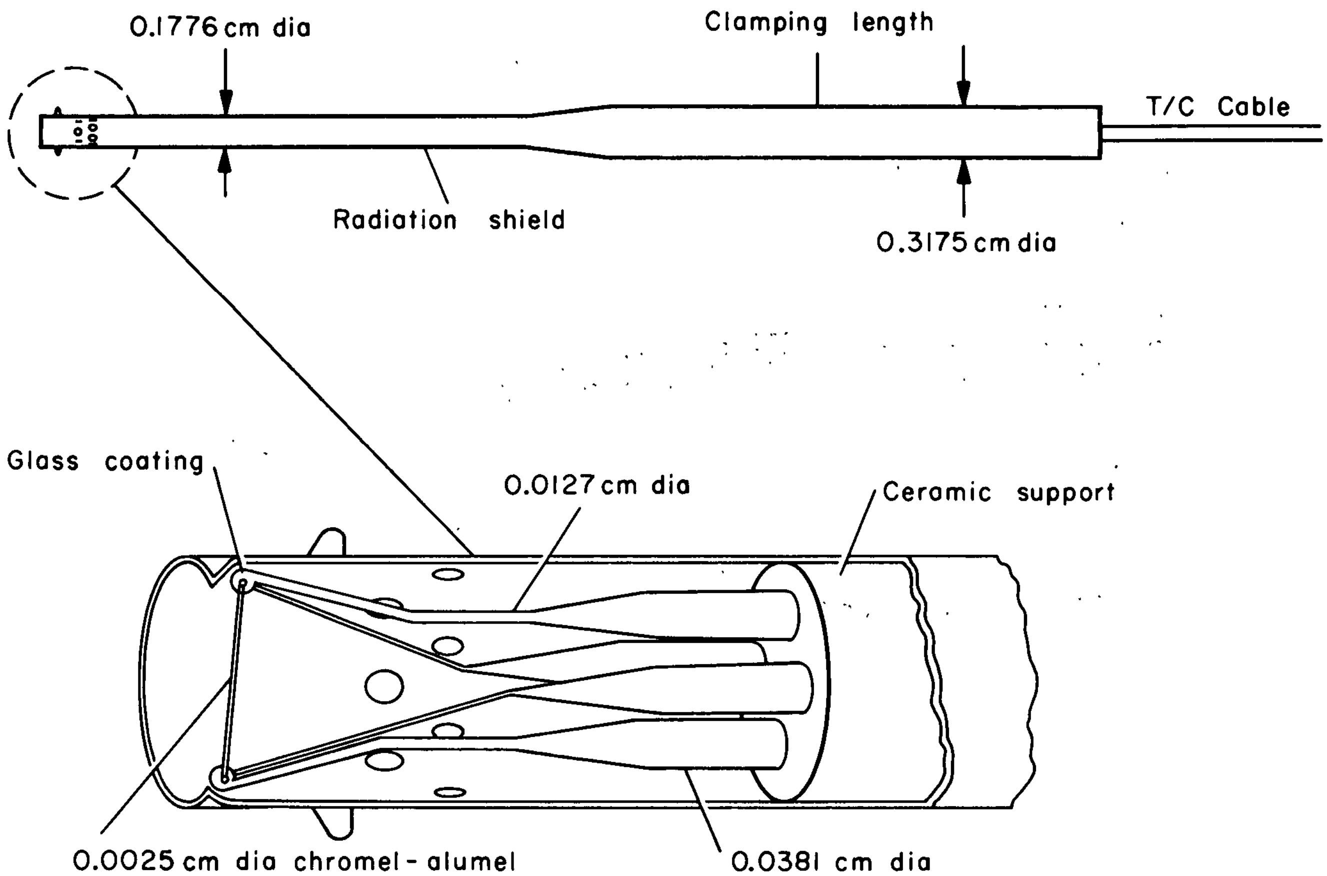

Figure 2.– Schematic of stagnation-temperature probe.

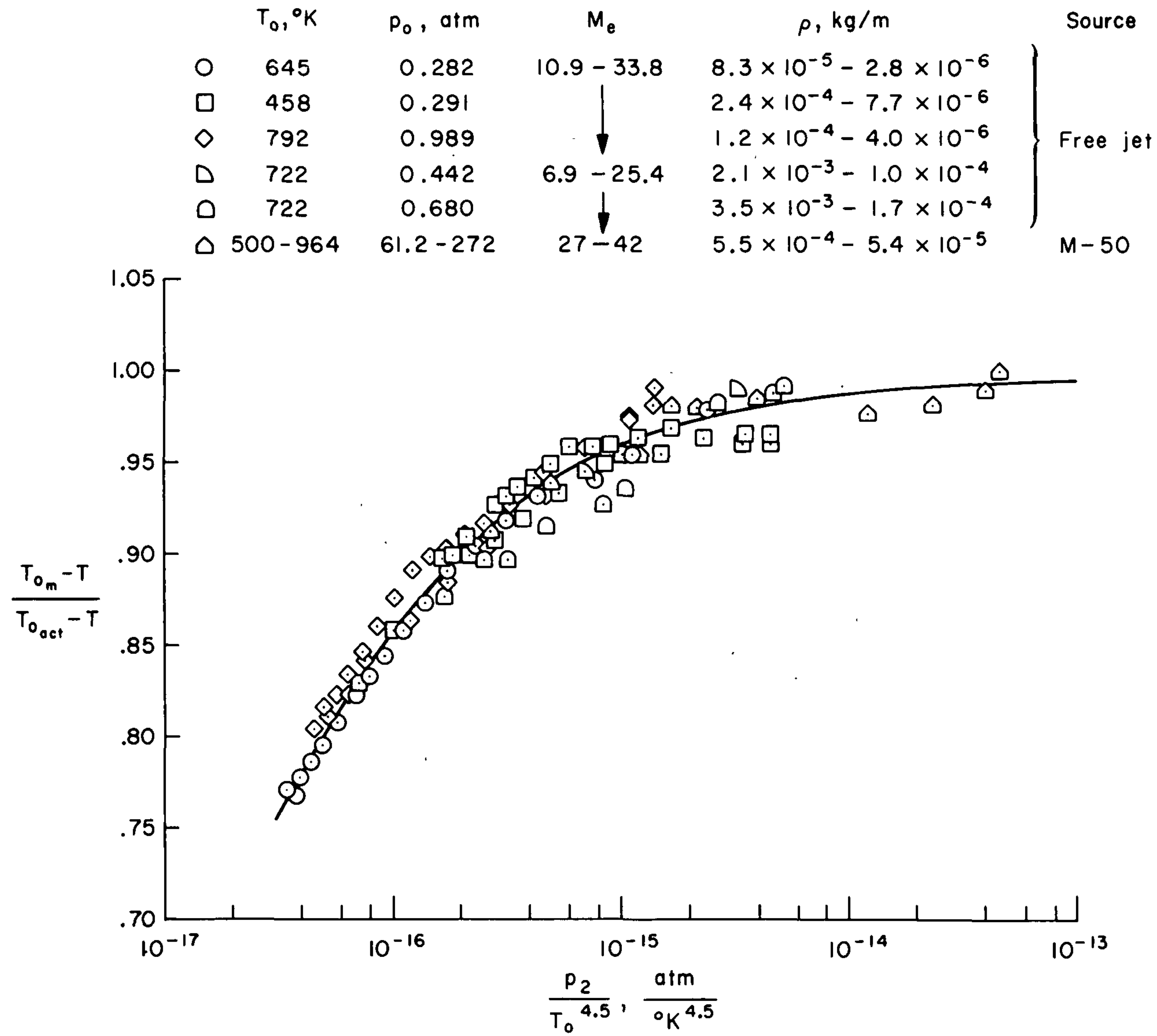

Figure 3.– Correlation of calibration data for the total temperature probe.

Station, x,m	Skin thickness, t, cm	Thermocouple wire diameter, d, cm
1.067	0.0152	0.0075
1.625	0.0127	0.0075
2.793	0.0076	0.0025
3.56	0.0051	0.0025

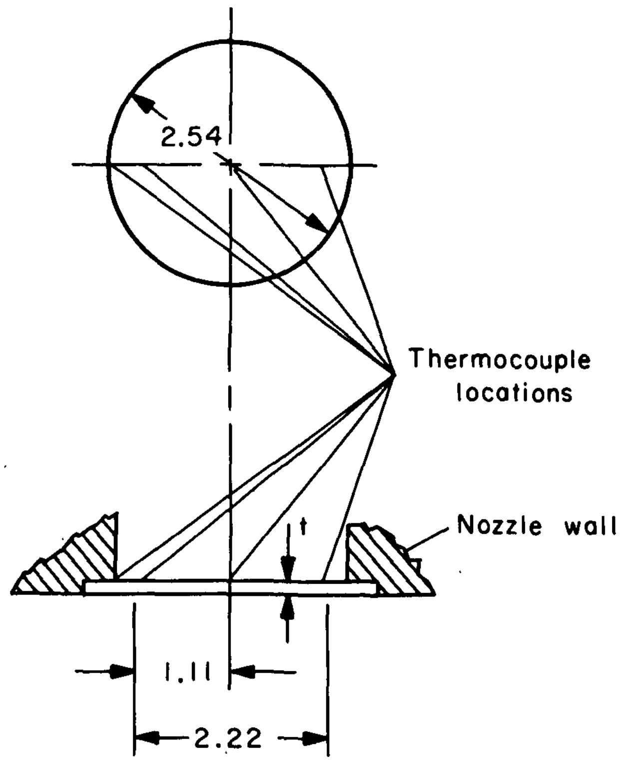

Figure 4.– Schematic of the heat-transfer gage.

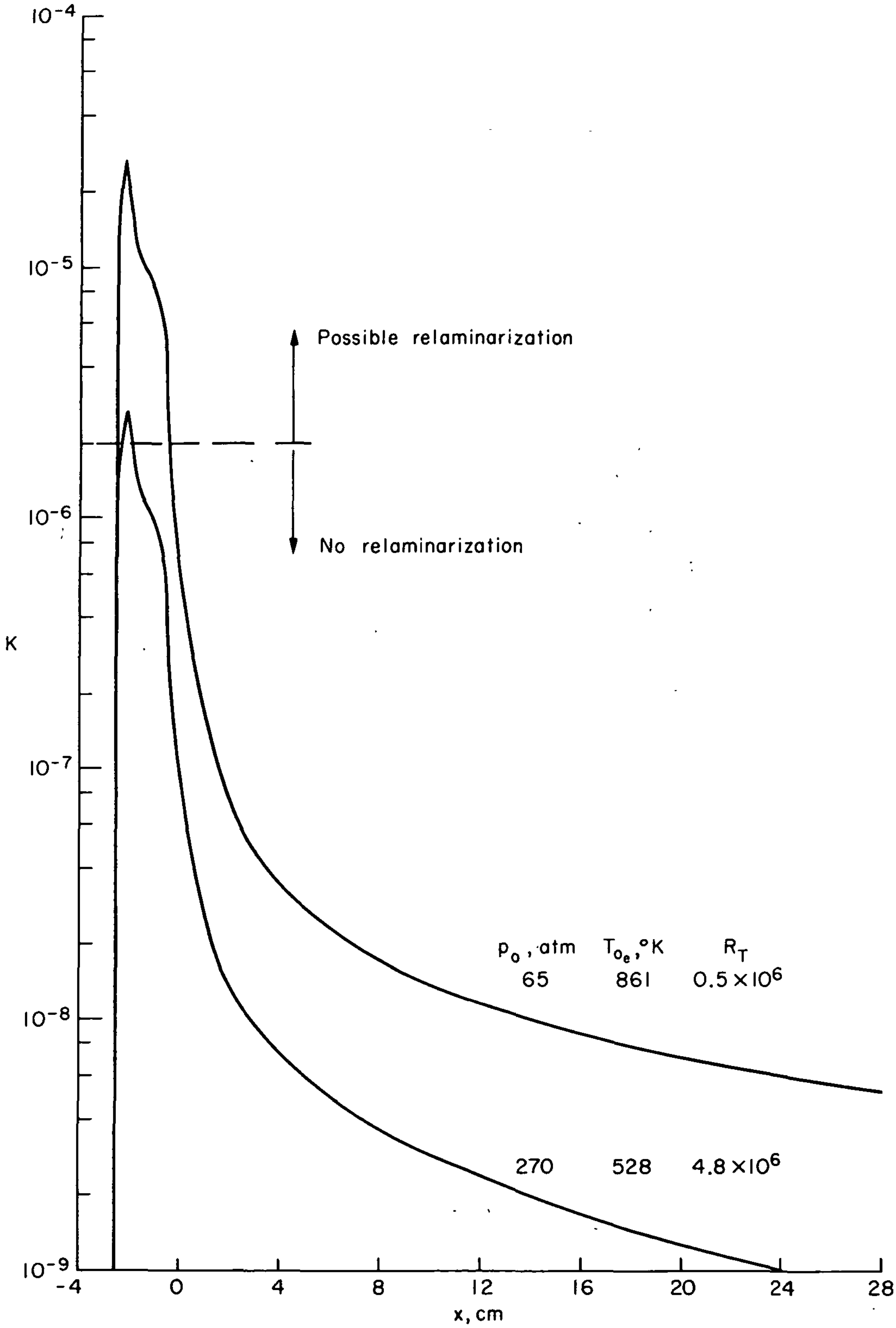

Figure 5.– Variation of the relaminarization parameter, *K*, along the nozzle.

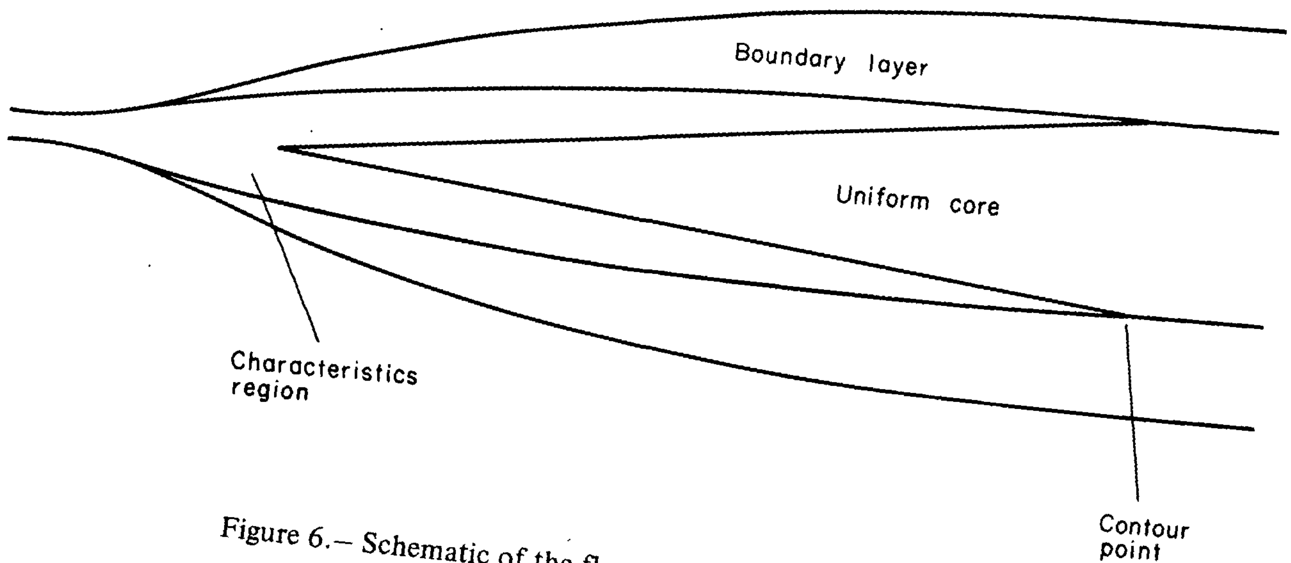

Figure 6.– Schematic of the flow regions in a hypersonic nozzle.

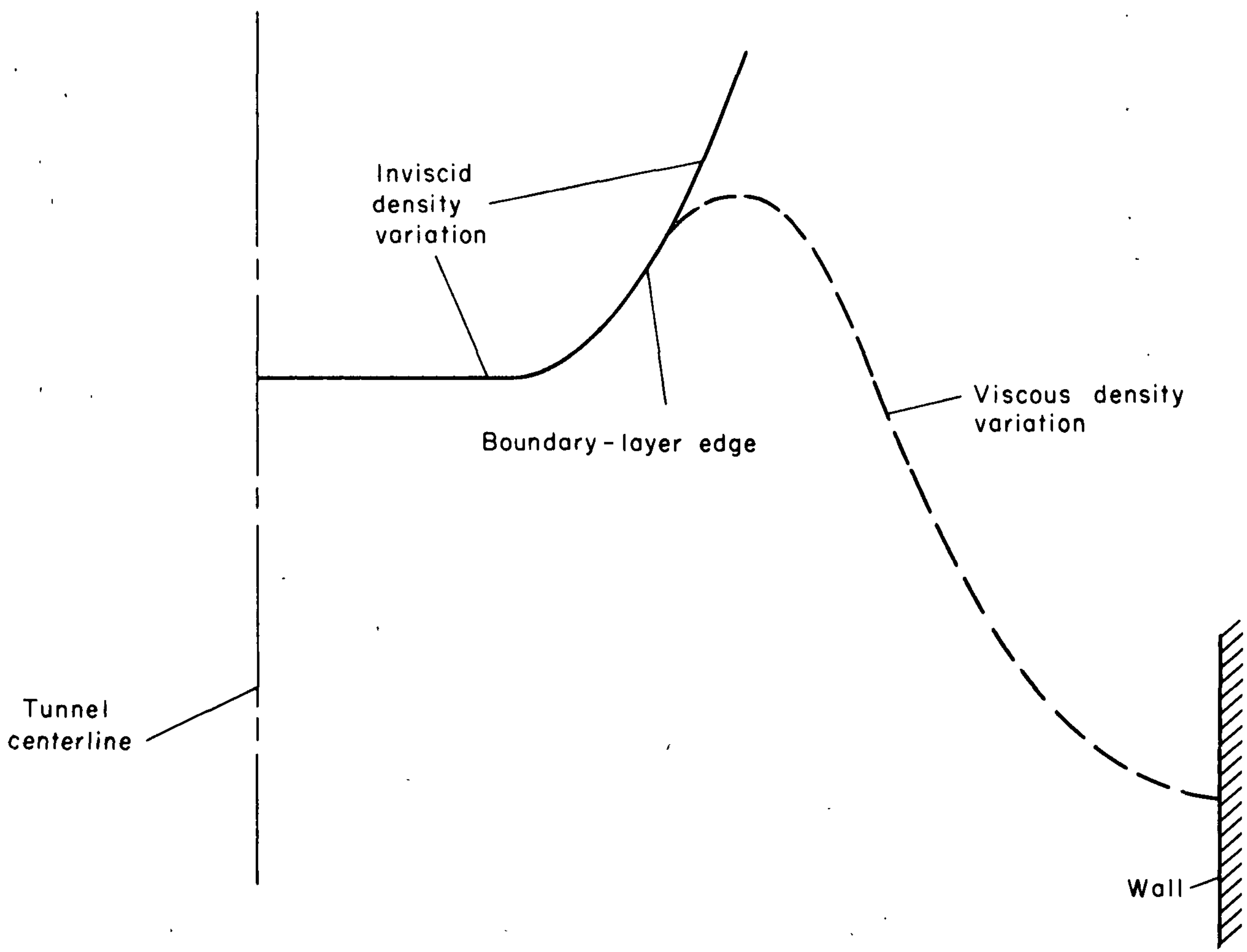

Figure 7.– Schematic of coupling between the inviscid and viscous density variations.

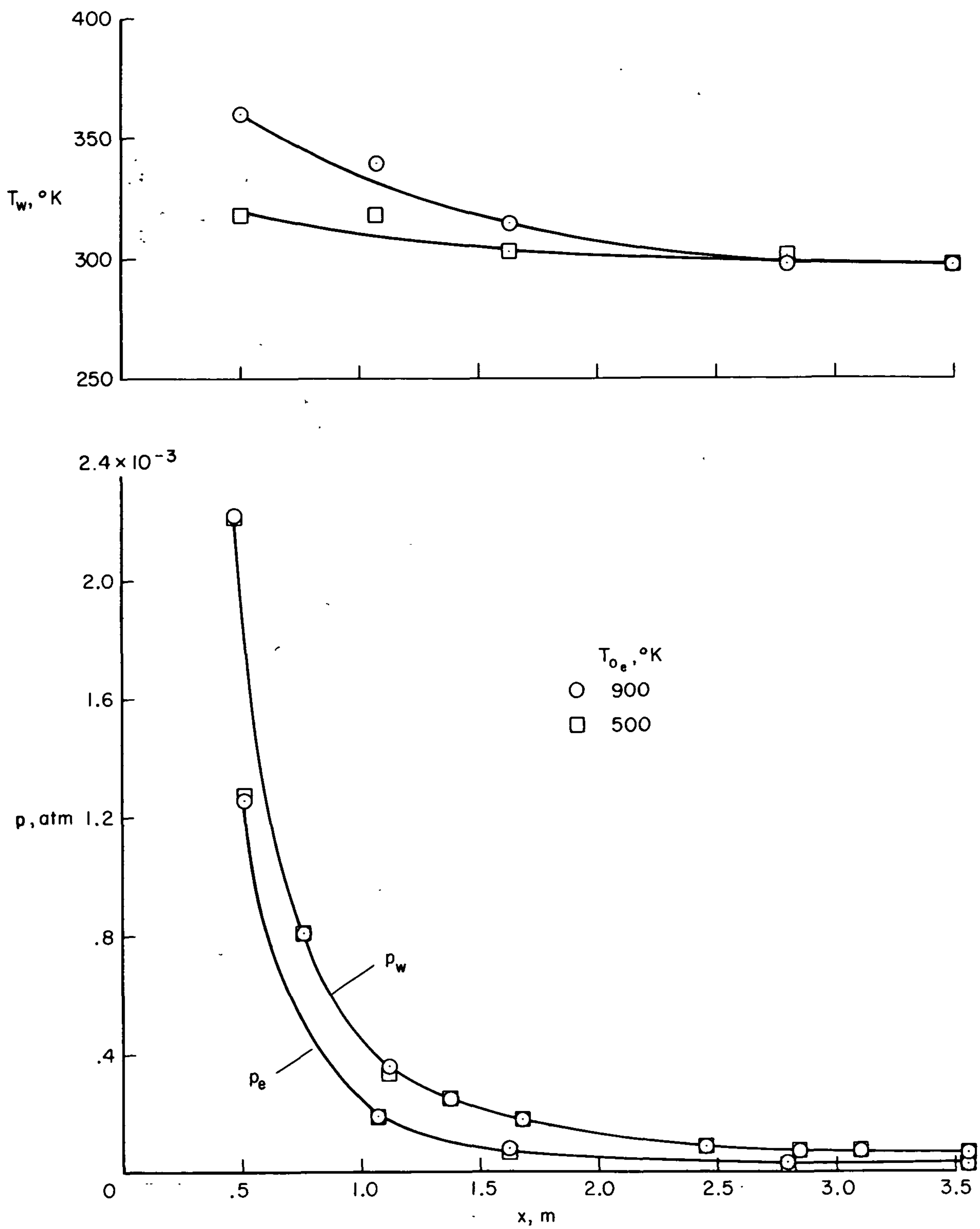

Figure 8.– Pressure and temperature variations along the nozzle.

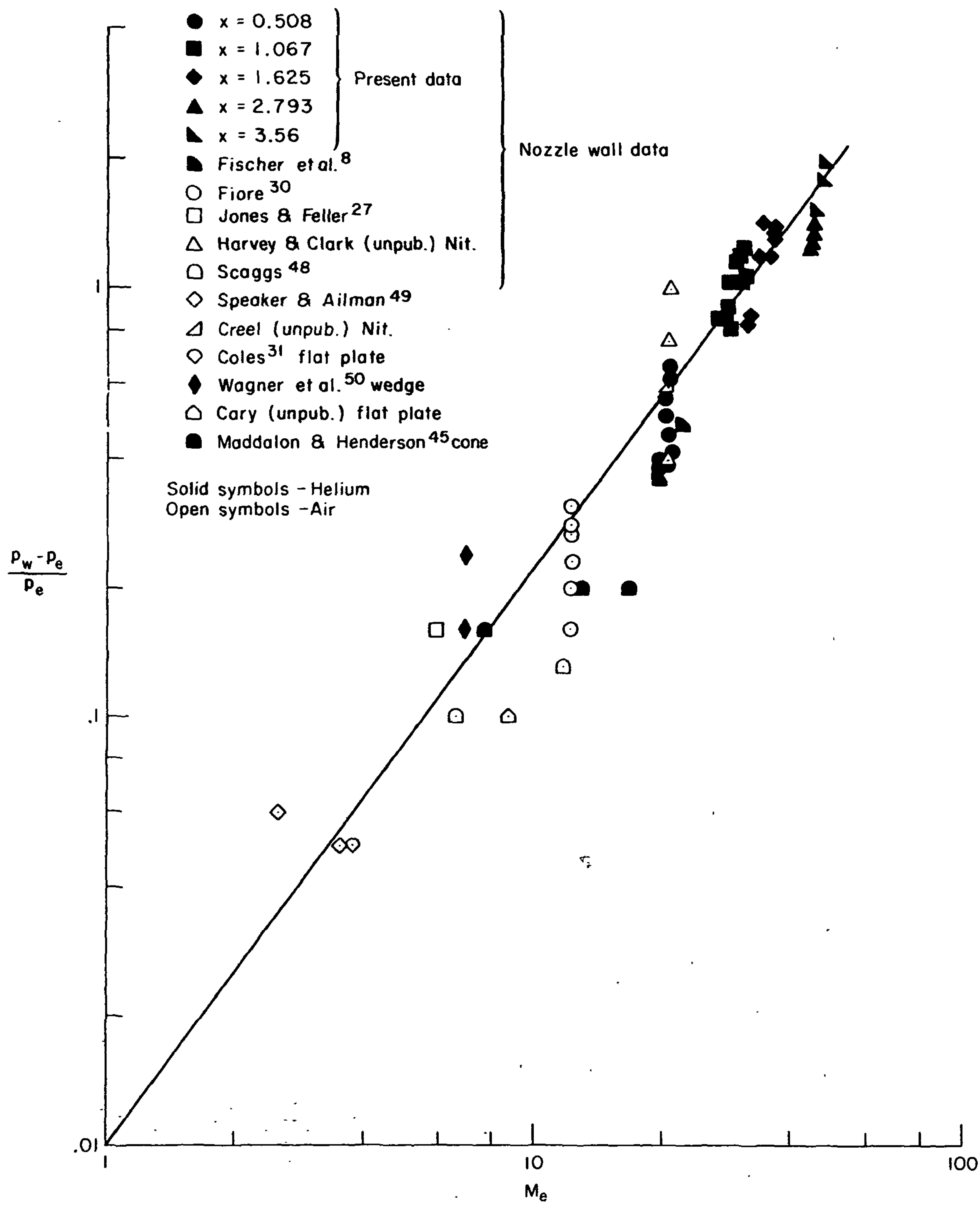

Figure 9.– Variations in wall pressure ratio with edge Mach number.

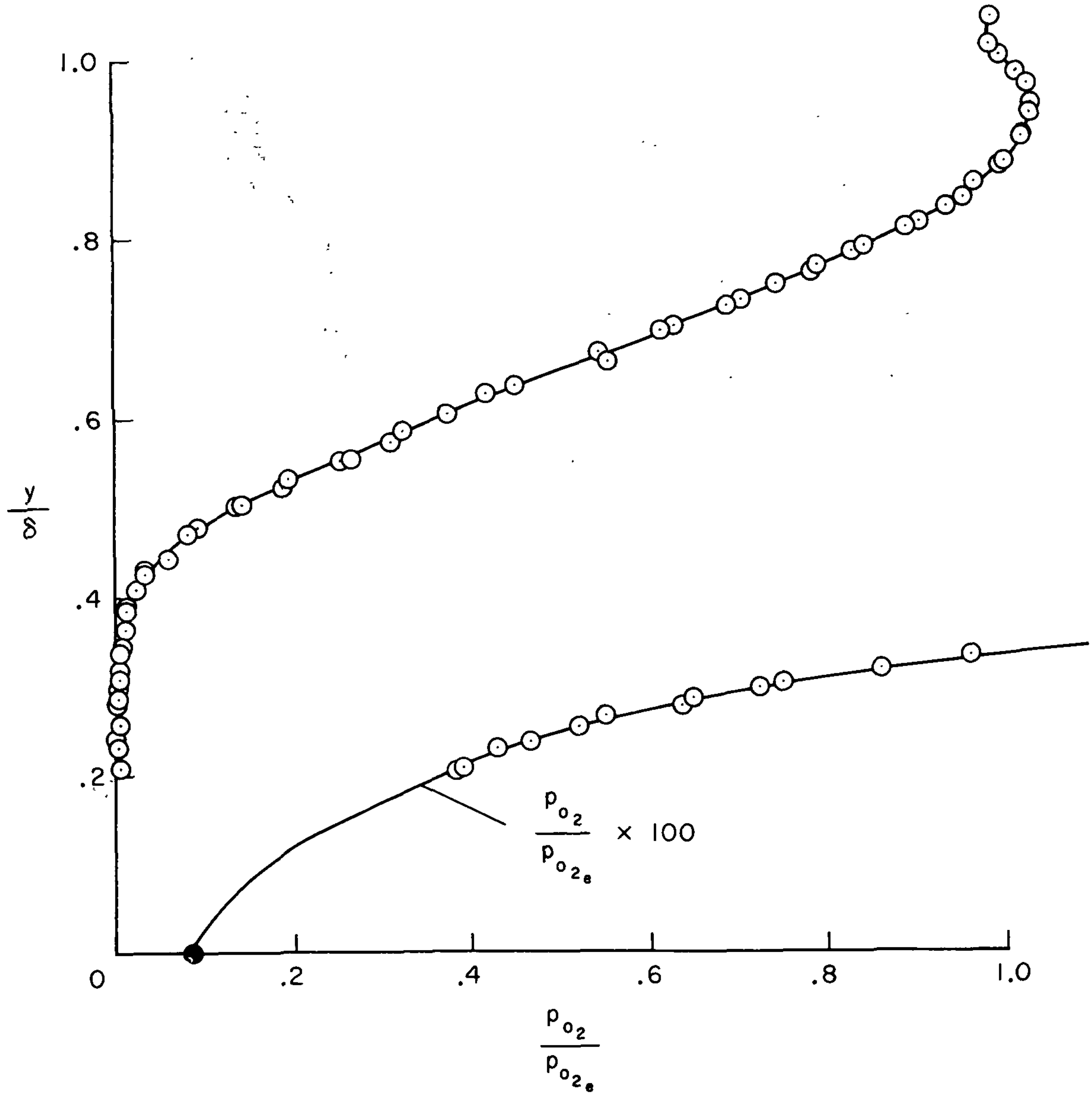

(a) Pressure profile.

Figure 10.– Typical pitot-pressure and stagnation-temperature profiles; x = 2.793 m, p_o = 201 atm, T_o = 958° K.

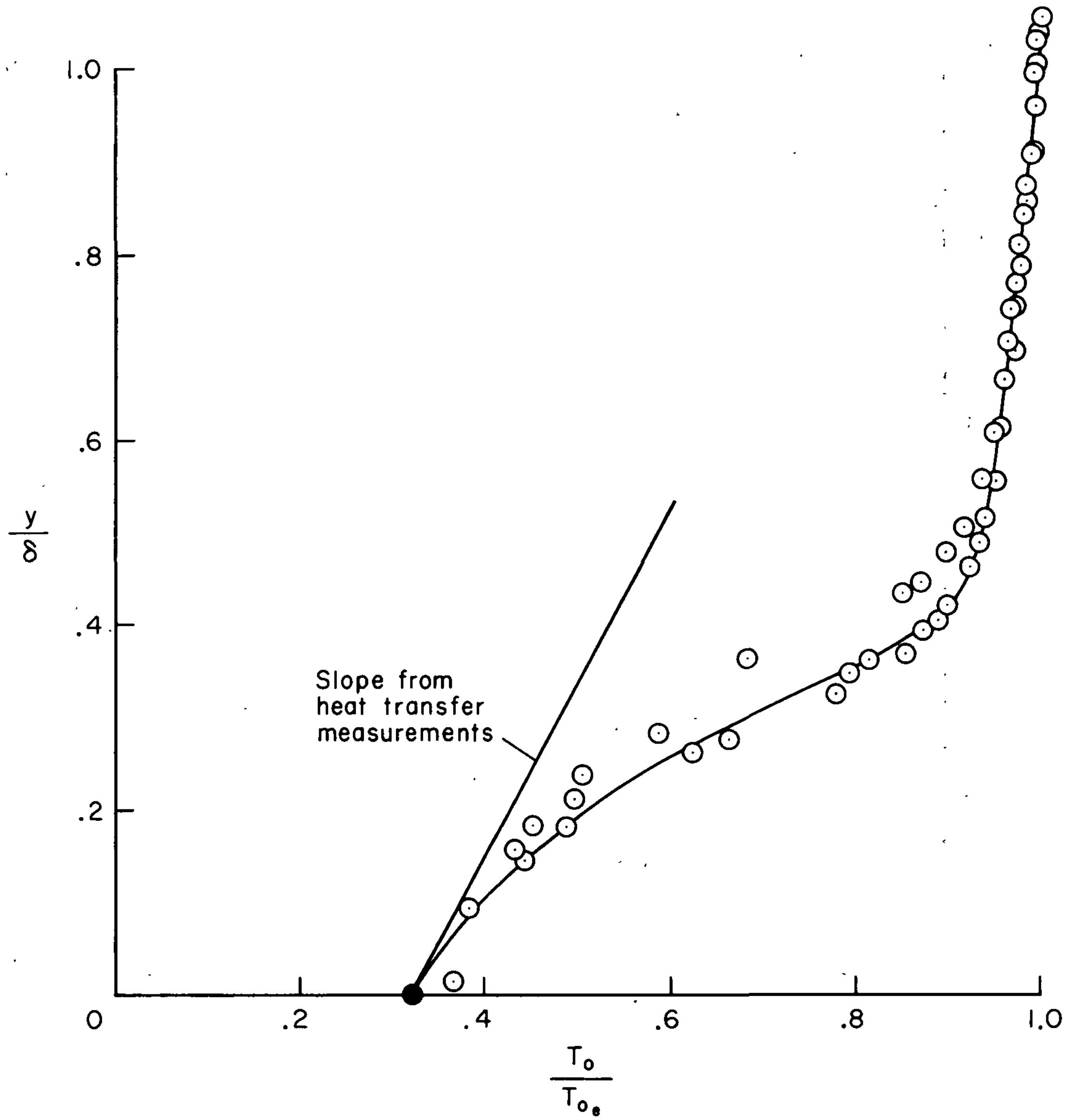

(b) Temperature profile.

Figure 10.– Concluded.

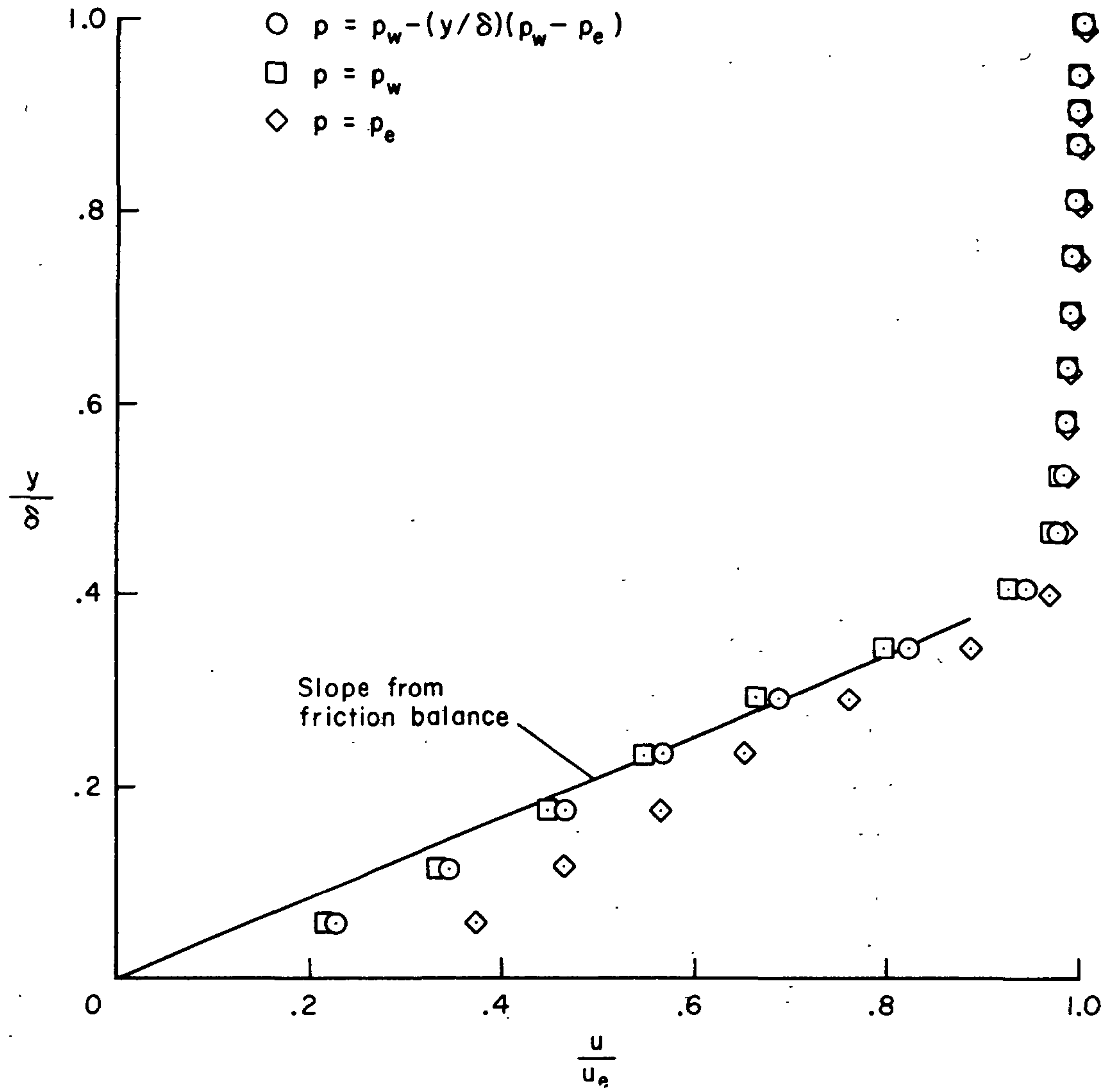

(a) Velocity profile.

Figure 11.– Typical velocity and density profiles; $x = 2.793$ m, $p_O = 201$ atm, $T_O = 958°$ K

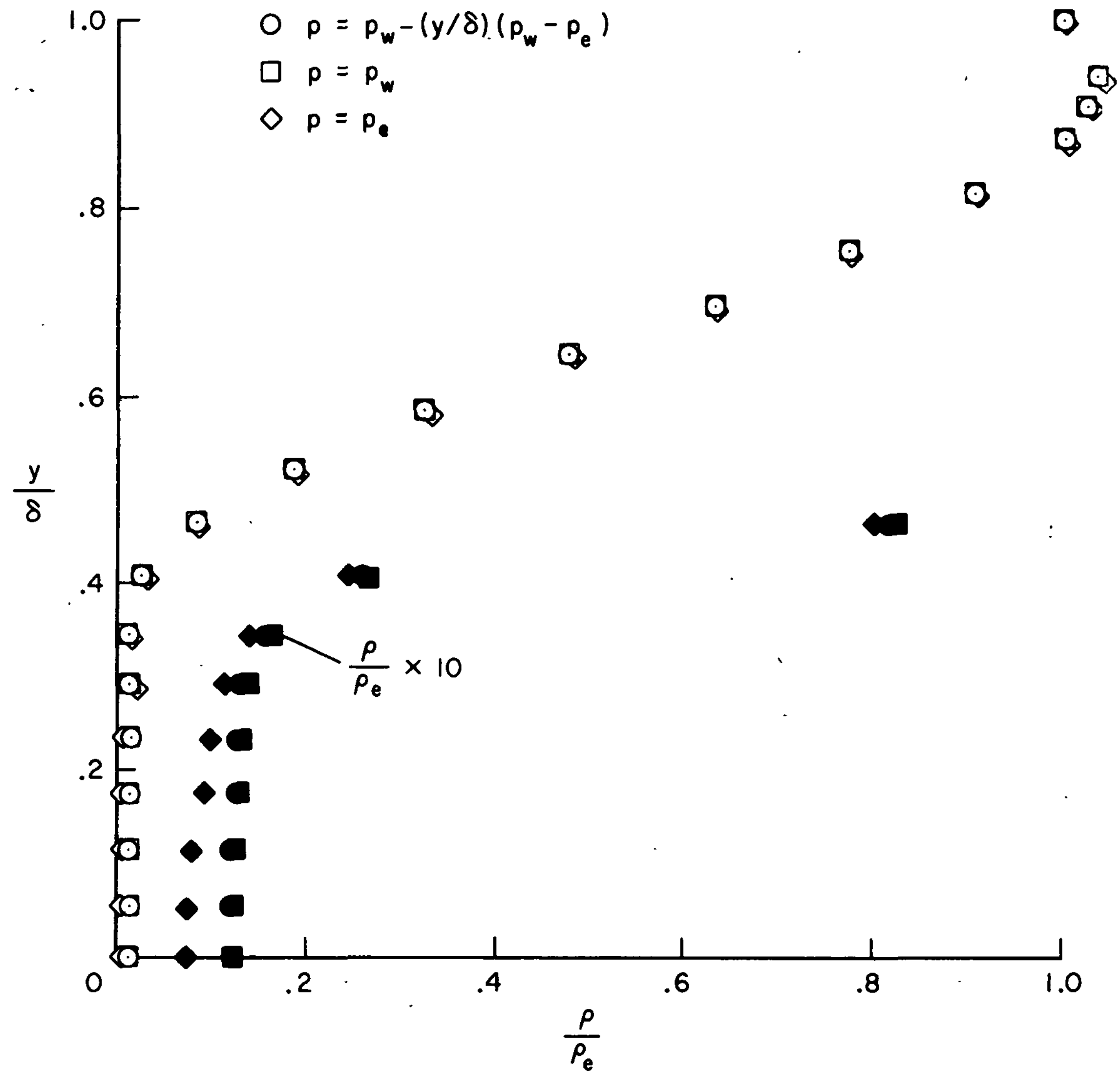

(b) Density profiles.

Figure 11.– Concluded.

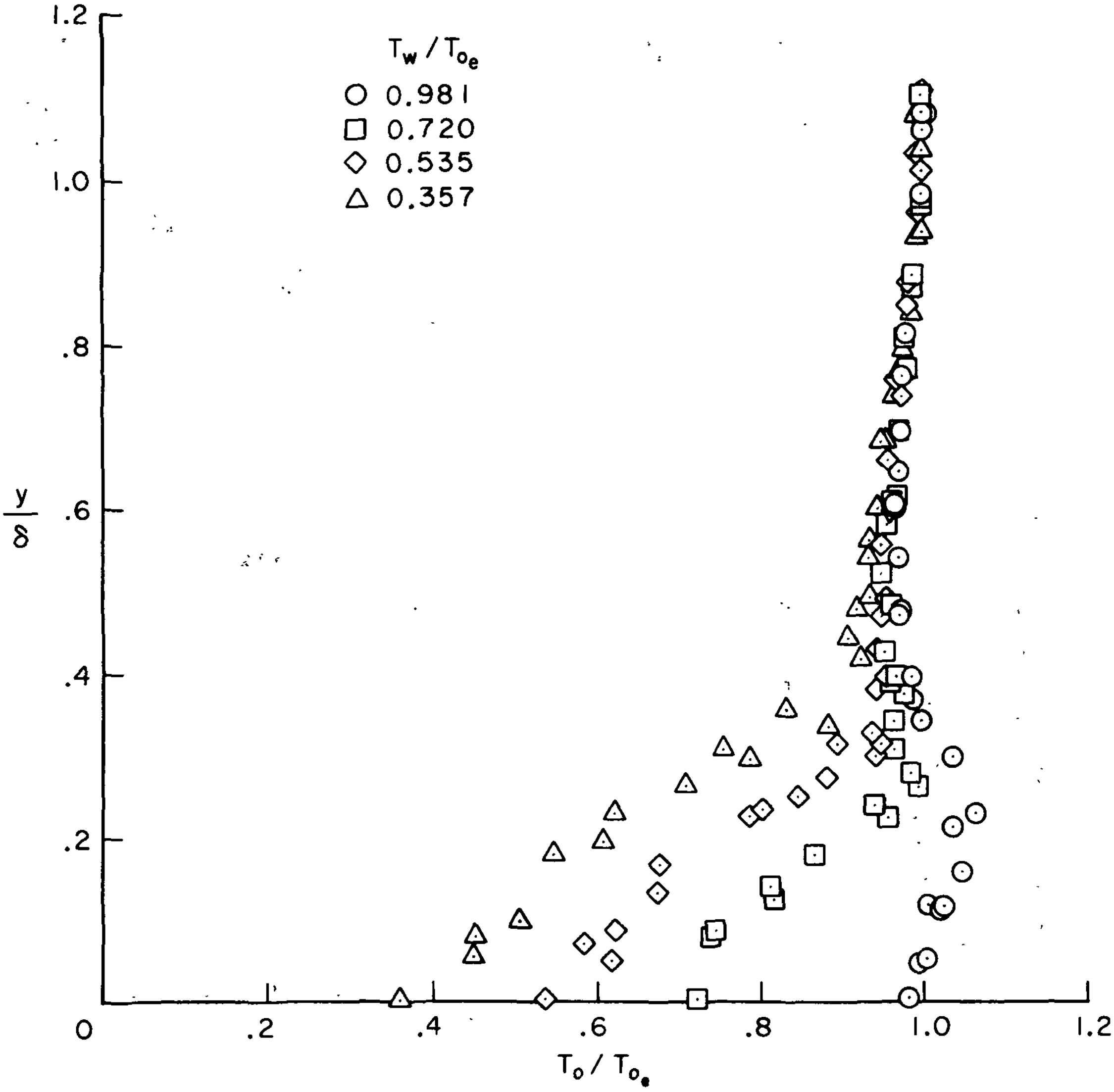

(a) Total temperature ratio.

Figure 12.— Variations in stagnation-temperature and pitot-pressure profiles with wall temperature; p_o = 108 atm, M_e = 27, x = 1.067 m.

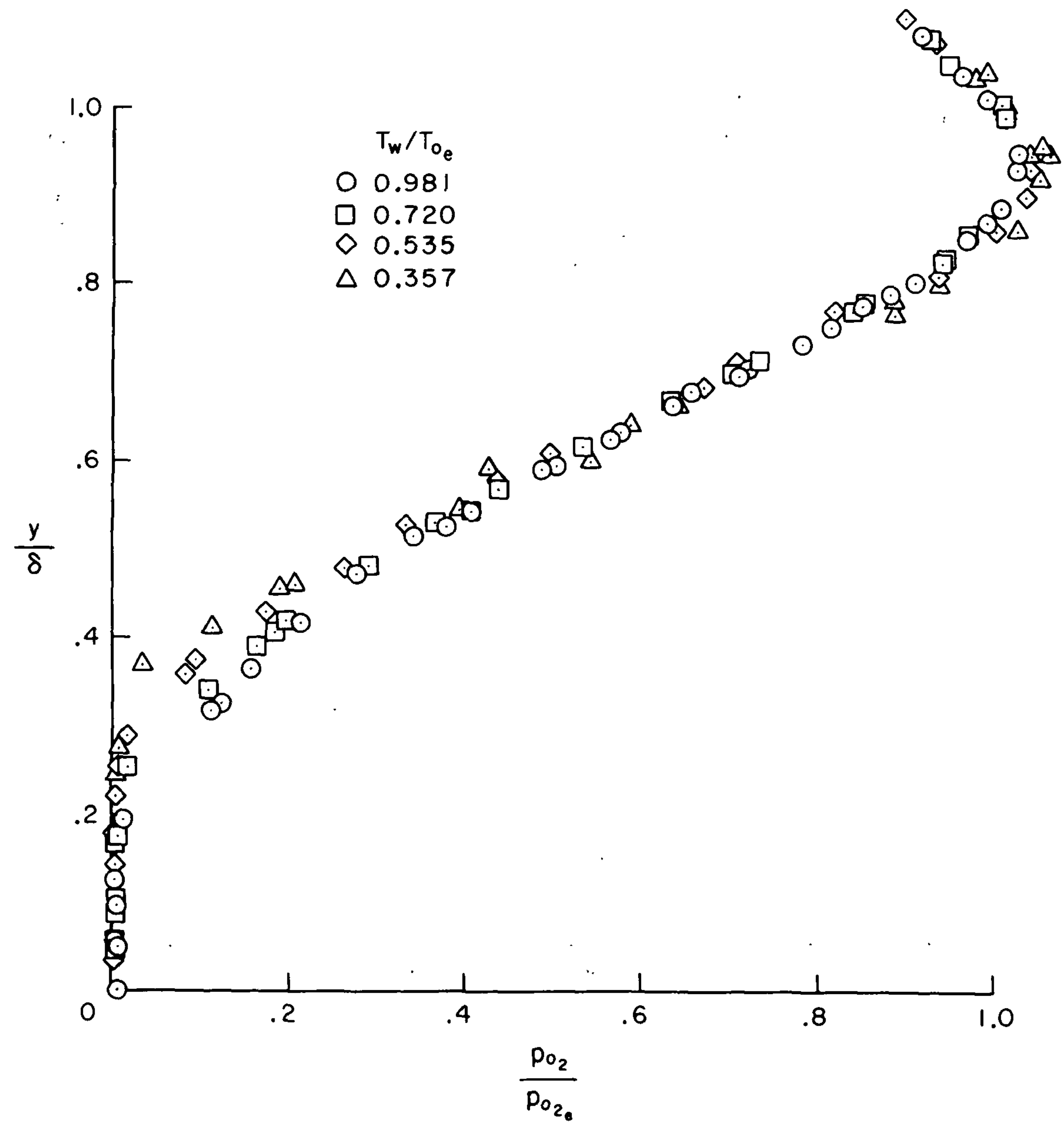

(b) Pitot-pressure ratio.

Figure 12.– Concluded.

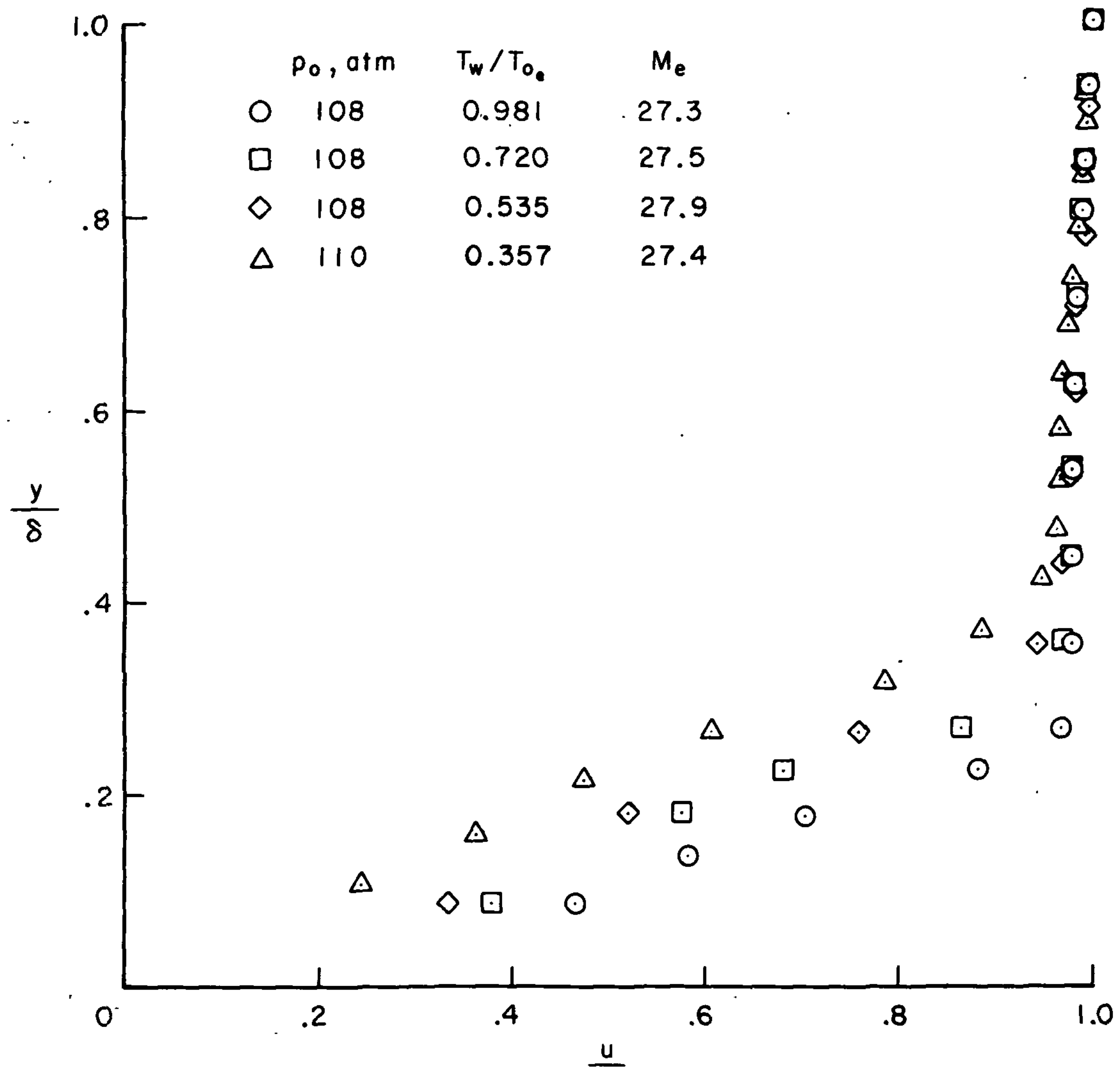

(a) Velocity.

Figure 13.– Variations in velocity, density, and Mach number profiles with wall temperat
$x = 1.067$ m.

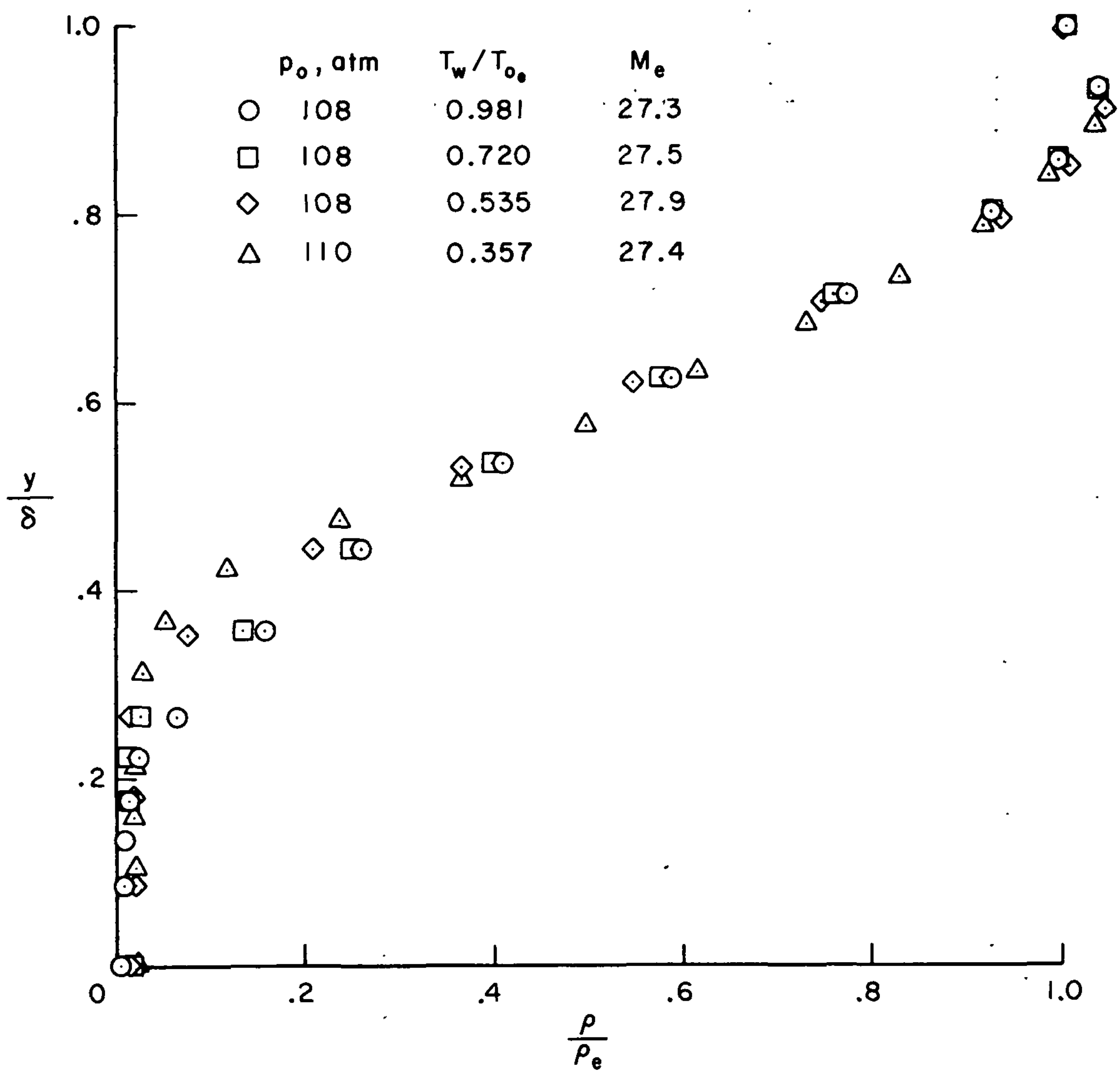

(b) Density.

Figure 13.– Continued.

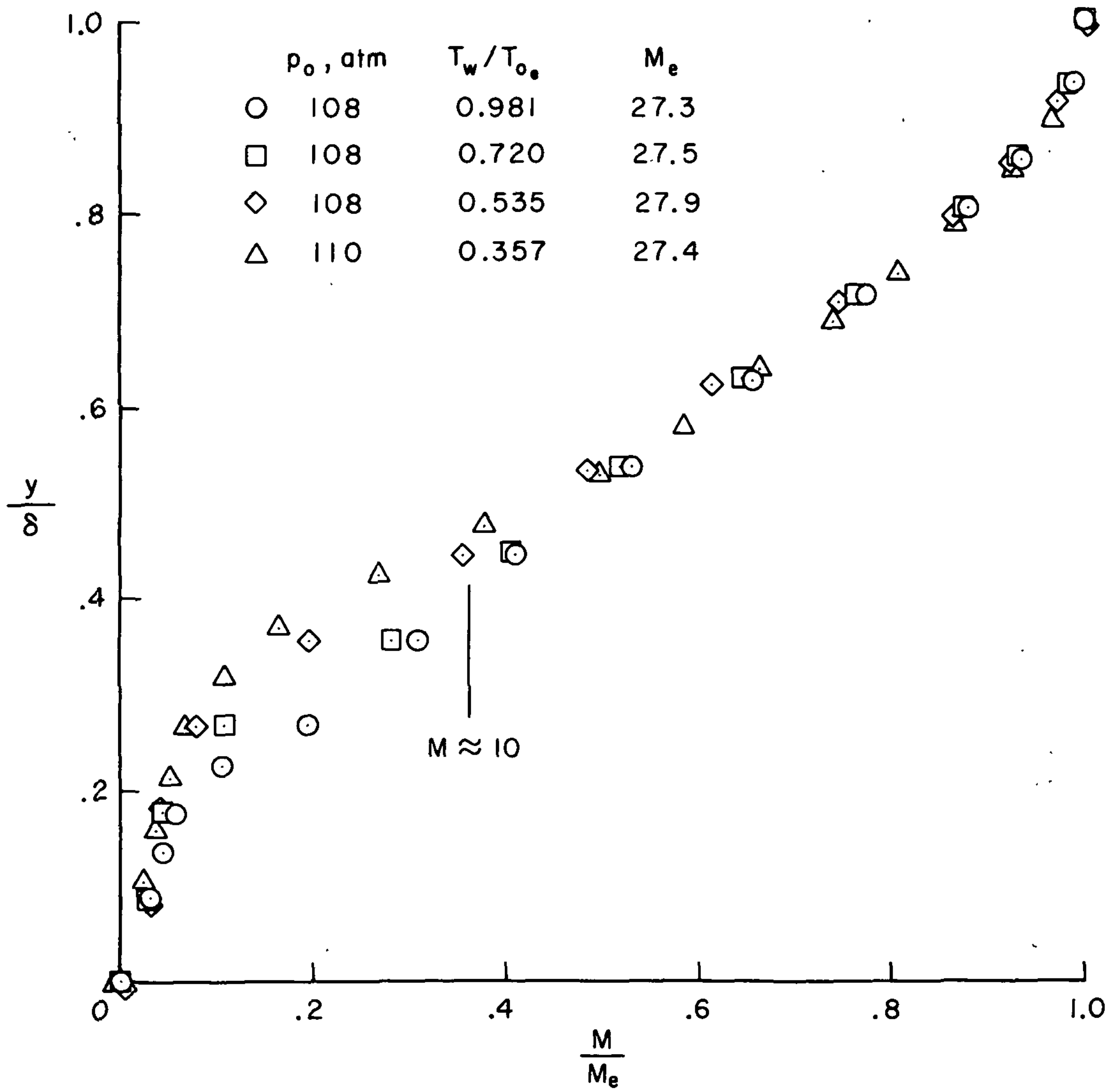

(c) Mach number.

Figure 13.– Concluded.

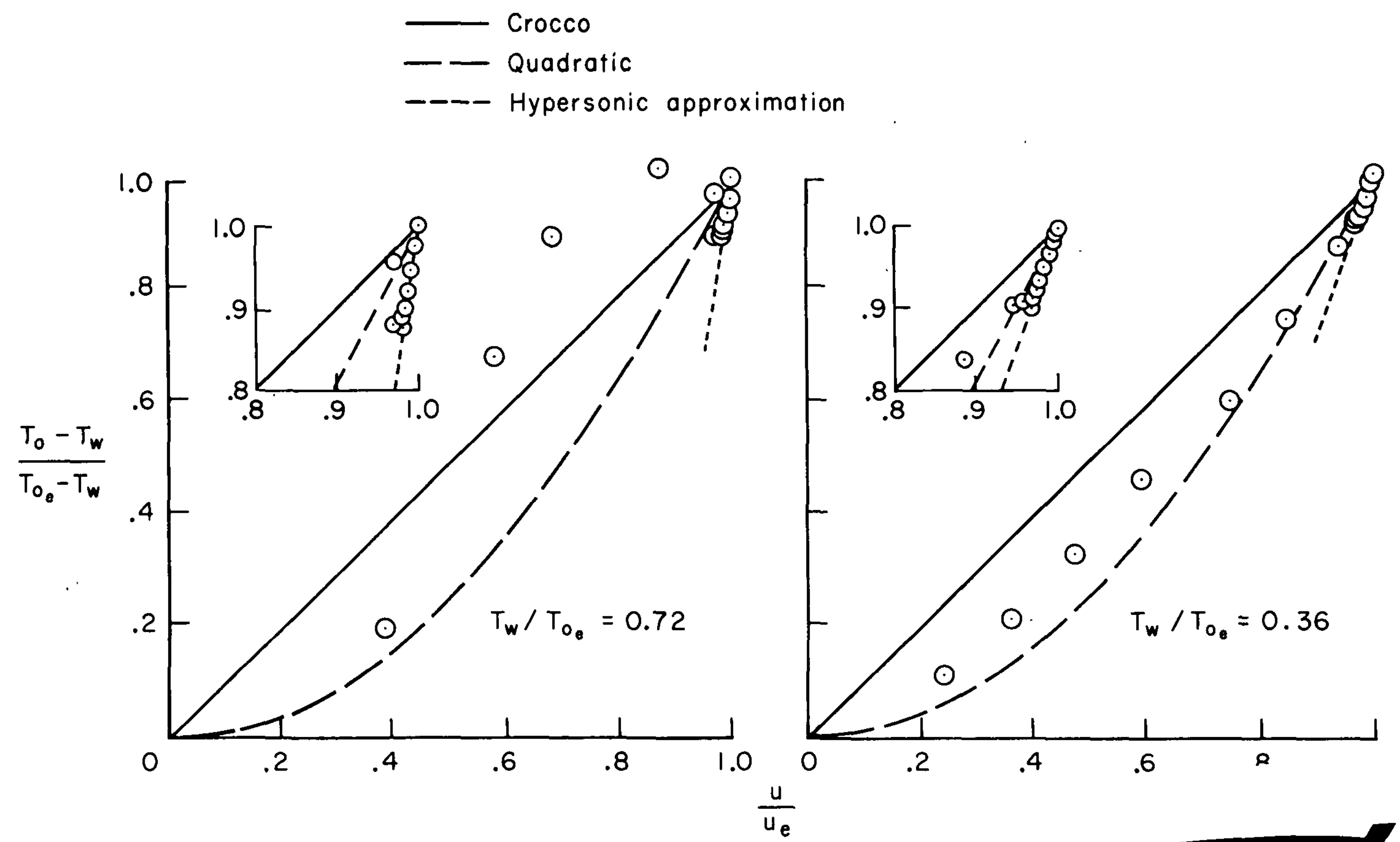

Figure 14.– Variations in velocity-temperature profiles with wall temperature ratio; $M_e = 27, x = 1.067$ m.

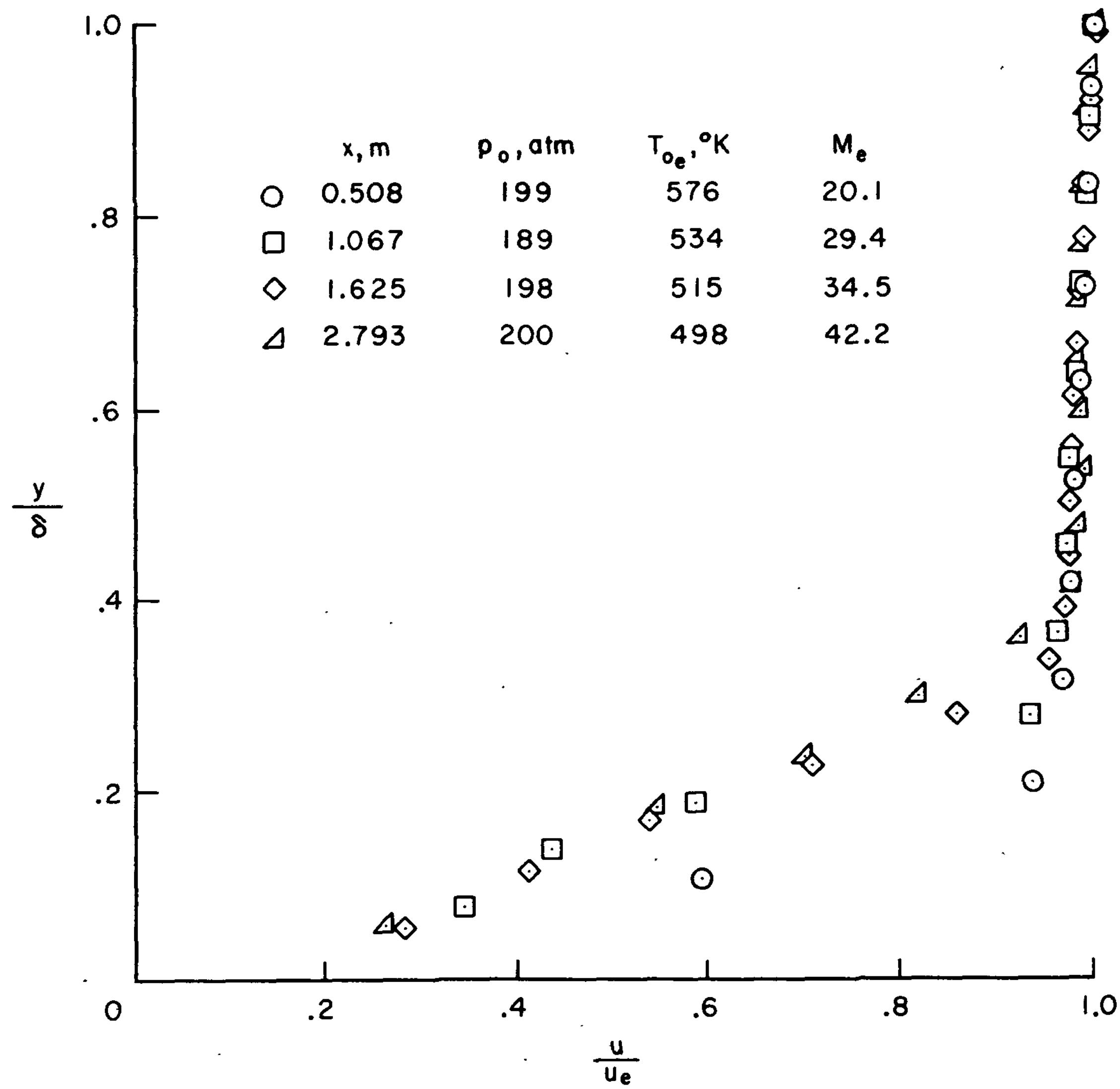

(a) Velocity.

Figure 15.– Variations in velocity, density, and Mach number profiles with nozzle station.

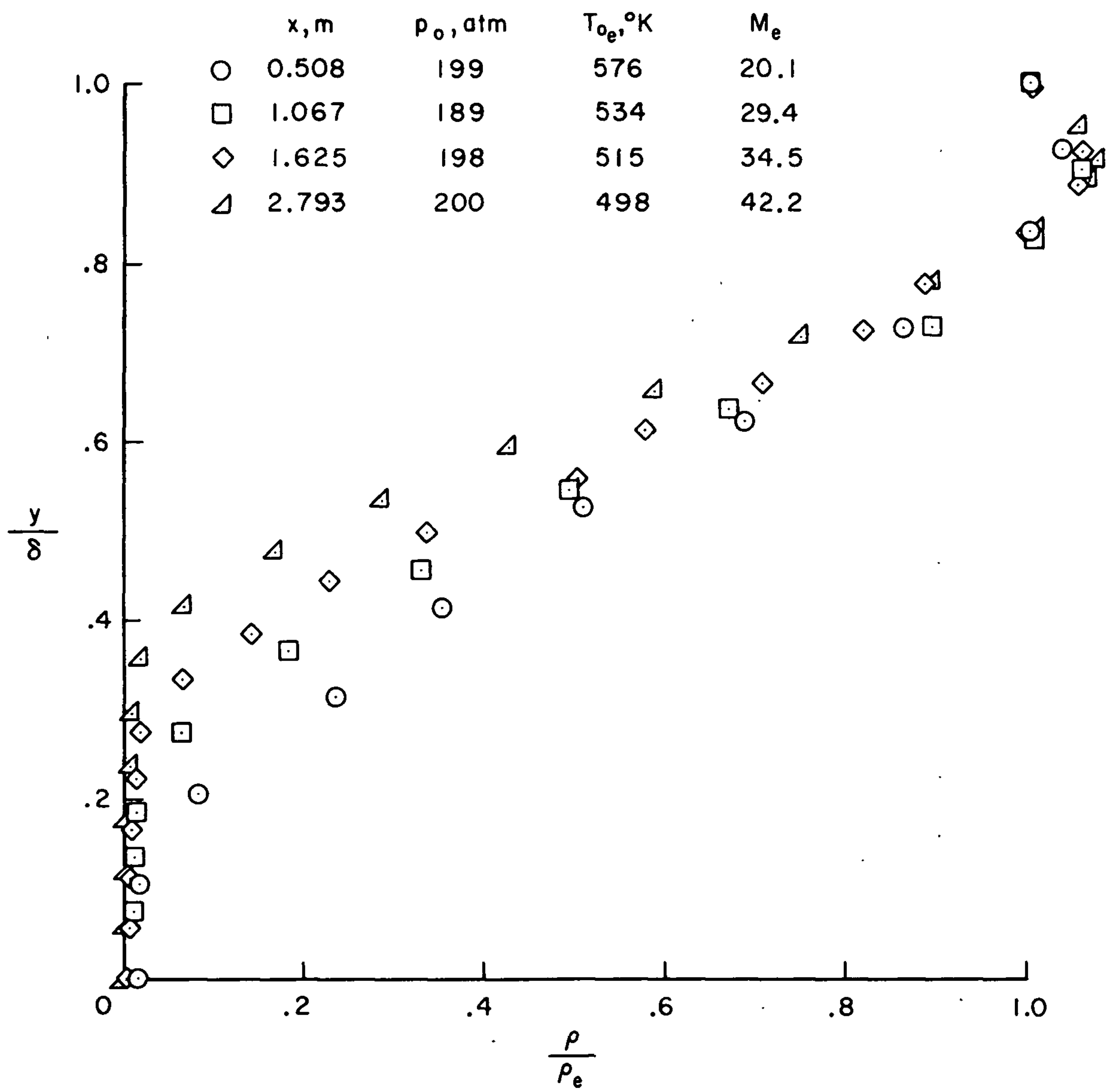

(b) Density.

Figure 15.– Continued.

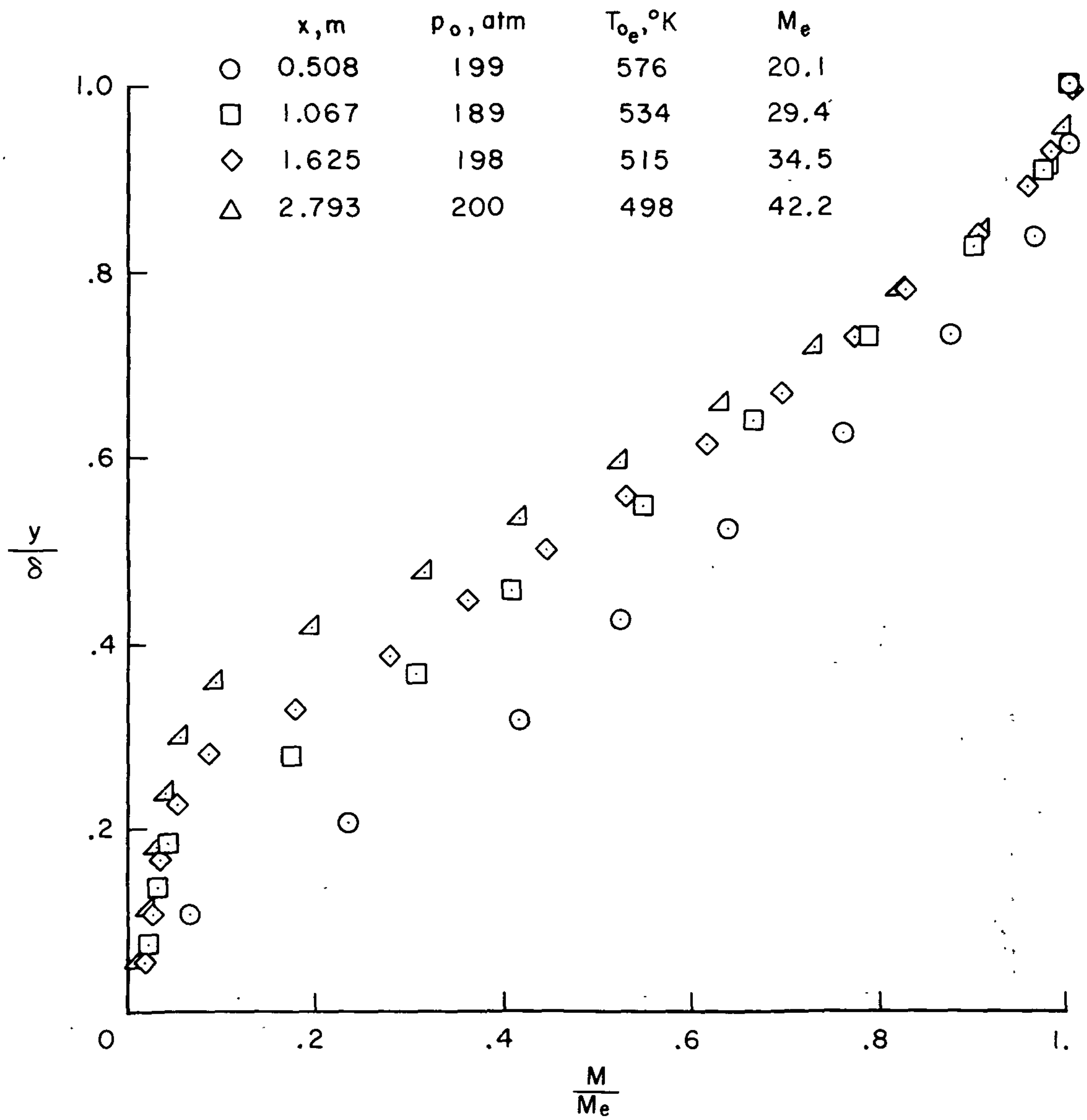

(c) Mach number.

Figure 15.– Concluded.

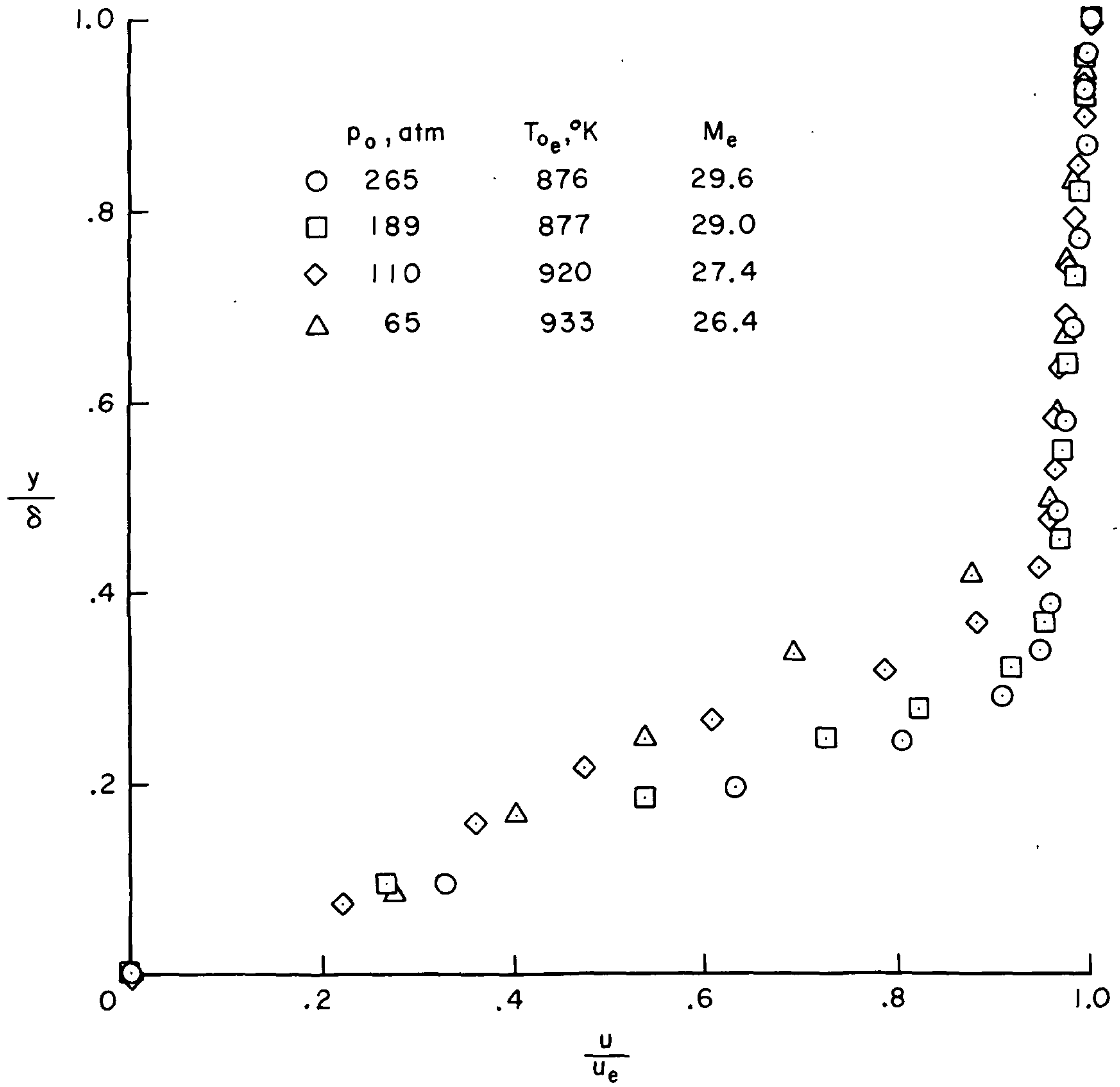

(a) Velocity.

Figure 16.– Variations in velocity, density, and Mach number profiles with pressure; x = 1.067 m.

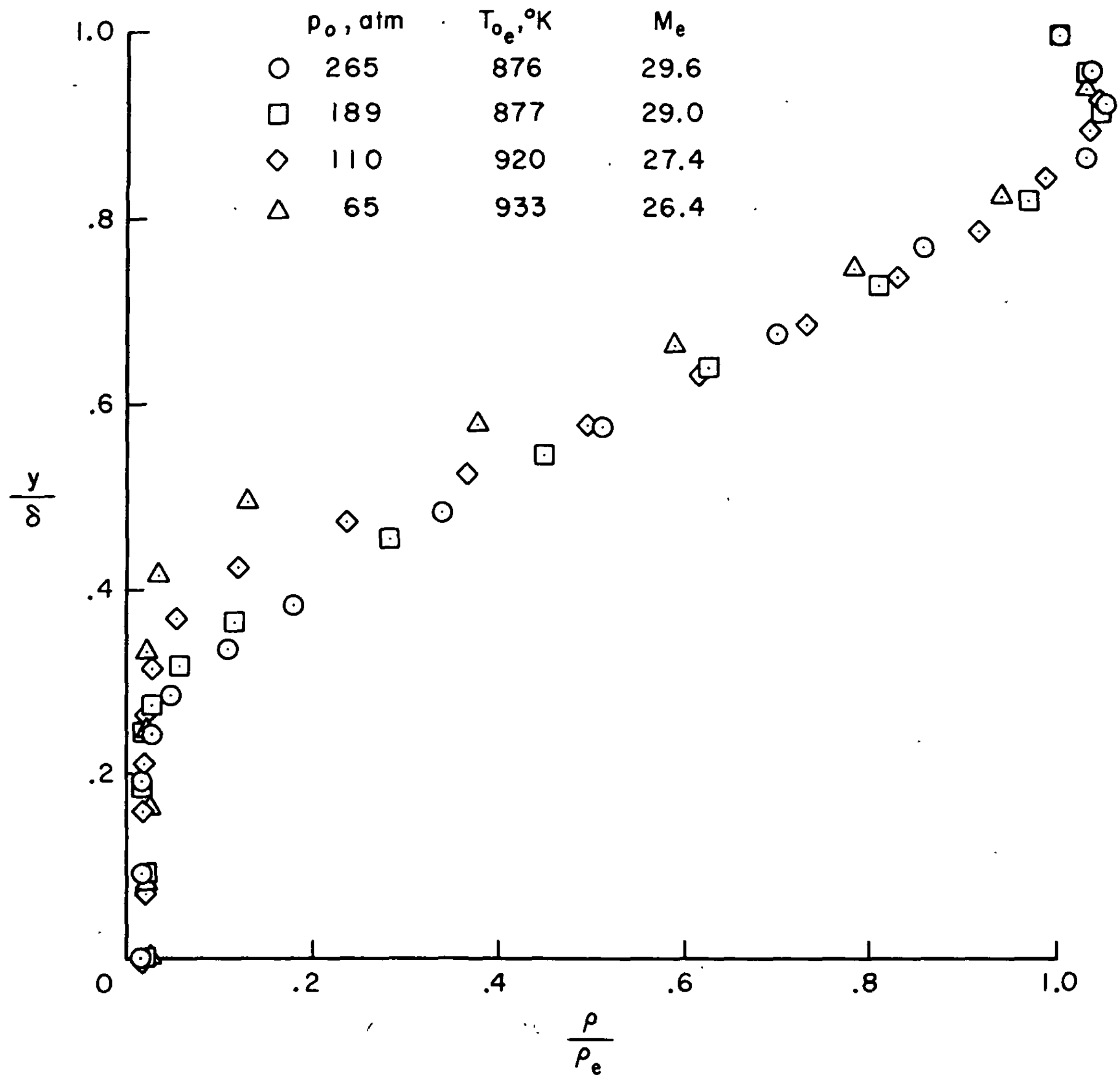

(b) Density.

Figure 16.– Continued.

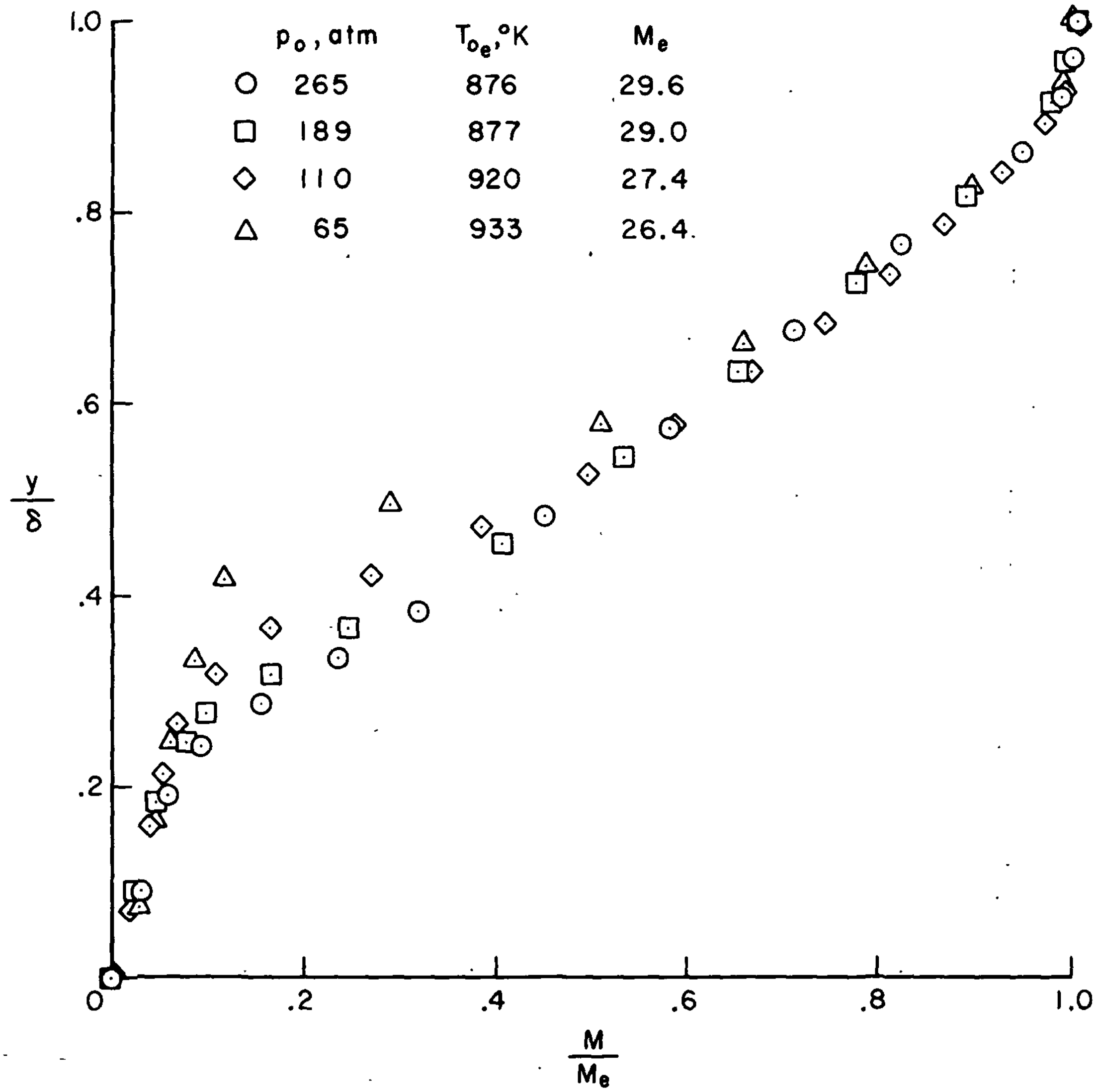

(c) Mach number.

Figure 16.– Concluded.

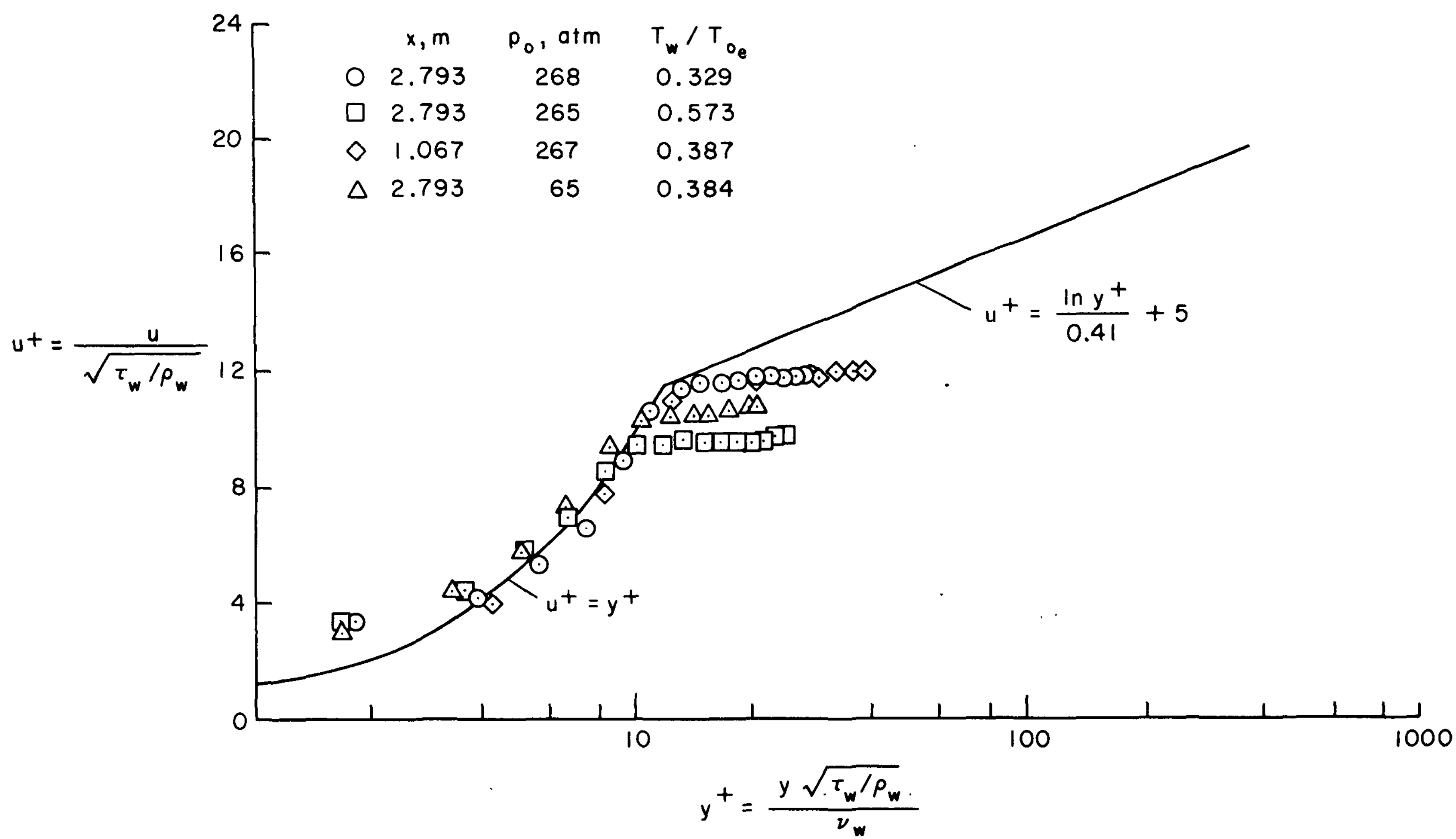

Figure 17.– Law of the wall correlation of present velocity measurements using wall values.

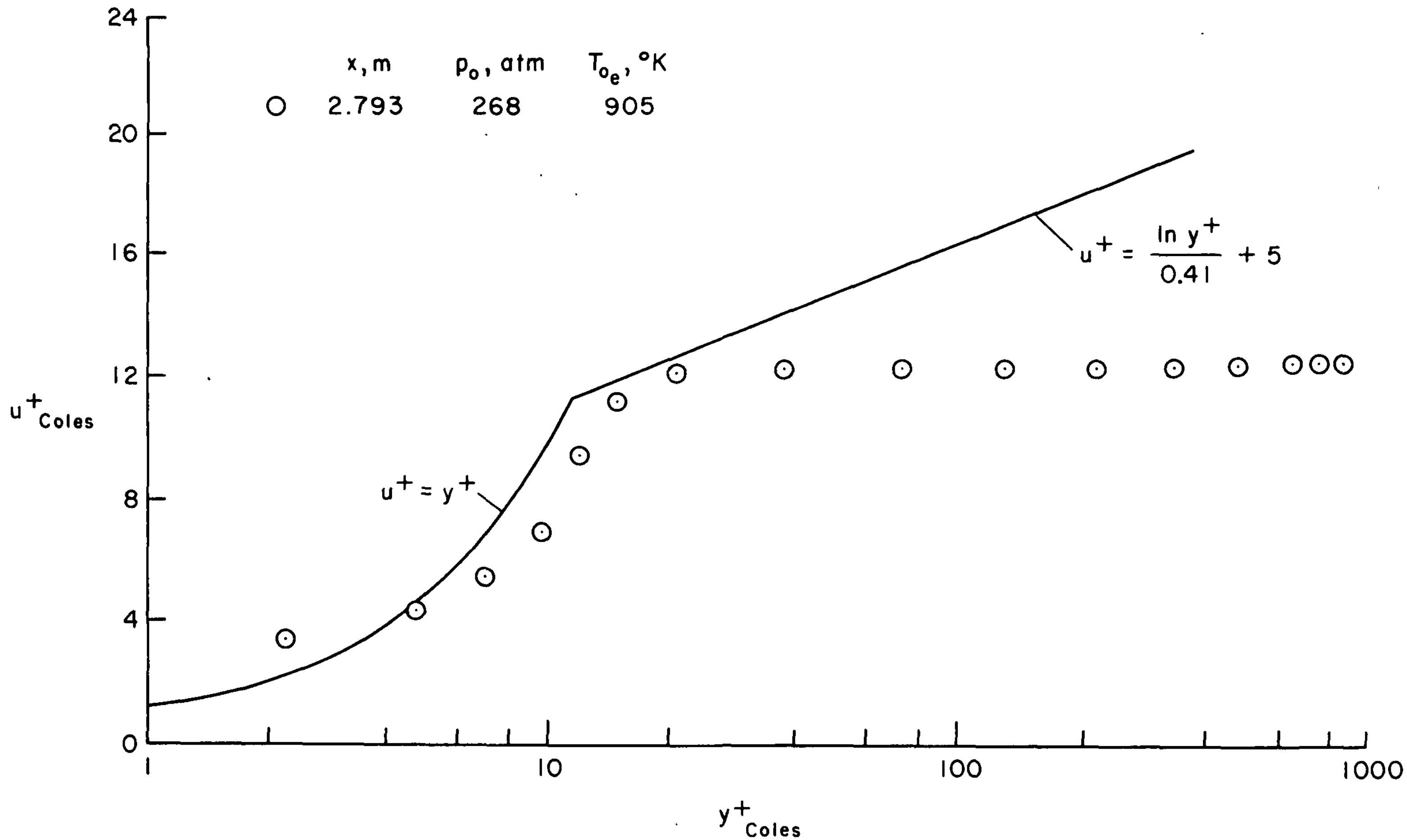

Figure 18.– Law of the wall correlation of present velocity measurements using Coles' transformation.

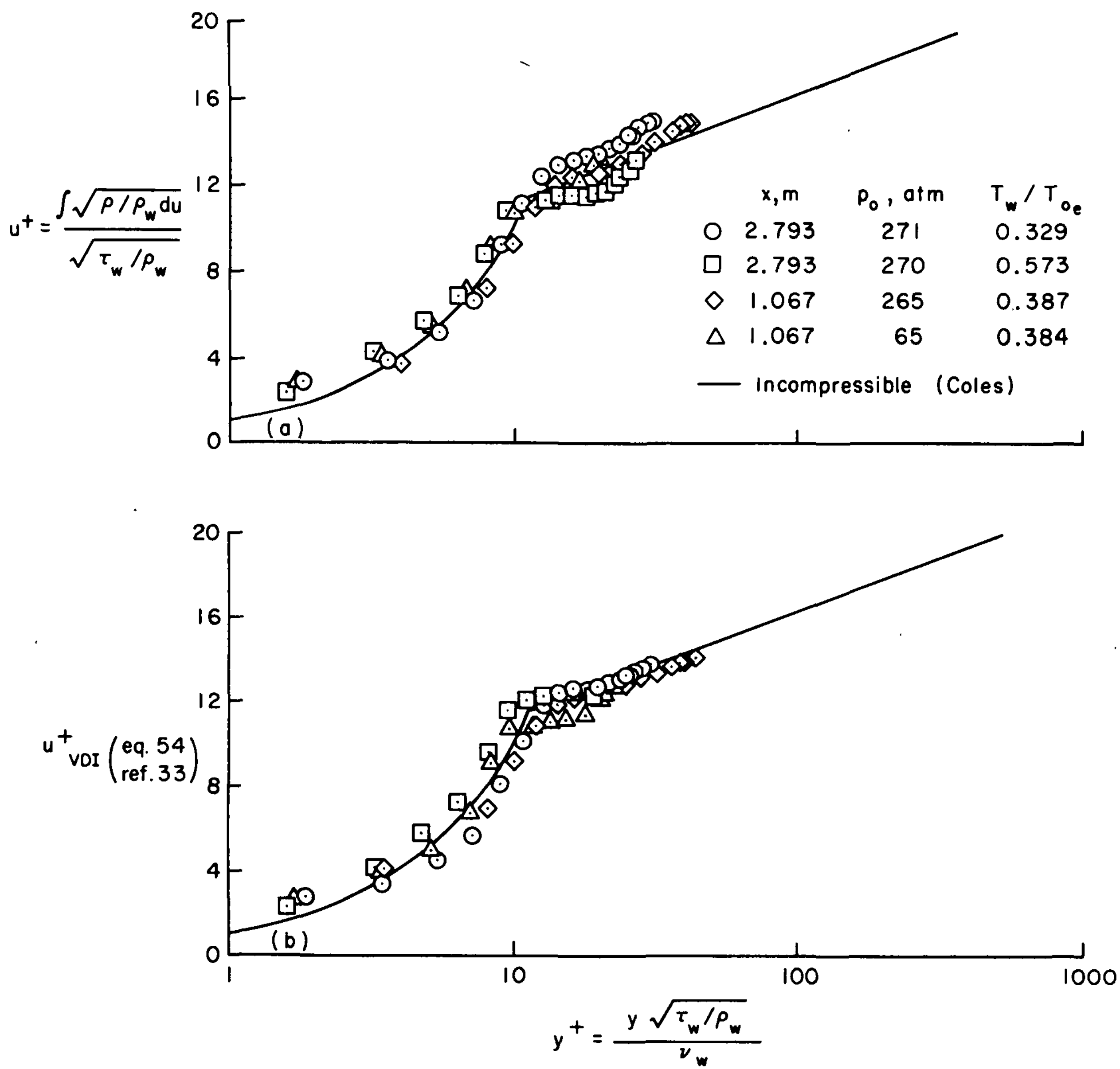

Figure 19.– Law of the wall correlation of present velocity measurements using Van Driest's transformation.

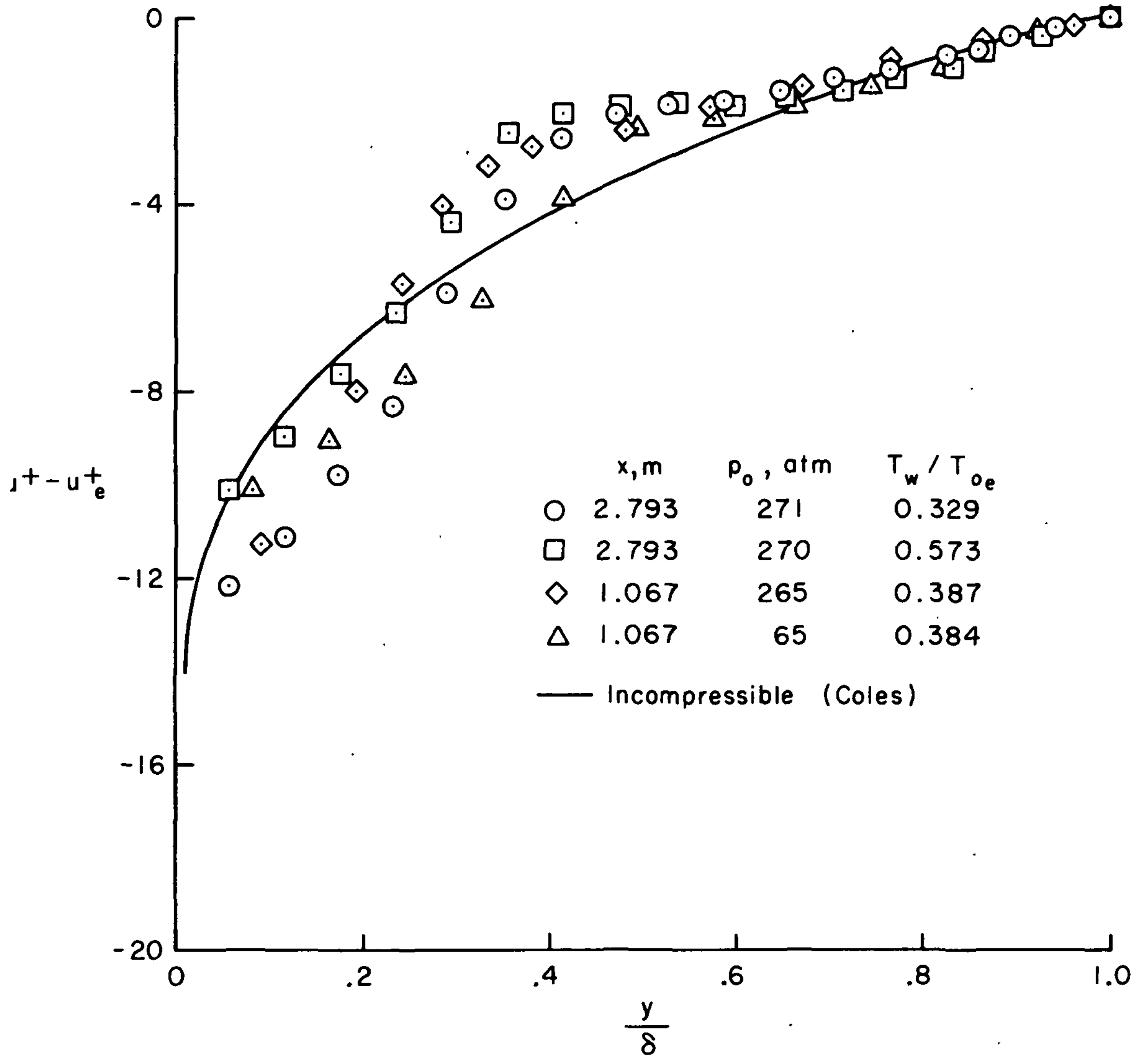

(a) $u^+ = \dfrac{\rho/\rho_w \, du}{\sqrt{\tau_w/\rho_w}}$

Figure 20.– Velocity-detect law correlations of the present velocity measurements using Van Driest's transformation.

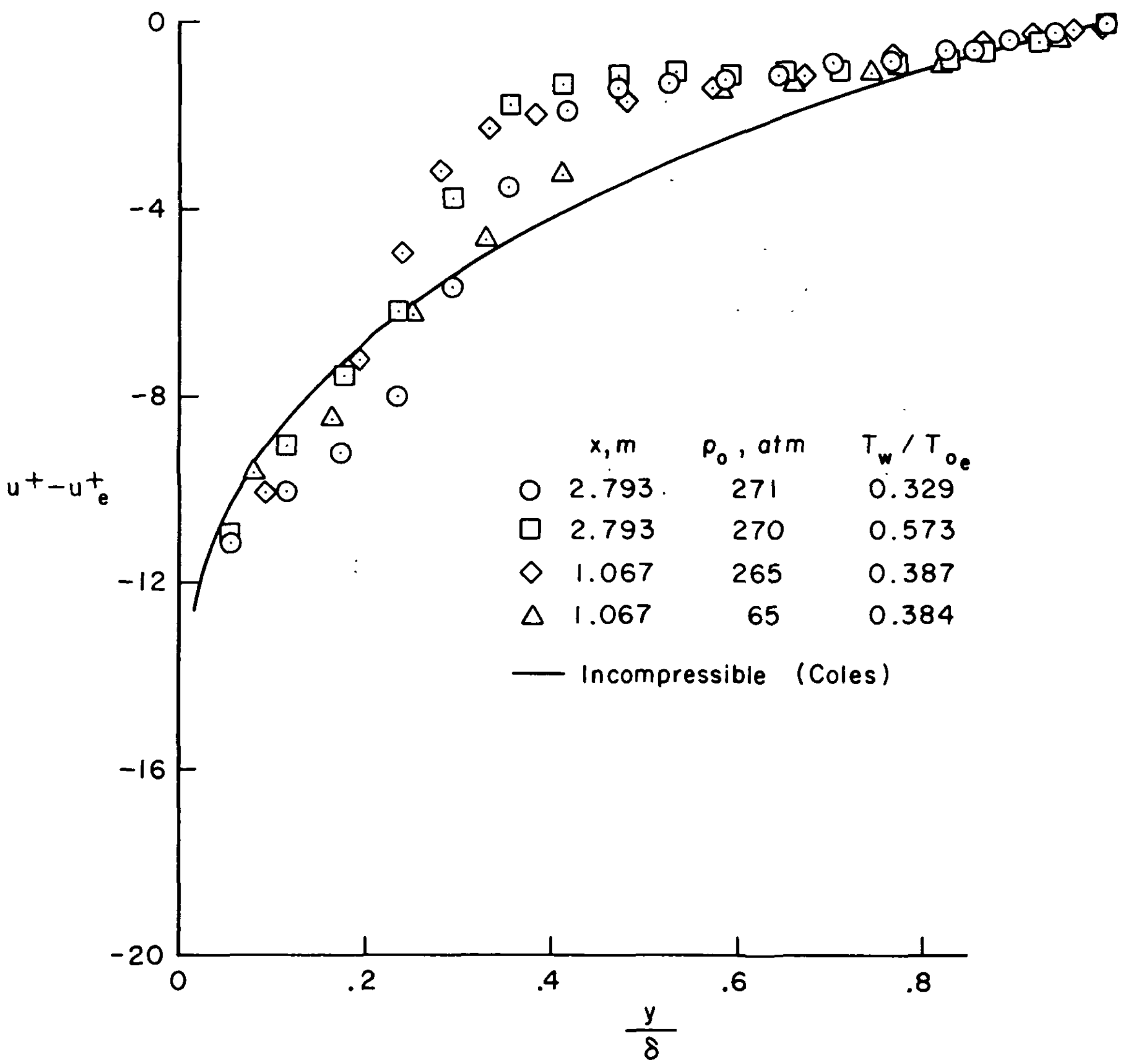

(b) u^+ from equation 54 (ref. 33).

Figure 20.– Concluded.

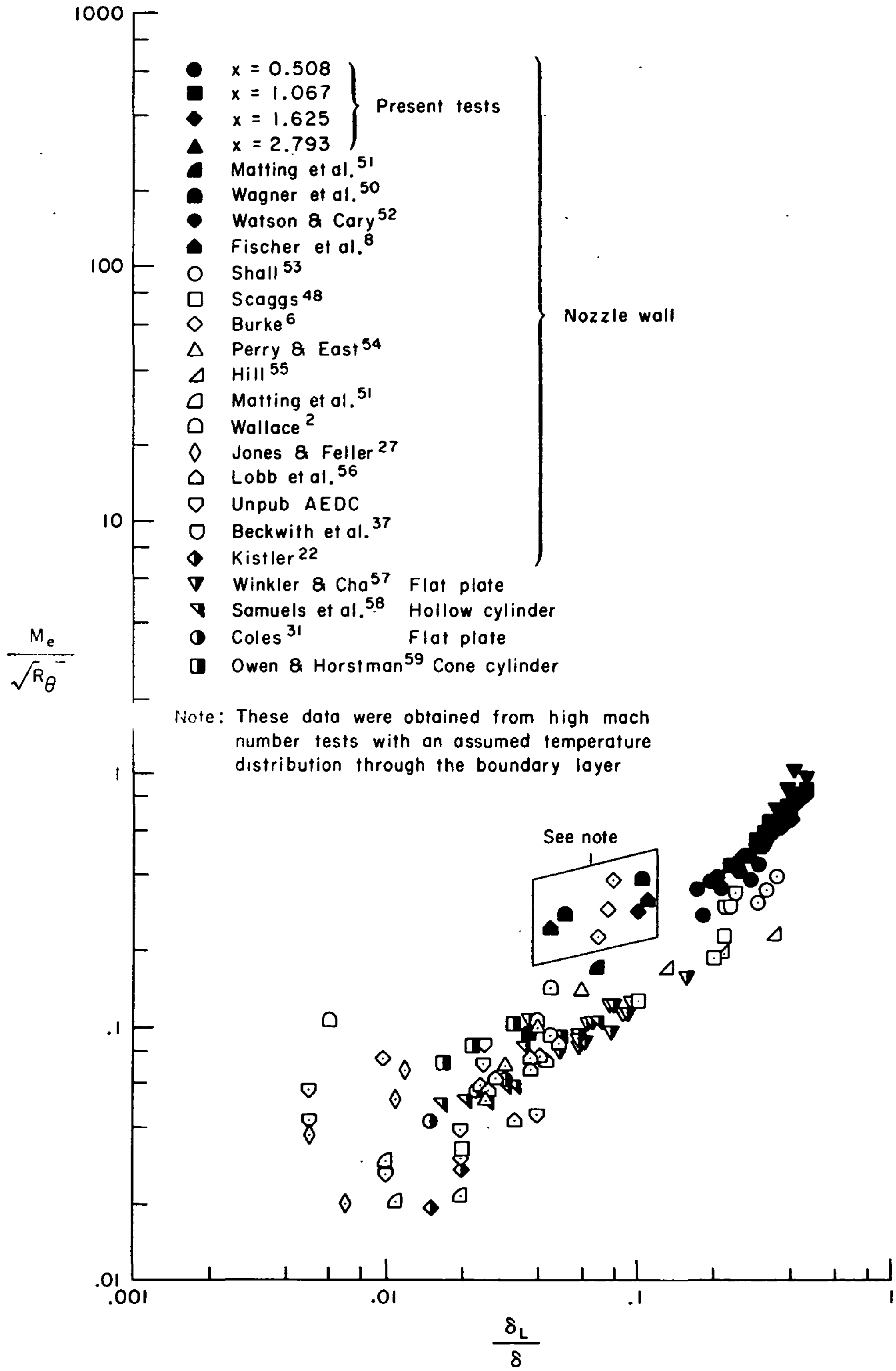

Figure 21.– Variations in sublayer thickness with $M/\sqrt{R_\theta}$.

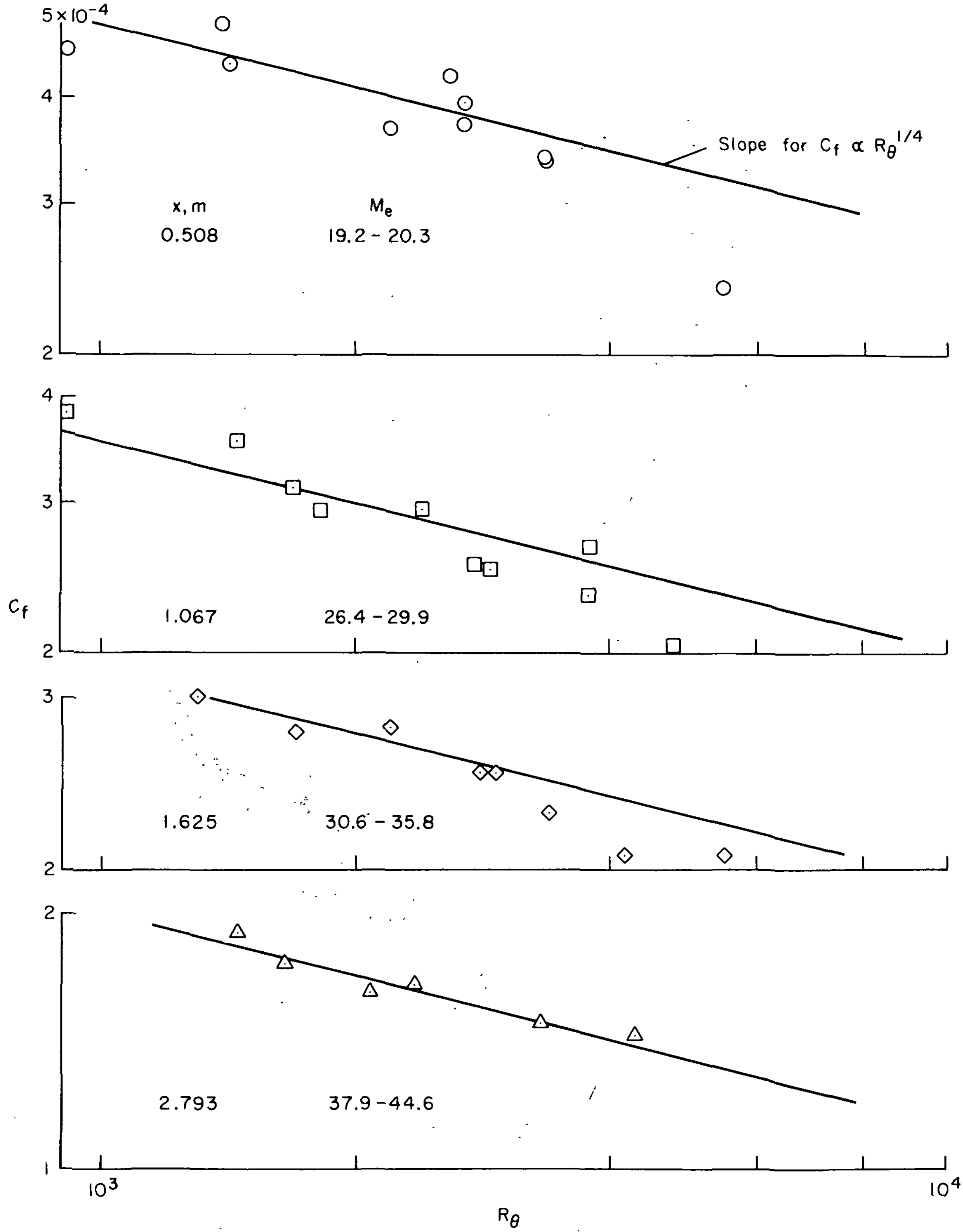

(a) Skin friction.

Figure 22.– Variation in skin friction and heat transfer with R_θ.

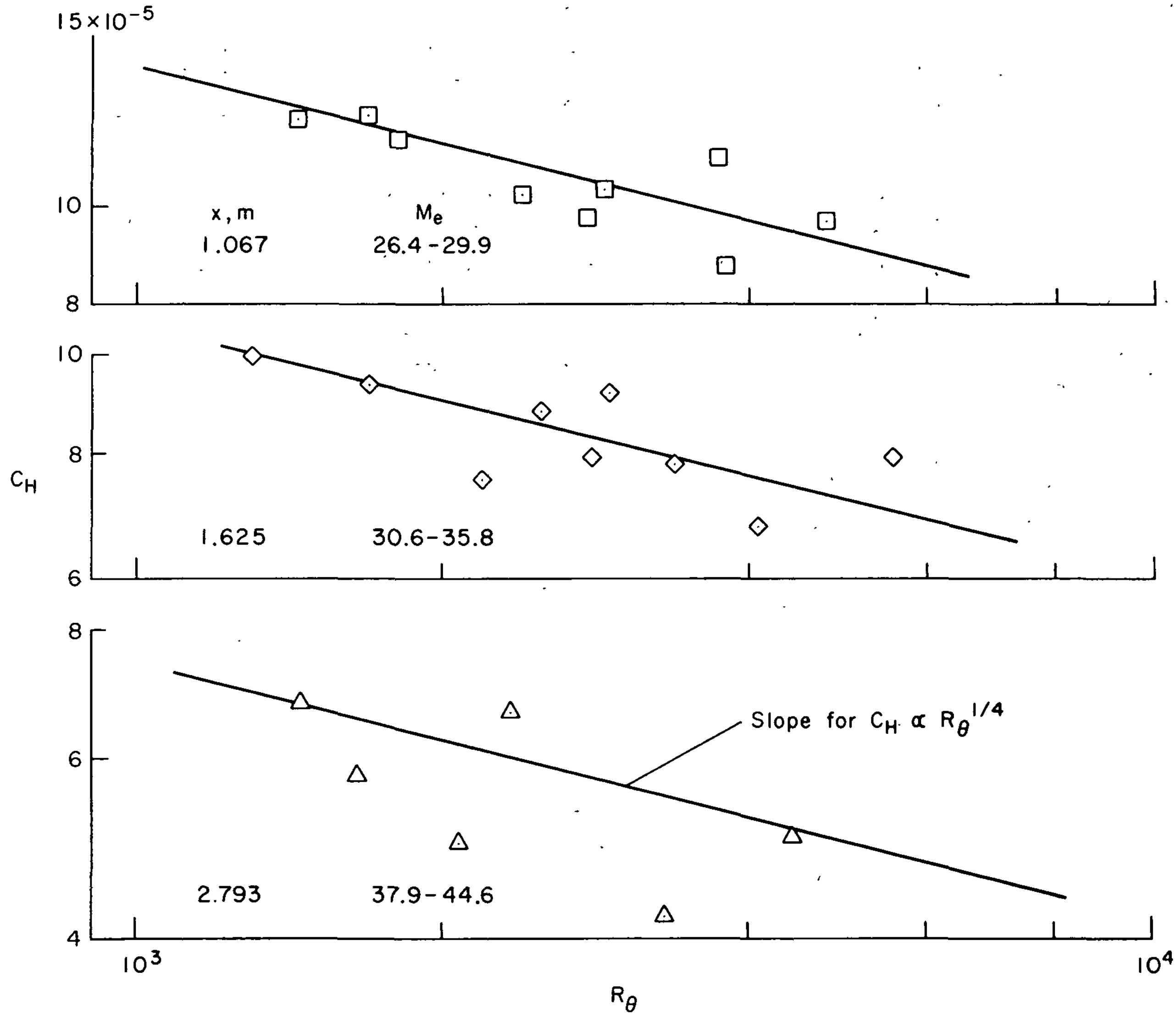

(b) Heat transfer.

Figure 22.– Concluded.

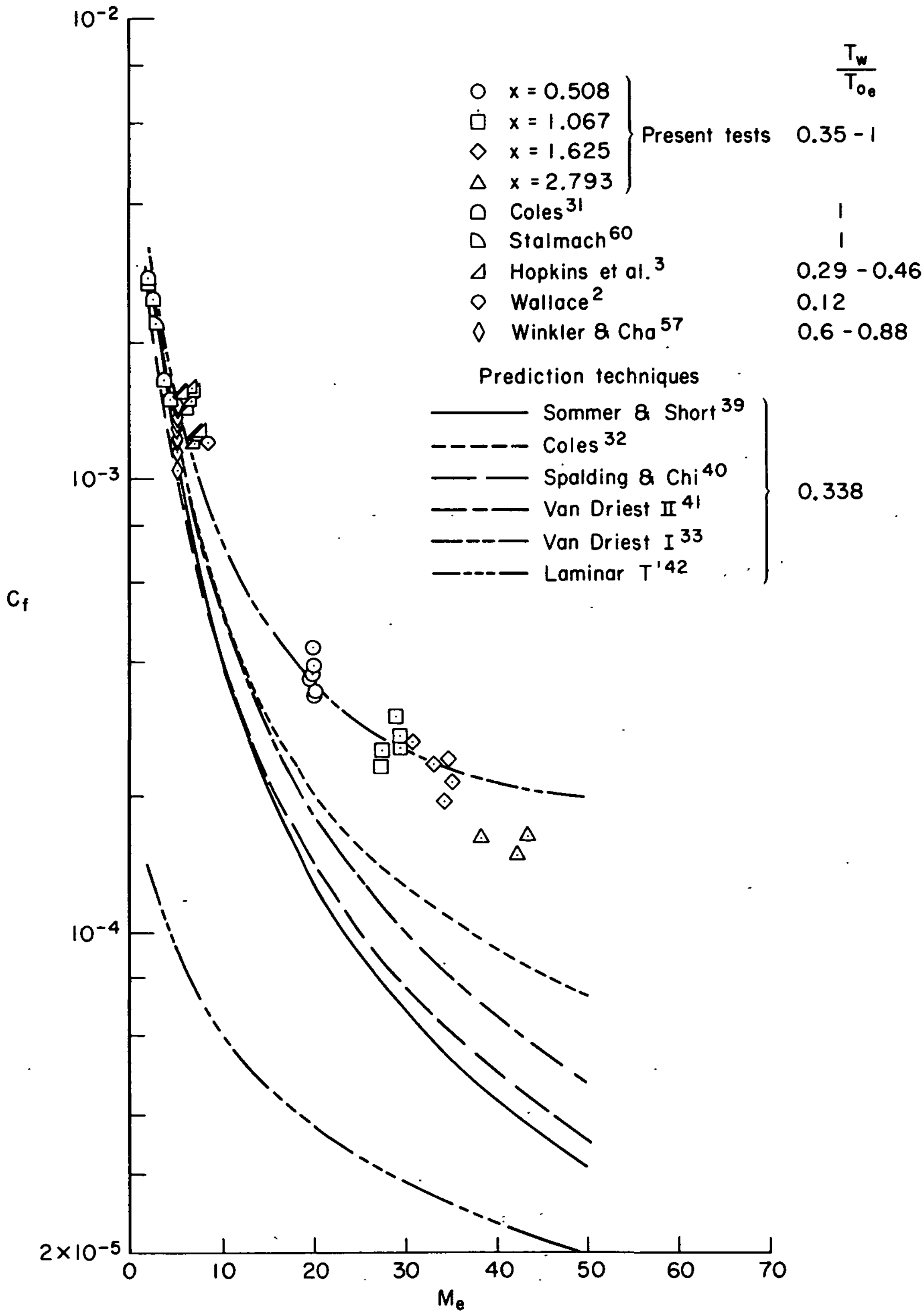

(a) Skin friction.

Figure 23.– Variations in skin friction and heat transfer with Mach number.

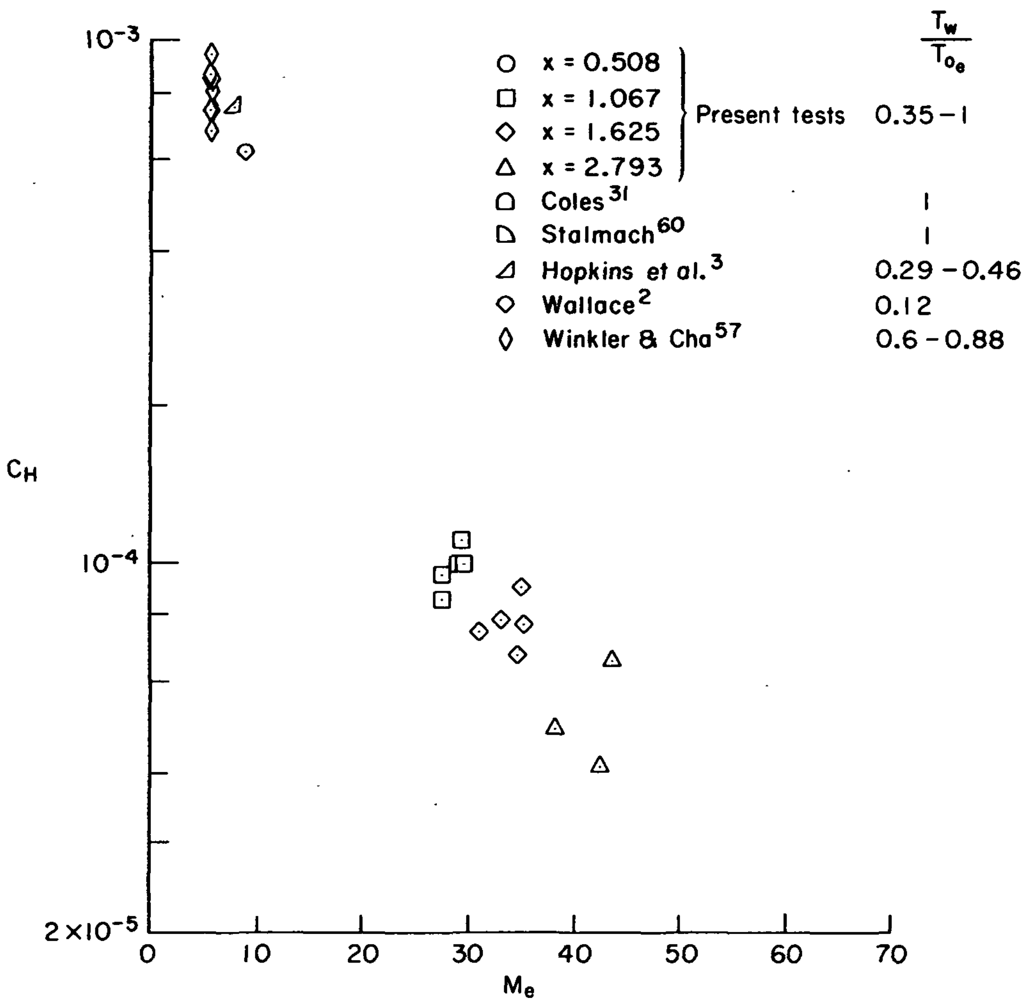

(b) Heat transfer.

Figure 23.– Concluded.

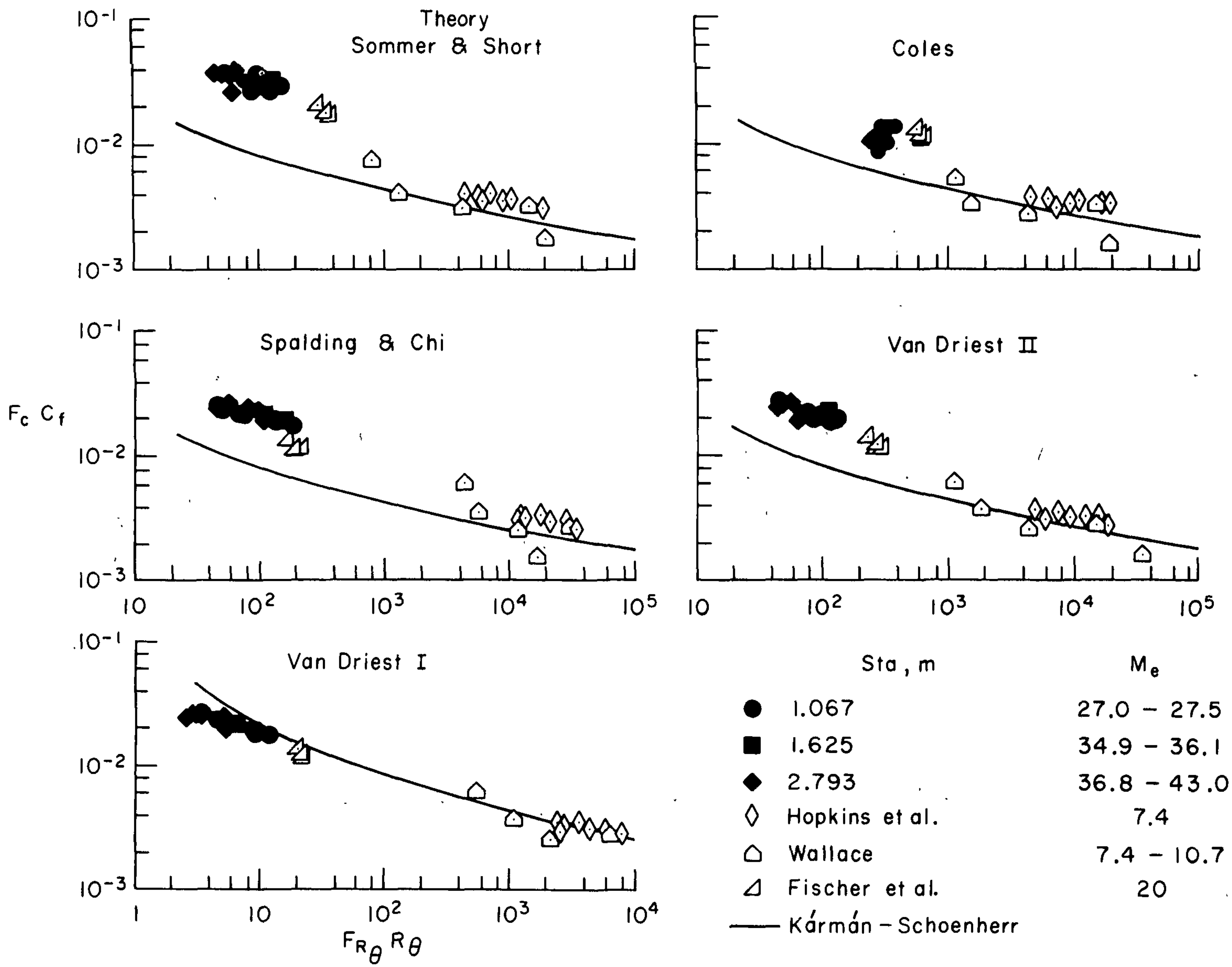

Figure 24.– Comparisons between measured and predicted skin friction.

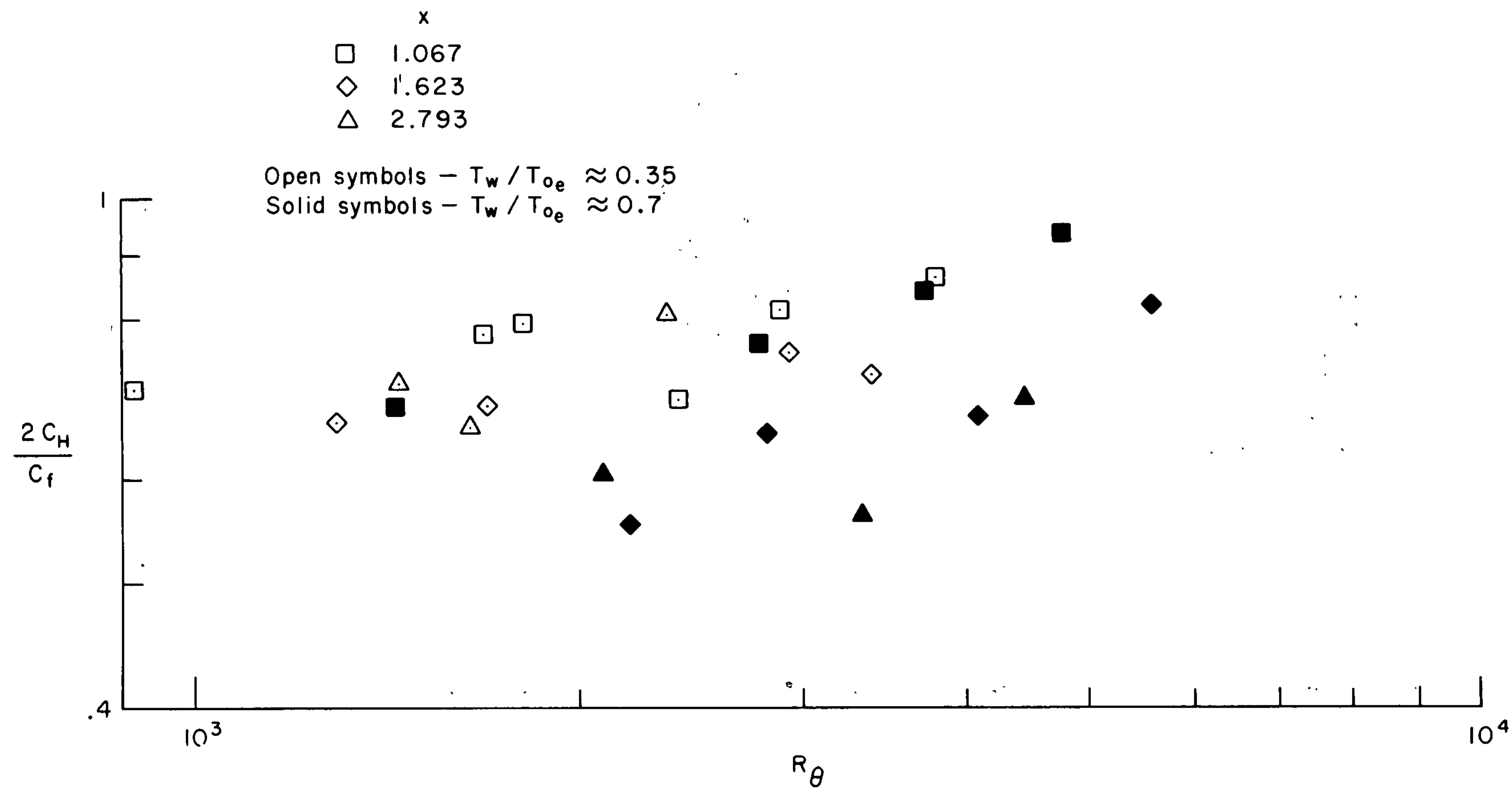

(a) R_θ

Figure 25.– Variation in Reynolds analogy factor.

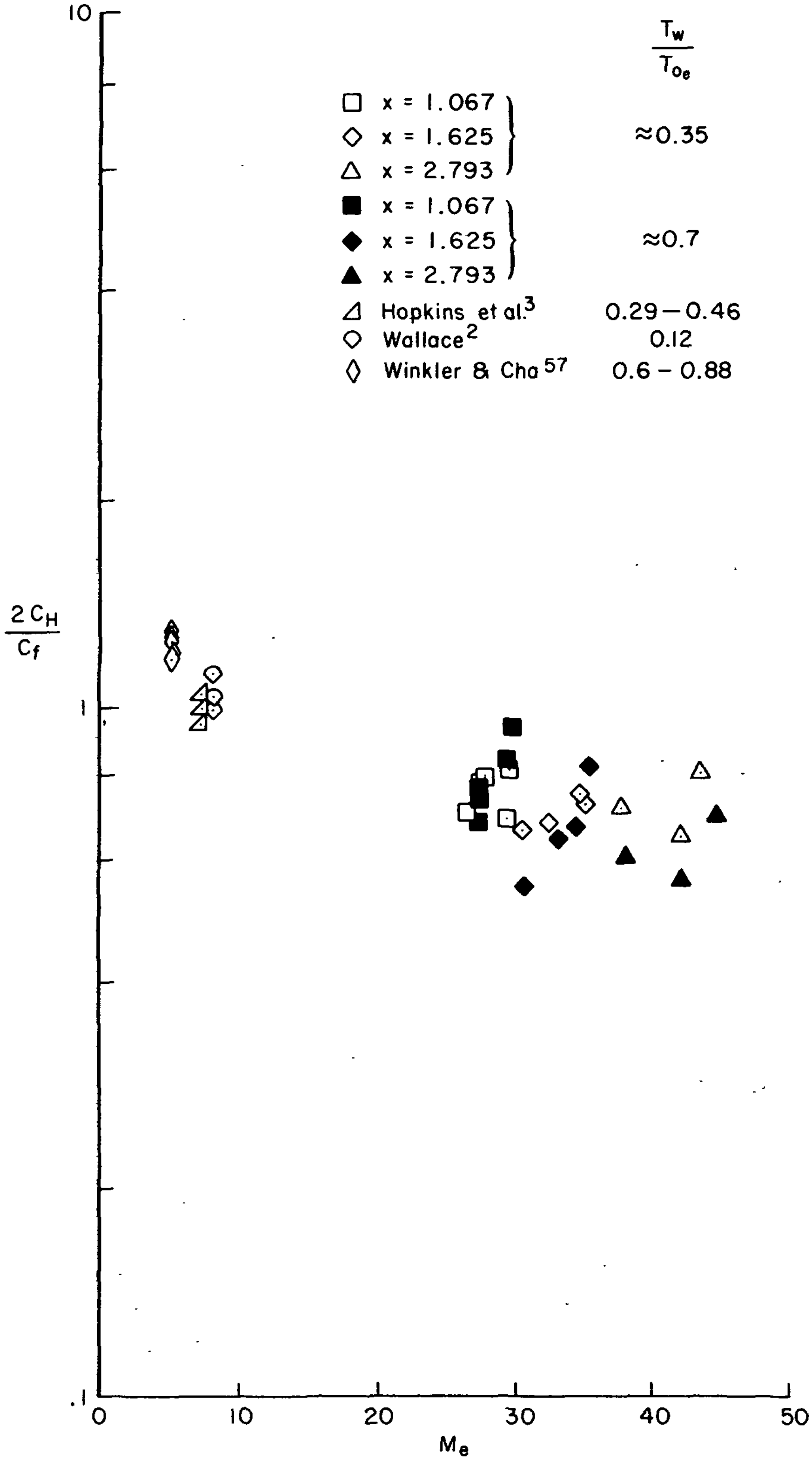

(b) *M*

Figure 25.– Concluded.

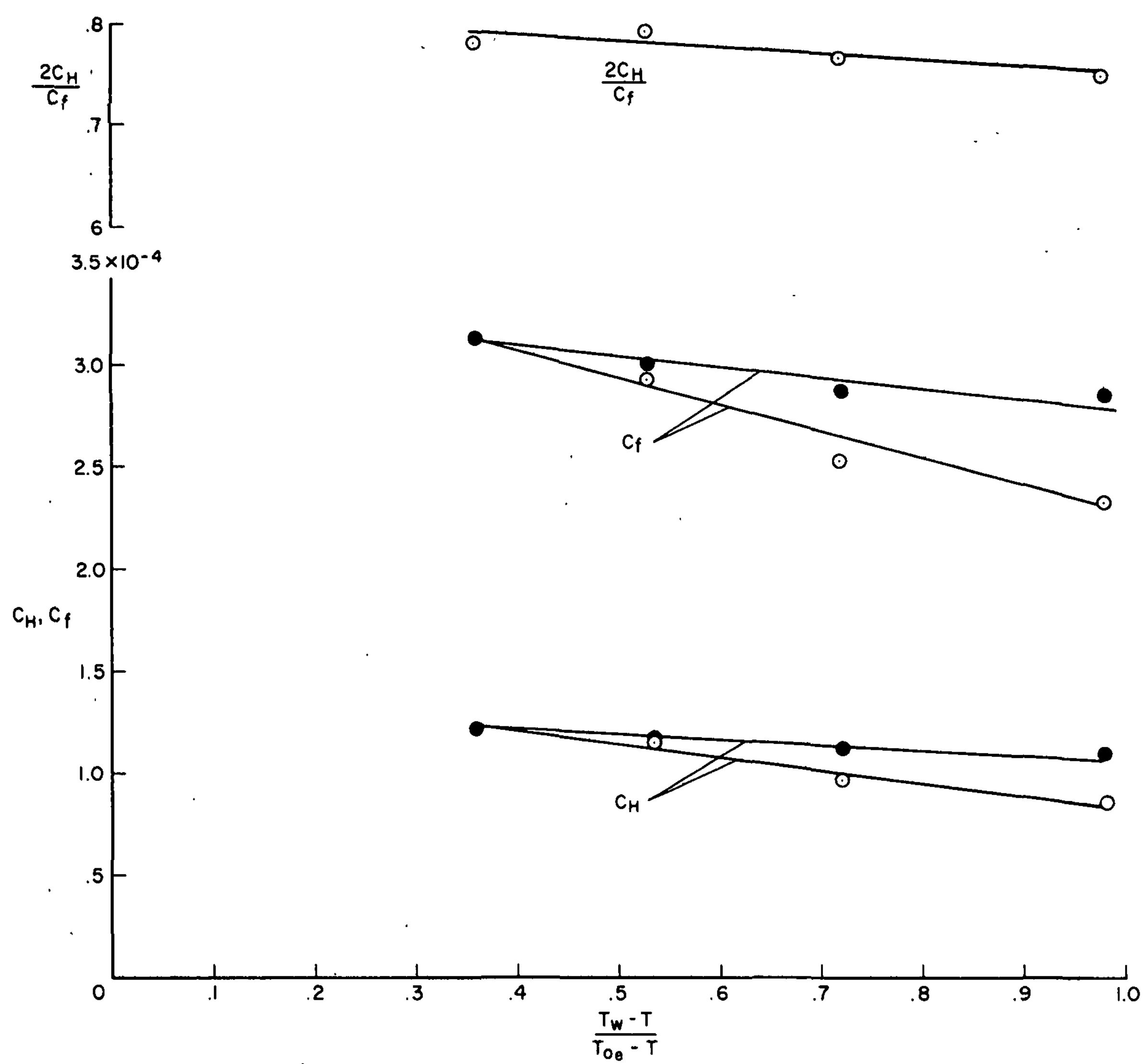

Figure 26.– Variations in skin friction, heat transfer, and Reynolds analogy factor with wall temperature ratio; $M_e \approx 2$ $x = 1.067$ m.

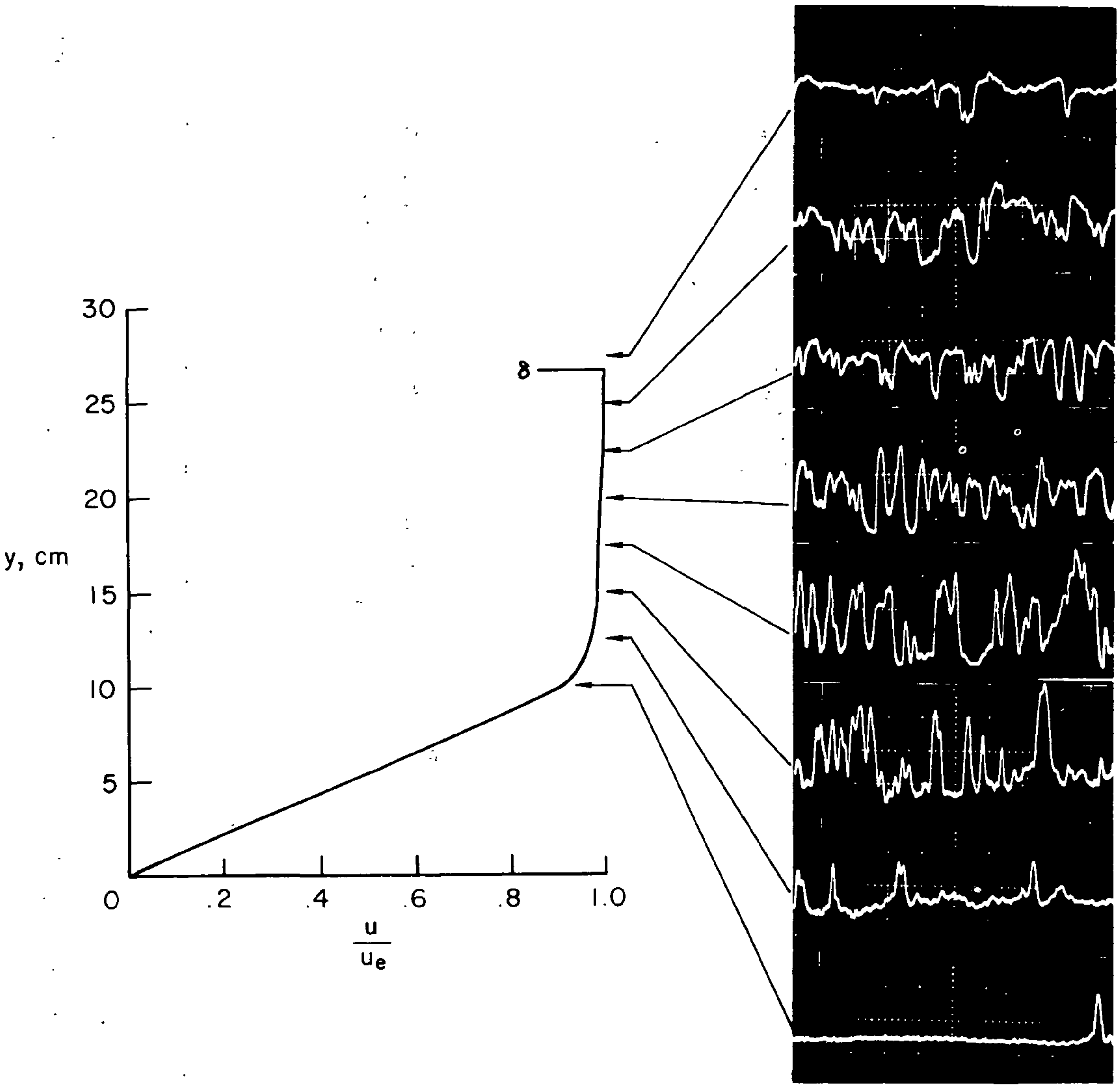

Figure 27.– Profile of heat-transfer fluctuations to cooled film probe.

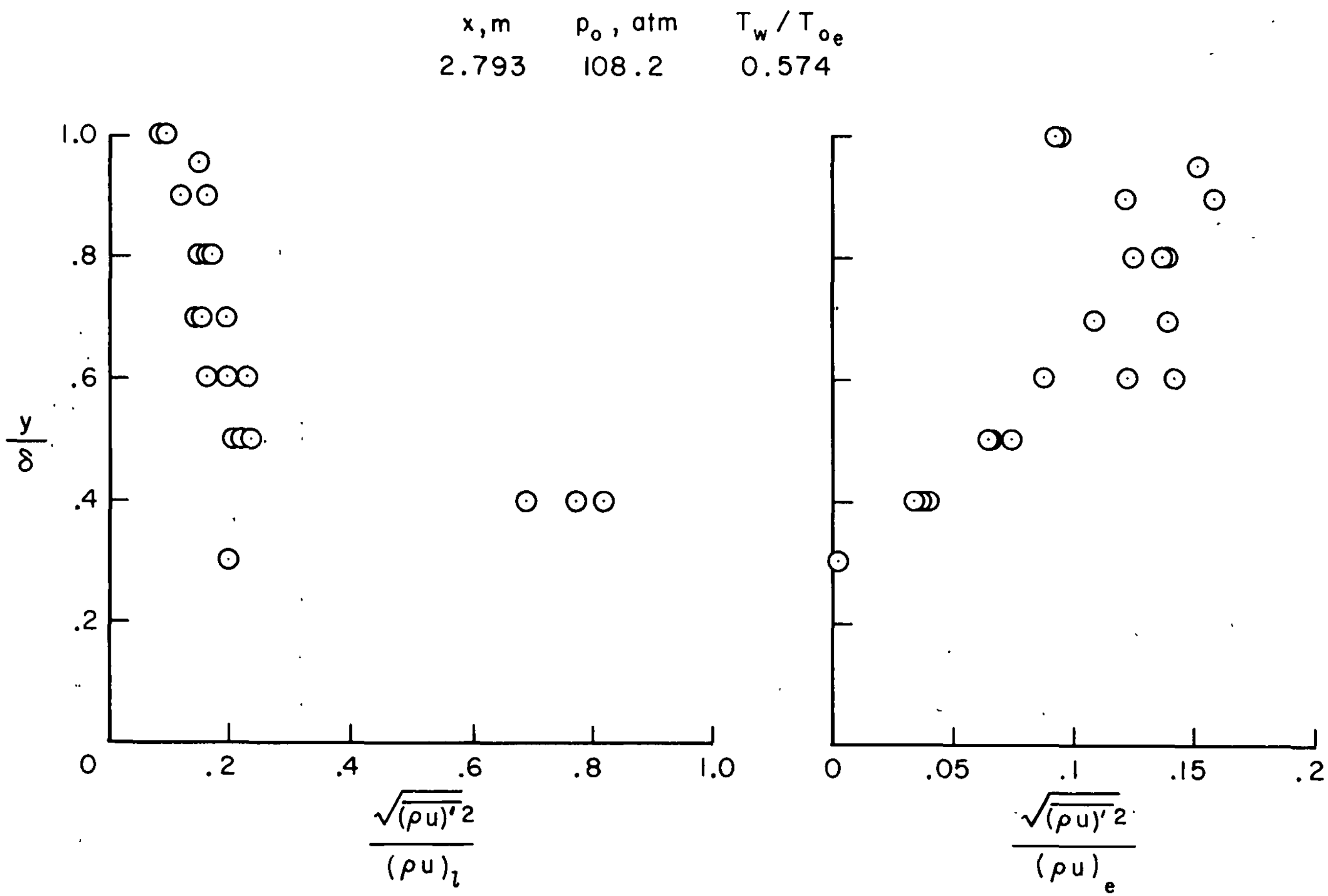

Figure 28.– Mass-flow fluctuations through the boundary layer; $M = 38.1$, $p_{o_e} = 108$ atm, $T_{oe} = 500°$ K.

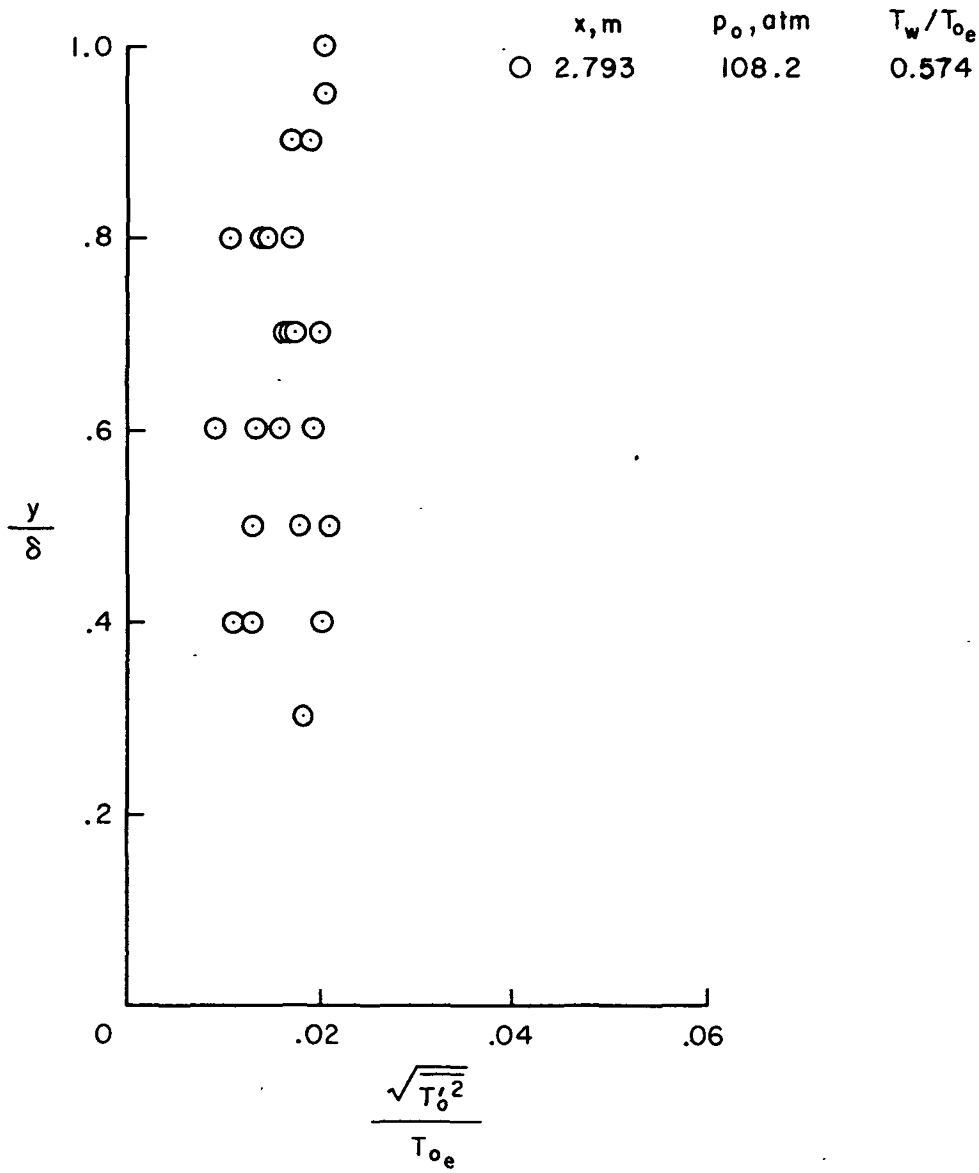

Figure 29.– Temperature fluctuations through the boundary layer; $M = 38.1$, $T_{o_e} = 500°$ K.

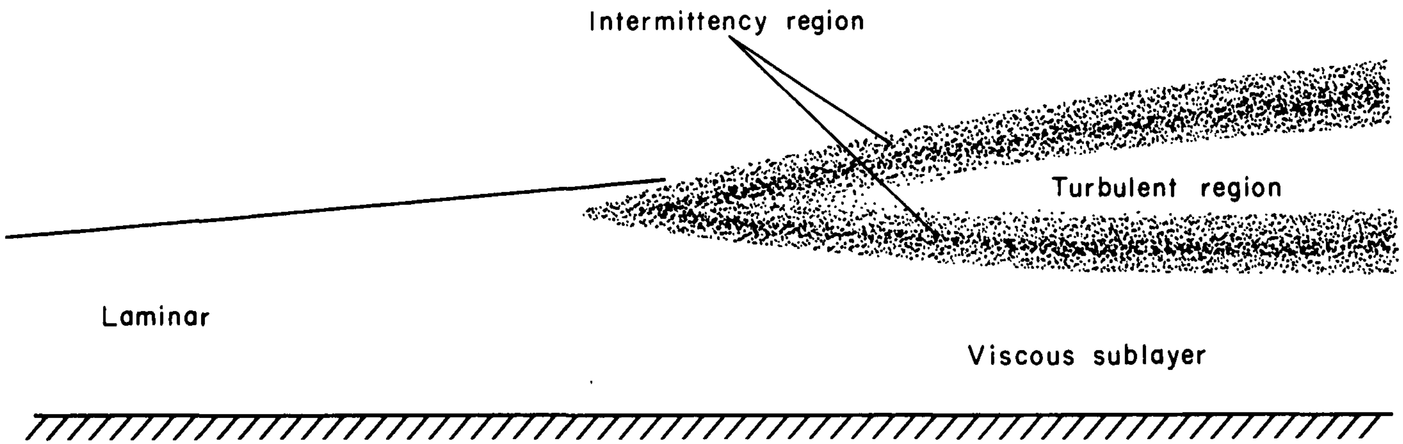

Figure 30.– Schematic of proposed hypersonic turbulent boundary-layer flow model.

NATIONAL AERONAUTICS AND SPACE ADMINISTRATION
WASHINGTON, D.C. 20546

OFFICIAL BUSINESS
PENALTY FOR PRIVATE USE $300

FIRST CLASS MAIL

POSTAGE AND FEES PAID
NATIONAL AERONAUTICS AND
SPACE ADMINISTRATION
451

U.S.MAIL

POSTMASTER: If Undeliverable (Section 158 Postal Manual) Do Not Return

---

"The aeronautical and space activities of the United States shall be conducted so as to contribute . . . to the expansion of human knowledge of phenomena in the atmosphere and space. The Administration shall provide for the widest practicable and appropriate dissemination of information concerning its activities and the results thereof."

—NATIONAL AERONAUTICS AND SPACE ACT OF 1958

NASA SCIENTIFIC AND TECHNICAL PUBLICATIONS

TECHNICAL REPORTS: Scientific and technical information considered important, complete, and a lasting contribution to existing knowledge.

TECHNICAL NOTES: Information less broad in scope but nevertheless of importance as a contribution to existing knowledge.

TECHNICAL MEMORANDUMS: Information receiving limited distribution because of preliminary data, security classification, or other reasons. Also includes conference proceedings with either limited or unlimited distribution.

CONTRACTOR REPORTS: Scientific and technical information generated under a NASA contract or grant and considered an important contribution to existing knowledge.

TECHNICAL TRANSLATIONS: Information published in a foreign language considered to merit NASA distribution in English.

SPECIAL PUBLICATIONS: Information derived from or of value to NASA activities. Publications include final reports of major projects, monographs, data compilations, handbooks, sourcebooks, and special bibliographies.

TECHNOLOGY UTILIZATION PUBLICATIONS: Information on technology used by NASA that may be of particular interest in commercial and other non-aerospace applications. Publications include Tech Briefs, Technology Utilization Reports and Technology Surveys.

Details on the availability of these publications may be obtained from:

SCIENTIFIC AND TECHNICAL INFORMATION OFFICE

NATIONAL AERONAUTICS AND SPACE ADMINISTRATION

Washington, D.C. 20546